Integrating Environmental Considerations in Technology Selections Under Uncertainty

by

Yue Chen

B.S. Chemical Engineering
Tsinghua University, Beijing, 2000

M.S. Chemical Engineering Practice
Massachusetts Institute of Technology, 2002

SUBMITTED TO THE DEPARTMENT OF CHEMICAL ENGINEERING IN PARTIAL FULFILLMENT OF THE REQUIREMENTS FOR THE DEGREE OF

DOCTOR OF PHILOSOPHY IN CHEMICAL ENGINEERING
AT THE
MASSACHUSETTS INSTITUTE OF TECHNOLOGY

JUNE 2005

Author.....
Yue Chen
Department of Chemical Engineering
May 2005

Certified by.....
Gregory J. McRae
Hoyt C. Hottel Professor of Chemical Engineering
Thesis Supervisor

Certified by.....
Karen K. Gleason
Professor of Chemical Engineering
Thesis Supervisor

Accepted by.....
Daniel Blankschtein
Professor of Chemical Engineering
Chairman, Committee for Graduate Students

Integrating Environmental Considerations in Technology Selections Under Uncertainty

By

Yue Chen

Submitted to the Department of Chemical Engineering
on May 18, 2005 in Partial Fulfillment of
the Requirements for the Degree of Doctor of Philosophy in
Chemical Engineering

ABSTRACT

Competition requires companies to make decisions that satisfy multiple criteria. Considering profitability alone is no longer sufficient. Ignoring environmental considerations will not only expose a company to potential regulatory costs, but also damaged public image, both of which in turn have negative effect on the economic well-being of companies. At the same time, the fast changing business environment requires companies to reach decisions in a speedy fashion. This work describes a decision-making framework that addresses the obstacles in integrating environmental considerations into technology selections with focus on the semiconductor and flat panel industry. It addresses data availability and data quality issues in environmental evaluations through the uncertainty analysis. It tackles the mismatch between the short innovation cycles in the industry and the long environmental analysis time by a combination of the uncertainty analysis, non-linear sensitivity analysis, hierarchical modeling, and the value of information analysis. It bridges the gap between environmental evaluations, economical evaluations, and technical evaluations by a unified modeling platform that links the process model, the cost-of-ownership model, and the environmental valuation model along with the databases and the random number generators for the uncertainty analysis. It is a generic framework and can be applied to various decision scenarios that face uncertainty in their systems. The paper also reviews sensitivity analysis methods and includes a survey on the current status and needs on environmental, safety, and health in the industry. A case study on Cu CVD illustrates the methods of the evaluations models. A case study on comparing NF_3 and F_2 as the chamber cleaning gas illustrates the decision-making framework.

Thesis Supervisors: Gregory J. McRae, Karen K. Gleason
Titles: Hoyt C. Hottel Professor of Chemical Engineering, Professor

ACKNOWLEDGEMENTS

I would like to first thank my thesis advisors Dr. Gregory J. McRae and Dr. Karen K. Gleason for the positive influences they had on me during my years at MIT. I learned from them to enjoy life while working hard. They allowed me much freedom in my research while giving me visionary directions. Greg introduced me to seeing the world as probabilistic, but yet the fact that uncertainty should not equal to ignorance (I now feel so empowered to deal with all the risks in my own life!) Karen's insights in how the semiconductor industry works steered me away from many vain pursues. I would also like to express my sincere appreciation to the other members of my thesis committee Dr. Herbert H. Sawin and Dr. Joel P. Clark. Herb gave me great suggestions upon how to make my research more relevant to the industry. Joel helped me in my learning of the life cycle analysis , which is a key part of my research.

I would also like to thank my parents Chen Jianchun and Wu Fuping who give me love, freedom, and infinite emotional support to pursue my dreams. Their encouragement for me to explore and always do better, shaped the way I approach and view this world. Their abundant collection of books opened up my imagination and enticed me to venture to a new continent. Another person who had great influence on me after coming to the US is my dearest friend Dr. Chahriar Assad Bakhtiari. His generosity and compassion filled me with energy. He advised me on adapting to this new culture while maintaining my uniqueness. His own graduate school experiences also helped me in putting my seemingly endless efforts in perspective.

I also had the great luck to work with a group of wonderful and delightful labmates: Sara Passone whose thoughts have always been intellectually stimulating, Federico San Martini whose passion for the environment made me feel I am not alone in my pursue, Jeremy Johnson with whom I had many ideological discussions, Bharthwaj Anantharaman who helped me with many technical problems, Patrick de Man, Gerald Bode, Jose Ortega, Chuang-Chung Lee, and Darren Obrigkeit. To Jose Alejandro Cano Ruiz with whom I never shared the office, yet whose work laid the foundation for mine.

This research was supported in part by the Engineering Research Center (ERC) for Environmentally Benign Semiconductor Manufacturing. This support is gratefully appreciated. Through the ERC, I have met many students, industrial practitioners , and faculty who are working on similar topics as mine. Their support has made my research possible. Here I especially would like to thank Dr. Nikhil Krishnan, Tim Yeakley, Terry Francis, Mike Sherer, Laura Losey, David Bouldin, Dr. Paul Blowers, and Dr. Farhang Shadman.

There are many other people who have made my five years at MIT enjoyable and rewarding. Some of them showed me the infinite possibilities in life as long as I dream and I try, while some of them shared my joys and sorrows. I salute you all!

Table of Content

List of Figures

List of Tables

Chapter 1 Introduction

1.1 Thesis Statement

Decision makers often need make choices based on uncertain information. The source of uncertainty may be limited understanding of the system of interest or the innate variability of the system. Because of time constrain, resource constrains, and real physical constrains, it is impossible to make decisions only after all the uncertainties are perfectly resolved. Therefore, a systematic framework and relevant tools have been developed to support decision making in technology selections under uncertainty. This framework is generic and can be applied to different contexts. This framework has been applied to integrating life cycle analysis (LCA) into technology selections in the semiconductor and flat panel industry since the problems of uncertainty and time constrain are particularly acute in this setting. The framework allows uncertainty to be quantified and propagate through the evaluations from inputs to outputs, and identifying important parameters that contribute the most to the uncertainty in the outputs. It uses hierarchical modeling to avoid excessive details in analysis. It also includes a unified modeling platform to link the technical, economic, and environmental evaluation models and databases.

1.1.1 Driving Forces for Tools to Support Effective EHS Decision Making for Semiconductor Manufacturing

There is an increasing need for manufacturers to assess and improve life cycle environmental impacts of their products. For example,

- European union (EU) directives, such as the waste from electrical and electronic equipment (WEEE) directive, state reduction of life cycle impacts as a primary goal [1].
- The Swedish Confederation of Professional Employees (TCO), for instance, has developed the detailed environmental requirements and an accompanying certification system for personal computers and monitors (TCO 95 and TCO 99). The initiative is widely recognized internationally, and purchasers world-wide use the criteria [2].
- The European Commission has also issued the Integrated Product Policy (IPP). "IPP advocates 'life-cycle thinking', which means that when pollution-reduction measures are identified, consideration is given to the whole of a product's life-cycle, from cradle to grave. That way appropriate action can be taken at the problem stages in the life-cycle." [3].

At the same time, life cycle awareness of environmental impacts is leading to the communication of environmental requirements along fabrication supply chains (for the electronics industry - from consumers and governments to electronics manufacturers, device manufacturers, equipment suppliers, materials suppliers, and onwards). For example,

- the ISO 14000 standards, and the 14040 series in particular, directly address life cycle and supply chain environmental issues as part of holistic environmental management strategies.
- Emerging regulations such as the as EU restriction of the use of certain hazardous substances in electrical and electronic equipment (ROHS) [4] and WEEE directives emphasize environmental supply chain requirements. The ROHS directive places restrictions on materials that can be present in electronic products. Such restrictions directly transmit environmental requirements along the electronics supply chain. The WEEE directive leaves manufacturers responsible for products at their end-of-life, and therefore links design issues throughout the supply chain with environmental impacts.

There is also an increasing recognition of the intrinsic correlation between EHS and conventional cost factors. Eco-efficiency frequently results in manufacturing efficiency. Less "waste" can mean reduced cost of raw materials and disposal. For instance,

- This "win-win" between economic and environmental factors has been pioneered through work in pollution prevention.
- There are numerous well known examples of companies who have combined environmental improvements with economic savings, such as 3M 's pollution prevention pays program, which has prevented 857,282 tons of pollutants and saved $894 million since 1975 [5], Ford motor company made significant environmental and economical improvement through intelligent design, during improvements of their Rouge plant in Deaborn, MI [6]

There is also increasing dialogue around including extended costs and impacts into environmental decision making. Awareness of cost factors such as the long-term health and safety costs of introducing new chemicals and community costs is growing. Also there is an increasing recognition that fixing environmental problems 'after the fact' leads to increased costs for all parties.

- Regulations like the EU Registration, Evaluation and Authorization of chemicals proposal begin to shift burdens of proof for chemical safety, from governments to manufacturers and drive generation and use of data on chemical health and safety in decision making [7].
- Clean-up of MTBE contamination of ground water or requirements in semiconductor manufacturing to phase out Perfluorooctanyl sulfonate (PFOS) indicate the need for better evaluation of potential EHS problems in the design of products and processes [8].

Last but not the least, EHS decision tools could result in much improved environmental (and economic) performance of the semiconductor industry.

- Lashbook and colleagues identified processes which have superior environmental and economic performance from three options for deep ultraviolet (DUV) lithography using CARRI, ESH cost Model and Mass/Energy Balance [9].

- Through the water recycling strategies, Texas Instruments was able to save 263 million gallons every year, for a cost savings of $700 K/yr. Here the economic interest is in line with environmental interest [10].
- Applied Materials has effectively used EHS decision tools to identify cost-effective options to treat copper CMP wastewater that may also reduce net water use. Such tools have also been used to characterize equipment environmental performance [11].

1.1.2 Motivations for Developing the Decision Framework

There are several practical barriers to the integration of environmental considerations into decision-making: (1) A frequently cited barrier is that the data available for environmental, safety, and health (ESH) evaluations are very limited and their quality varies greatly. For example, the typical uncertainties in the cancer toxicity indicators for discharge to water range from 2 to 3 orders of magnitude, while those in the non-cancer toxicity indicators range from 3 to 6 orders of magnitude [12]. To further complicate the situation, new chemicals are introduced into the manufacturing processes at a very fast pace. These new chemicals lack much biological and environmental information. What's more, the material, energy, and emission inventories for many processes are not readily available. The lack of accurate data impairs the confidence in the ESH results. When uncertainty in ESH evaluations is represented in a qualitative or semi-quantitative manner, it becomes harder to integrate the results into cost analyses, which are quantitative. (2) Another related uncertainty comes from the technologies under study. It is widely understood that in a technology design lifecycle, decisions made at earlier phases have more influence on future cost, revenue, and ESH impacts of the technology than those at later phases. However, there is also less information known about the technologies at a very early stage. (3) The third barrier is that the inputs for ESH activities are mostly unconnected to those of process and equipment design and operation, even though the parameters central to the latter are also the ones that directly drive the ESH impacts such as the material usage, the energy usage, and emissions. The communication between process engineers, equipment engineers, and the ESH engineers is often arduous, which makes it harder for the effects of ESH and cost on each other to be presented together to decision makers. (4) Because of the first three barriers, a comprehensive ESH analysis is very time consuming if not impossible at an early design stage, which does not fit into the fast pace of the industry. (5) Lastly, the correct system boundaries to be used in ESH analyses is unclear to many decision makers. Upstream processes and downstream disposal generate significant environmental impacts. Yet they are not always under the control of the decision maker. This complicates the definition of system boundary.

Besides the barriers mentioned above, there are also innate difficulties in decision making. To illustrate these difficulties, let us look at a case of choosing between two gases for chamber cleaning. A comprehensive decision requires the consideration of technical performance, cost, worker safety and health, and environmental impacts. The performance of these criteria is shown in Table 1.1. It can be seen that there is a clear advantage of the variable costs of the F_2 process. Its lifecycle global warming effects are

smaller, too. However, it may pose worker safety and health hazard, requiring special procedures to protect workers, as well as ensure F_2 not to interfere with other processes in the fab. Besides the complexity in finding acceptable tradeoffs, there is also much uncertainty in these numbers due to the imperfect inputs, limited understanding of the systems, and the inherent variability of the factors.

Table 1.1 Comparison of NF_3 and F_2 as a Chamber Cleaning Gas

Criteria	F_2	NF_3	References
Variable Cost/mole of Fluorine	\$0.8	\$6	{MicroGenTM, #141}
Fluorine usage rate at the same etch rate (mole/min)	0.54	0.80	This work
Lifecycle Global Warming Effect (kg CO_2 equivalent/kg)	0.056	0.13	This work
Toxicity LC_{50} (ppm)	180	6700	[13, 14]

1.1.3 Objectives

Based on the motivations mentioned above, the objectives of the work are:

- To analyze environmental impacts with life cycle point of view.
- To construct a comprehensive framework for technology assessment.
- To use new uncertainty analysis tools to help focus resource allocation.
- To test methodology using industrially relevant case studies.
- And to identify win-win situations for the industry.

1.1.4 Major contributions

The major contributions of this work include:

- Identified major obstacles in the operation of integrating of environmental considerations into technology selections (motivation of this integration is beyond the scope of this work).
- Reviewed methods of identifying important parameters that contribute to the variances of the outputs.
- Constructed systematic framework for decision analysis that is particularly relevant to the semiconductor and flat panel industry.
- Introduced the concepts of value of information (VOI) and resources allocation in information collection into environmental assessments.
- Combined uncertainty analysis, hierarchal modeling, VOI, and global sensitivity analysis into decision analysis.
- Designed a unified modeling environment using existing commercial software to conveniently and simultaneously model the processes under study, evaluate the environmental and economical impacts of the processes, and perform the uncertainty analysis.
- Conducted a survey on various parties in the industry on their view and needs in ESH assessments.

1.2 Thesis Outline

Chapter 1 provides the background and motivation for this work, which is to develop a systematic framework and relevant tools in directly addressing uncertainties in technology selections.

Chapter 2 describes the past work and present view on integrating environmental considerations into decision making in the semiconductor industry. The literature review discusses multi-criteria decision making involving environmental considerations in process/equipment design from a few aspects: (a) evaluation methods, i.e. cost of ownership and LCA, (b) the use of decision theory in the above decision-making, (c) the use of uncertainty analysis in environmental evaluations, (d) unified modeling environment. These are also the topics that would be address in the later chapters. It was found that few literature on environmental evaluation methods resolve the data availability and quality problems. Uncertainty in the systems is treated naively. The considerations of system boundary and uncertainty are not the focus of the methods either. Env-S emphasizes the importance of linking the process information with economic and environmental evaluations without providing an implementation platform to realize the connection. The literature review reveals the value in developing the Tools. Chapter 2 also includes a survey that was conducted to understand the current status and needs in the industry regarding ESH assessments.

Based on the motivation from Chapters 1 and 2, Chapter 3 presents the how to understand the effects of the uncertainty in inputs on that of outputs, and given unacceptable level of uncertainty in outputs, how to reduce it. Both tasks call for direct representation of uncertainty in the analyses. Chapter 3 first reviews the sources of uncertainty and the importance of considering it in the context of selecting future technologies. Then it defines the uncertainty analysis in this thesis, i.e. representing system parameters including state parameters and control parameters as stochastic, propagating the uncertainty through the evaluation models, and obtaining stochastic representations of the outputs. After that, it proceeds to sensitivity analysis, which has two undertones for uncertain systems: one is to see the responses of nominal values of outputs to inputs; the other one is to see the responses of the uncertainty, defined here to be variance of outputs to inputs. This work will focus on the latter. Sensitivity analysis methods discussed in this chapter are local linear sensitivity analysis, Analysis of Variance, linear correlation coefficient, and rank correlation coefficient, Fourier Amplitude Sensitivity Test (FAST), Deterministic Equivalent Modeling Method, and Global Sensitivity Indices (GSI). Focus was put on the non-linear global methods. Two common examples are used to compare the ease of use, the effectiveness, and the cost of the methods. It is suggested that for systems with a large number of inputs, rank correlation coefficients be used to first to identify the top ranking factors, then other more quantitative methods, such as the GSI and FAST can be used for the top few most important parameters to attain a more precise magnitude of the contribution accounting for the higher order non-linear effects.

There are three evaluation models used in the multi-criteria analysis in the Tools. They are the process model, the cost-of-ownership (COO) model, and the Process by Product Input-Output Life Cycle Analysis (PIO-LCA). Chapter 4 describes these models and demonstrated their use through a case study on Cu chemical vapor deposition (CVD). Process models are the basis of understanding a technology's technical, economic, and environmental performance. They provide the mass and energy balances, and the process time. The Cu CVD process was simulated in a modeling environment VisSim. The VisSim model provides the amount of precursors consumed, the precursor yield, the deposition time, and energy used. These factors are fed into the cost-of-ownership model and the PIO-LCA model. The former describes the costs of acquiring, installing, operating, and decommissioning a processing system in a factory environment. The latter considers not only the environmental impacts directly generated in the processes they design, but also those associated with the provision of input materials for the processes, and downstream disposal. It was built on the methodology of Economic Input-Output LCA. It allows investigation at the process level rather than only at the industry level. As aforementioned, there is large uncertainty in the data of LCA. Therefore, an environmental information management system EnvEvalTool was used which has toxicological and fate and transport data obtained from various data sources, as well as calculated using a fate and transport model. Most of the parameters in the EnvEvalTool have PDFs. For the missing one, their PDFs were estimated.

The tools described in Chapter 3 and 4 are put to use in Chapter 5 to compare two alternative chamber cleaning technologies. The decision framework is also described in details in this chapter. The concepts of hierarchical modeling and value of information (VOI) are presented here. The idea of hierarchical modeling is to start with simple models and rough estimations, carry out the analysis, and based on whether the results are satisfactory or not to determine whether the next level of detail is required. There are two aspects of the hierarchy: one is from the model structure, meaning the simplifications and assumptions in the model; the other is from the accuracy of the parameters. These two aspects correspond to the sources of uncertainty. Chapter 3 only addresses the parametric uncertainty. Hierarchical modeling considers the structural one. Because there is cost associated with collecting more information, the decision maker needs to compare the value that the new information brings to the cost of obtaining it before deciding whether to move from the lower hierarchy to the higher one. The net VOI is therefore defined as the additional value (or reduced cost) of the project that the new information brings compared to the value (or cost) of the project without the information minus the cost of obtaining the information. Both hierarchical modeling and VOI require quantification of the uncertainty in data and identification of important parameters. They are done by uncertainty analysis and non-linear global sensitivity analysis. Due to the nature of the decision context, which is to distinguish two alternatives, relative measures rather than absolute values for comparison. This takes away the variability that is common to both alternatives, therefore reduces the uncertainty in the relative output measures. The modeling of the cleaning process was done in Excel®.

To address the data gap problem mentioned in Chapters 1 and 2, Chapter 6 describes an integrated modeling platform for process, cost, and environmental modeling.

With this platform, it is easier for a decision maker to see both the economic and environmental consequences of a process/equipment design. It also facilitate the communication among the process developers, process engineers, and ESH personnel. The modeling platform consists of commercially available software: the process modeling is done is Aspen; the COO and PIO-LCA modeling is done in Excel; the ESH database is based on Access. Codes written in Visual Basic connects the programs together. The chamber cleaning case is revisited to demonstrate the modeling environment. The database structure needed for this environment is also described in this chapter. The chemical data for the three evaluation models are linked together by CAS numbers.

Chapter 7 proposes the future work, which include: (1) building more unit operation models for the semiconductor and flat panel industry; (2) propagating the database of chemical life cycle information using QSAR or other predictive methods; (3) using real options to evaluation the VOI; (4) making the PIO-LCA and the EnvEvalTool available on line to the public.

The thesis concludes by Chapter 8 which summarize all the previous chapters. Figure 1.1 shows the relationship of the chapters. It is also the proposed framework of the thesis.

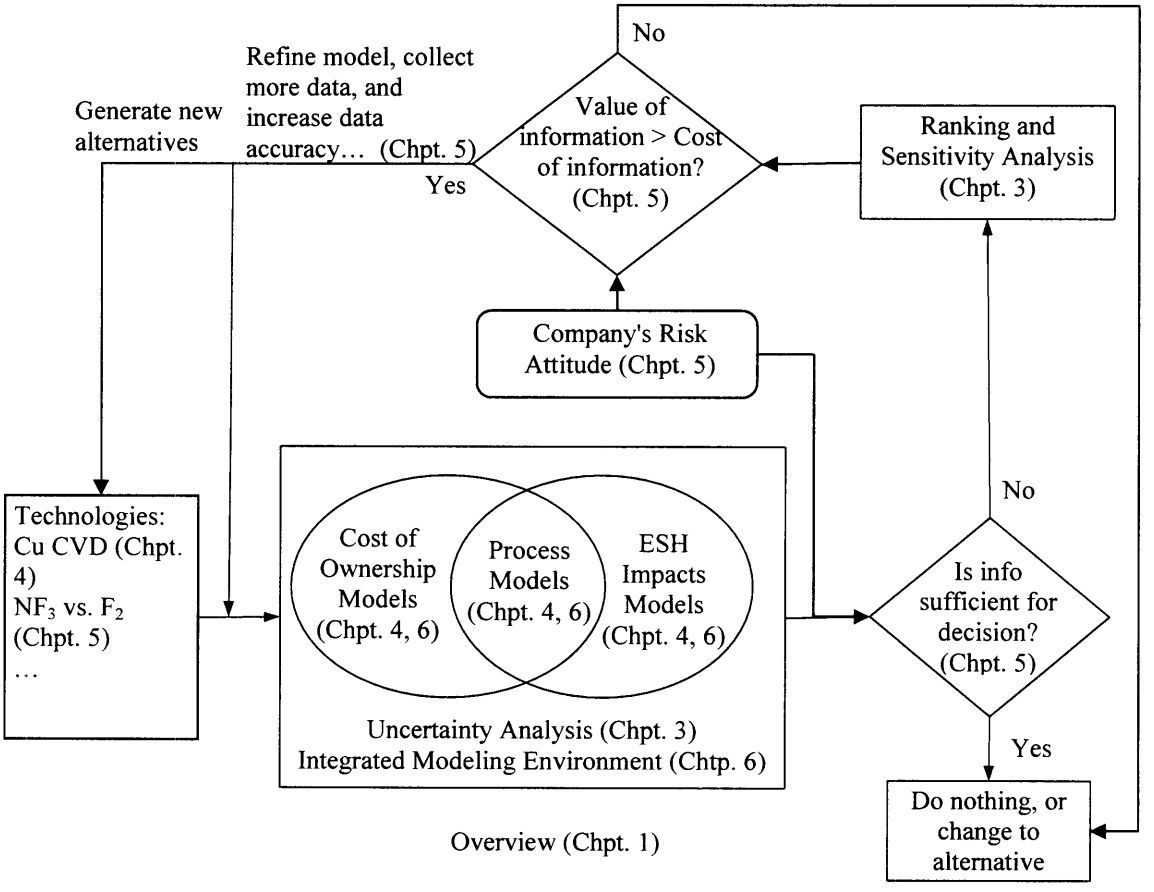

Figure 1.1 Proposed Decision Making Framework and Structural of the Thesis

Chapter 2 Past Work and Present View on Integrating Environmental Considerations into Decision Making

2.1 Literature Review on Environmental Evaluation Tools in the Semiconductor Industry

The increasing demand for environmentally benign manufacturing calls for a methodology that directly addresses data availability and quality. It needs to be able to provide sensible results under limited and imperfect information, and give directions for future effort on data collection. The methodology also needs to integrate environmental evaluation with cost and process modeling. The past literature has addressed parts of these demands. The Lifecycle Assessment White Paper [15] provides a good account of environmental evaluation cases and methods related to the semiconductor industry. These methods address some of the problems mentioned above in different manners. Table 2.1 compares the existing environmental valuation methods for the semiconductor industry.

In Computerized Assessment of Relative Risk Impacts (CARRI^{TM}), the uncertainty in the data is represented qualitatively by high, medium, low, or N/A [16]. Even though this method gives users an idea of the uncertainty, it does not inform the user about where improvement in data accuracy will reduce the uncertainties in the results. CARRI^{TM} ranks the impacts of processes based on the amount chemicals used in the processes and emissions, which is not directly linked to the real impact because different chemicals can have very different impacts on human health and the environment with the same mass amounts. A simple example can be H_2SO_4 vs. HF. It does not consider the impacts arising from energy or water consumptions. The system boundary of CARRI^{TM} is limited to include manufacturing processes. The sources of data used in CARRI^{TM} are restricted to databases, including a chemical characteristics database, a process description database, and a weighting factors database. While a valuable tool for qualitative understanding the process impacts, the reliance on databases for process description precludes CARRI^{TM} from evaluating new technologies whose data are not available in the database.

Developed by Applied Materials Inc. and UC Berkeley, the Environmental Valuation System (EnV-S) models the processes based on industrial data and physics and chemistry principles, thus enabling the evaluation of future technologies. The modeling is done at the tool level, the platform level, and the facility level [17-20]. When evaluating a system, the technical performance, the COO, and the health and safety impacts are considered. Its COO calculation includes downstream treatment and disposal emissions. Understanding these downstream costs encourages designers to improve environmental performance by lowering treatment and operating costs. The inputs of the process models can be treated as random variables upon which Monte Carlo simulations

can be performed to obtain the confidence bounds of the outputs. However, the uncertainty analysis is relatively simple. Only the sources of safety and health impacts inside the fab are considered. Nevertheless, the concept of EnV-S of linking process modeling, health and safety modeling, and economic modeling is very valuable. It is also currently implemented by the Applied Materials, Inc.

The computer software Tool for Environmental Analysis and Management (TEAM™) by Ecobilan alleviates the data requirement problem of LCA by providing 309 predefined data modules on industrial sectors such as transportation, energy, and aluminum [21]. Users can directly adopt these modules in modeling an life cycle analysis (LCA) rather than collecting the data in the field. Unfortunately, there is not yet a sector for semiconductor industry. The program itself does not support process or equipment modeling. Yet, it allows users to generate data from parameter-controlled simulations using customized control panels. To assess the uncertainty in data, Monte-Carlo simulations can be launched in TEAM™. Supported probability distributions are normal, lognormal, triangular, and Boolean distributions. TEAM™ does not have an expert system that can help the user with defining system boundary, or performing sensitivity analysis.

The S70 Mass and Energy Balance Model was another attempt in providing data for environmental evaluations [22] by SEMATECH besides CARRI™. It is a collection of 57 models of unit operations that are commonly used in semiconductor manufacturing. It functions as a spreadsheet calculator rather than a process-modeling environment. For example, users need to provide flow rates and process time to calculate the mass amount of materials used in the processes. Emissions are calculated by multiplying inlet flow rates with conversion factors, which can only be obtained through modeling outside the S70 or through measurements. It offers users a quick way to estimate the mass and energy balance of a process. Since it is static, uses averaged data, and does not consider in depth kinetics and transport processes, it cannot predict the mass and energy amount required for changes in process conditions.

None of the environmental evaluation methods described above was conceived to resolve the data availability and quality problems. The considerations of system boundary and uncertainty were not the focus of the methods either. However, system boundary and uncertainty are crucial to the conclusions of the evaluation and their confidence levels. Without considering them, the evaluation can be either incomplete, or too large to be manageable. The decision framework in this thesis was constructed to address these two issues in a systematic manner.

Table 2.1 Comparison of Existing Environmental Valuation Methods for the Semiconductor Industry

	CARRI	EnV-S	TEAM	S70
Impact Categories Considered	Work space safety and health, broad characterization of environmental toxicity, regulatory, COO	COO, human health (cancer, acute toxicity, etc), regulatory	More than 50 categories such as global warming effect, human toxicity, aquatic/terrestrial eco-toxicity	Mass and energy consumed, transformed, and discharged
Applications	Relative risk of chemical usage	Tool design, choosing between alternative tools	Quantifying environmental impacts of the operations associated with products, processes, and activities	Determine the overall material and energy usage and waste products generated by the unit operations
System Boundary	Fab, downstream	Upstream, fab, downstream	Upstream, fab, downstream	Fab
Inputs Based on Database or Model	Database	Process model	Based on user input, databases	Static, average process model
Site Specific	Yes	Yes	No	Yes
Impact Database Available	Yes	No	Yes	No
Inventory Database Available	Yes	Yes	Yes	Yes
Which Stage of a Production Cycle to Be Applied to	Process selection	Tool design, tool selection	ISO investigation, valuation of existing processes	Process design
Aim at ISO 14000 Compatibility	No	No	Yes	No
Linked to Cost	Yes	Yes	No	No
Include Uncertainty	Qualitative	Probability distributions, Monte Carlo simulation	User can set up limited probability distributions	No

2.2 Survey on Current Status and Needs of Semiconductor Industry for Environmental, Safety, and Health (ESH)

In order to better align our research with the needs and concerns of the semiconductor industry, a survey was carried out between January 2004 to May 2004 among various players in the industry.

2.2.1 Methodology

Firstly, we selected the organizations to be surveyed to spam the whole spectrum of the industry, including chip manufacturers, chemical suppliers, equipment manufacturers, and consortia. Key individuals in these organizations were identified. They are mostly ESH experts, some process, equipment, and chemical experts. Please see Appendix C for details and the questionnaires.

Secondly, we structured the interview topics to be as follow:

- Decision making process on product development
  - Time frame of development
  - Criteria in choosing chemicals and equipment
  - For tool suppliers: life time of tool, facilitization issues.
  - For chemical suppliers: knowledge on chemical handling in the fab
- ESH considerations in decision making
  - System boundary
  - Motivations
  - Roles of safety, worker health, and environment in decision making
  - Barriers
- Relationships among IC manufacturers, tool and chemical suppliers
  - Burden of providing chemical and emission information
  - Information sharing of chemicals
- Uncertainty and risk
  - How do you deal with missing or uncertain data in ESH evaluations
  - Value of information
  - Chemical property estimation tools: QSAR, group contribution method
- Assessment of existing ESH tools
  - CARRI®
  - Chemical Data Matrix
  - Cost Analysis Tool

2.2.2 Survey Results

- **Common Findings from All Companies**

Product Development

Most product development follows the time frame we presented. Performance is always the key issue. ESH enhancement cannot compromise performance. In order to achieve a certain technical performance, ESH issues can be engineered around.

Regulations and customer requirements (which are probably driven by regulations) are the biggest drivers for ESH considerations. However, it is hard to comply with different ESH requirements from different customers and regions.

ESH Evaluations

Companies all have chemical review and approval process. The system boundary for most of the companies is around the fab. The mindset for environmental protection is end-of-pipe type of downstream treatment. Most companies focused on one or a few aspects of the environmental impacts. For example, they would focus on reducing the global warming potential of the emissions from the processes, but would not usually consider whether other emissions or the resources needed to treat other emissions may increase.

ESH COO is often not separately calculated because it is considered small compared to equipment cost. One rule of thumb we heard is that, "ESH COO issues with a process only become important when the overall cost of abatement devices becomes equivalent to the cost of a new tool"

Due to the large data gap and uncertainty in data, there is a need for decision support at early chemical screening stage. There is limited awareness of the value of information and matching decision context with required data quality. Even with chemical data present, they sometimes still have a hard time in translating these data into decisions.

Most R&D personnel and process engineers of the tool suppliers and IC manufacturers have limited or little understanding on the ESH impacts of their designs. There is a need for transparent environmental evaluation process.

It is easier to incorporate ESH considerations during major technology inflections. We therefore need a system to (i) evaluate options to fix ESH issues and (ii) look for emerging ESH issues during major technology changes.

There is a need for understanding the requirement on facility, abatement, and safety in scale-up. Understanding facilitization problems and capacity issues and related costs associated with new processes, chemicals and equipment is the most pressing need for the industry. Quantifying the environmental impacts and uncertainties in the impacts of new and untested chemicals and processes is more forward looking.

- **Findings from IC Manufacturers and Tool Suppliers**

- IC manufacturers often rely on suggestions from suppliers on what chemicals to test in the fab.

- Their customers such as the electronics makers usually care more about the environmental impacts of using their products such as the microprocessors and less on how the products are manufactured. Therefore, there is little incentive for the IC manufacturers and tool suppliers to reduce the impacts of the manufacturing processes, while they do working on reducing the energy consumptions of their microprocessors and so on.
- Environmental issues with product content is an emerging environmental concern. At the same time, the burden of safety, emission qualification and abatement is largely on tool suppliers.

- **Common Findings from Chemical Suppliers**

The burden of understanding the ESH properties of chemicals is largely on chemical suppliers. The advantage of chemical suppliers in providing this knowledge is that they have a good understanding of safety control, worker protection, ESH properties of chemicals, such as toxicity.

There are also some difficulties facing chemical suppliers, such as understanding how chemicals are used in the fab; human exposures in the formulator, distributors, and the fab; how the chemicals are used, stored. These constrain the chemical suppliers from better providing safety control recommendations and estimating the COO of the processes/tools that use their chemicals.

We also found that if a chemical has already been used in other applications, it is much faster to introduce it to a new application. The most time consuming part in chemical development is to find the right chemical for a certain application.

The survey results were also summarized in Table 2.2 (adopted from [23]).

2.2.3 Areas for Contribution from Academia

Based on the survey results, it was decided that the academia can contribute to the following areas:

- Predictive screening of chemicals and processes (systematic process, dealing with uncertainty)
- Capacity and facilitization issues for equipment and IC manufacturers
- Product content and equipment product content
- Brief training on ESH for process engineers
- Methods for coping with missing, inaccurate or uncertain data
- Well-worked out case studies with clear steps of analysis

Table 2.2 Summary of Industrial Survey Results

	Broad Areas	Semiconductor Manufacturers	Chemical Suppliers	Equipment Suppliers	Specific Research Topics	Challenges
1	**New Chemicals**					
	Screening at Early Stages	**Yes** (Also, need to know and predict regulations)	**Maybe** (Have some resources to do this already)	**Maybe** (More concerned with emissions)	(i) QSAR+tox studies+Experts (ii) Predict and Track Regulations (iii) Decision Making	Confidentiality and Data Sharing
	EHS Impacts during Ramp Up and High Vol. Mfg.(HVM)	**Yes**	**Maybe** (Did not emphasize this)	**Yes** Concerned about emissions during HVM	(i) Filling data gaps (ii) Decision Making	Data Sharing
2	**Life-cycle issues**					
	Downstream Issues	**Yes**	**Yes** (Difficult since do not know how chemicals are used)	**Yes**	(i) Emissions measurements (ii) Modeling treatment systems	
	Product Content	**Yes** (Related to chip packaging)	**No**	**Maybe** (With content in equipment at end of life)		
	Upstream LCA	**Maybe** Are beginning to work on this	**Maybe** (Have resources in this area)	**Maybe** (Acknowledge that this is where the industry should be going)	(i) Data gaps (ii) Uncertainty (iii) Rate of change in the industry	Need this perspective to make good environmental decisions
3	**Equipment and Facility Infrastructure**					

	COO	**Maybe** Some use SEMATECH Model EHS COO sometimes considered too small	**Yes**	**Yes**	Std. model, integrating environmental components including facility infrastructure	
	Bulk Chemicals/Resources	**Maybe** (Some already know this well)	**Maybe**	**Yes**	Integrate tracking these, with process databases/manufacturing software?	
	Predict waste streams, capacity requirements with scale up to HVM	**Maybe** (Some already know this well)	**Yes** (Emissions and interactions)	**Yes**		
4	**Training**					
	EHS Assessment Training for Process Engineers	**Maybe** (Some companies teams work well together. SEMATECH developing module)	**Yes** (They already do this)	**Maybe** (Some companies already have some programs)	Developing training modules	Encouraging increased communication and cooperation between groups
5	**Case Studies**					
		Supercritical CO_2 (2)	Spin on Vs. CVD low k	**Look at past changes, eg: NF3 remote cleaning**		
		Copper CMP and copper waste	**POU F_2 generation**	Rank different etch chemistries		

		PFC	Cu CVD Vs. Cu Plating	Analyze materials that are banned		
		NF_3 vs. ClF_3 (3)	Biometrics (DNA on chip)	**Replacement solvents used with supercritical CO2**		
		NF_3 Vs. F_2 (including economies of scale)	SAR (focus on PBT)	PFOS		
		Focus on major transformations such as phase out of lead	Lithography or deposition w/ potential for multiple exposures	PFC Replacements		
		Generate Tech Tr. Documents		Projects at the Center		
6	**Other Recommendations**					
		EHS decision making 3-4 years before large technology inflection	Partner with trade associations	Facility Models to be developed: clean room air, inert gases, UPW, etc.		
		Look at emerging issues 6-8 years ahead		Track pyrophoric, HAPs, haz waste, etc. And routes of exposure through breath, skin, etc.		

Chapter 3 Uncertainty Analysis and Sensitivity Analysis

3.1 Introduction

Given the large uncertainties in system inputs described in the first chapter, methods that can correctly represent these uncertainties and understand their effects on the decision outcomes are needed. If the confidence that can be place in the analysis results is low, appropriate methods need to be use to identify the input factors that contribute the most to the uncertainties in the results. This chapter will briefly explain the concepts of uncertainty analysis and sensitivity analysis. Then it will concentrate on the latter. Let's first describe the system under study in the mathematical term.

The kind of systems that is studied in this work can be described in function

$$Y = g(\underline{x}, \underline{\theta}) \tag{3.1}$$

where Y – a random variable (r.v.) with a distribution of $f_Y(y)$. Its expected value is μ_y. Its standard deviation is σ_y;

$\underline{x} = x_1 \ldots x_n$, where x_i are deterministic variables, i = 1 … n ;

$\underline{\theta} = \theta_1 \ldots \theta_p$, where θ_i are r.v.s defined in K^p, i = 1 … p, with joint distribution $f_{\underline{\theta}}(\underline{\theta})$. Their expected values are $\underline{\mu}_{\underline{\theta}}$. Their standard deviations are $\underline{\sigma}_{\underline{\theta}}$. The covariance between θ_i and θ_j is $Cov(\theta_i, \theta_j)$.

Figure 3.1 illustrates the system in a two-dimensional case.

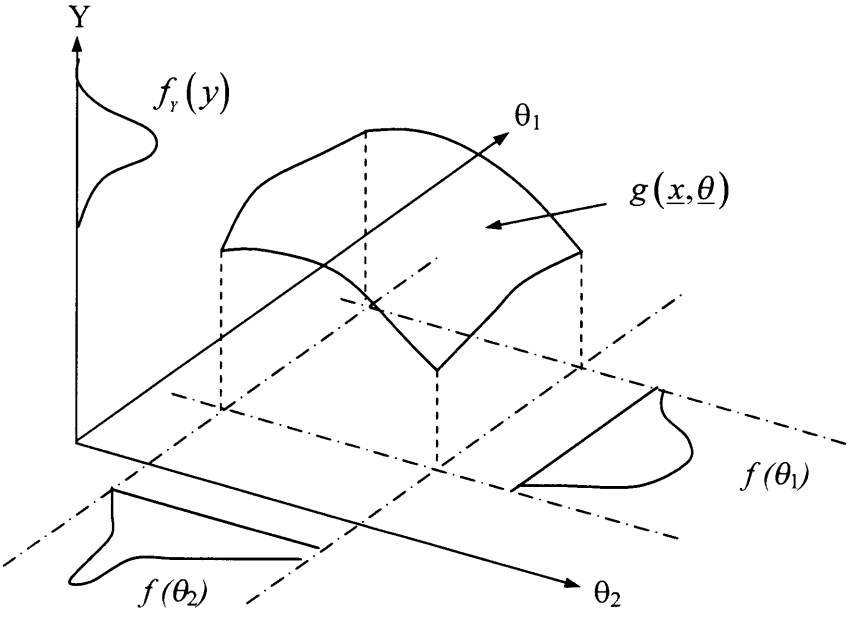

Figure 3.1 Random Variable Y as a Function of Random Variables θ_1 and θ_2

The goal here is to study the effect of $\underline{\theta}$ on Y. There are two branches of this problem: one focuses on the output uncertainty over the entire range of values of the input parameters; the other one focuses on the output value rather than its uncertainty. In the first branch, we are interested in obtaining the distribution of Y $f_Y(y)$, or the moments of Y. It is called uncertainty analysis. The second branch is called sensitivity analysis.

Uncertainty analysis aims at combining model response with parameter variability to better present reality. Both the inputs and outputs are expressed as probability distributions, which can present the full range of variation of the parameters. It studies the model response surface resulted from the collective uncertainties in all the uncertain parameters. With proper techniques it can consider the correlations among the uncertainties of the inputs. Figure 3.2 illustrates the basic idea of uncertainty analysis for a two-parameter system.

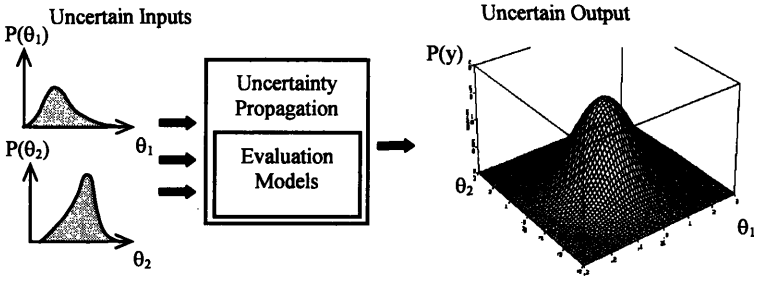

Figure 3.2 Illustration of Uncertainty Analysis. Uncertain inputs are represented by probability distribution functions. Uncertainty is then propagated through the evaluation models to generate probability distribution functions of outputs.

The primary task of uncertainty analysis is to obtain the probability density function $f_{y(\underline{\theta})}(y(\underline{\theta}))$ of the model response $y(\underline{\theta})$ given the joint prior PDF $f_{\underline{\theta}}(\underline{\theta})$. Another task is to obtain the moments of the outputs such as expected values:

$$E\{y(\underline{\theta})\} = \int_{-\infty}^{\infty} y(\underline{\theta}) f_{y(\underline{\theta})}(y(\underline{\theta})) dy(\underline{\theta}) \tag{3.2}$$

In this work, Monte Carlo simulations were used for these two tasks for Excel based models. The Monte Carlo method, or methods of statistical trials, refers to any method which solves a problem by generating suitable random numbers and observing that fraction of the numbers obeying some property or properties. The method is useful for obtaining numerical solutions to problems which are too complicated to solve analytically [24].

This method can be exemplified with a simple problem of finding the probability distribution of y = y(x), with x following a normal distribution. To solve this problem, Monte Carlo simulations generate a set of random numbers x_i, which all follow a normal distribution N(μ, σ). These numbers are then substituted into y = y(x) to compute the corresponding y_i. The probability distribution can be obtained from the values of y

generated in this manner. It can be seen intuitively that as the number of random numbers increases, the representation of the real distribution will become better and better. When the number approaches infinity, the collection of these random numbers eventually represents the normal distribution. The collection $\{y_1, y_2, \ldots, y_n, y_{n+1}, \ldots\}$ represents the reality.

To calculate the expect value of y, the Monte Carlo methods transform

$$\begin{aligned} E\{y(\theta)\} &= \int_{-\infty}^{\infty} y(\theta) f_{y(\theta)}(y(\theta)) dy(\theta) \\ &= \int \ldots \int y(\theta) f_{\theta}(\theta) \theta_1 \ldots d\theta_n \end{aligned} \tag{3.3}$$

into

$$E\{y(\theta)\} \approx \frac{1}{N} \sum_{i=1}^{N} y(\theta_1', \theta_2', \ldots \theta_n') \tag{3.4}$$

where N – number of sampling.

Practically the sampling of the random numbers cannot be infinite. Optimal sampling methods needs to be considered. The optimal sampling methods should be able to generate a sequence of random numbers that possesses the statistical properties of the random variable without too much computation time. This topic is covered in the study of random number generators [25-27].

Contrast to the uncertainty analysis, sensitivity analysis aims at attribute output responses to the individual parameters, either locally or globally. "Locally" means $g(\underline{\theta})$ at a certain point $\underline{\theta}^0$, i.e. $g(\underline{\theta}^0)$, or the change of output response y with $\underline{\theta}$, i.e. $\partial y / \partial \underline{\theta} \Big|_{\underline{\theta}^0}$. "Globally" means the function $g(\underline{\theta})$ or the average $\int_{\underline{\theta}} g(\underline{\theta}) d\underline{\theta}$. Both analyses are called sensitivity analysis. In this study, we focus on the latter. One goal of understanding the global effects is to reduce the variance in Y by reducing the variance in $\underline{\theta}$ given limited resources:

$$\begin{aligned} &\min \ \sigma_Y^2 \\ &\text{s.t.} \quad Y = g(\underline{x}, \underline{\theta}) \\ &\qquad \sum_{i}^{p} t(\sigma_{\theta_i}^2) = C \end{aligned} \tag{3.5}$$

where $t[\sigma_{\theta_i}^2]$ is the resources available to reduce the variance in θ_i;

C is the total resources available.

The procedure of solving this problem are in two steps: one is to identify important parameters that contribute the most to σ_y^2 ; the second step is to allocate resources to reduce the variance in these important parameters. This paper will only address the first part.

First we will review how to find the distribution of Y and its moments. To obtain $f_Y(y)$ from the function of $g(\underline{\theta})$ and $f_{\underline{\theta}}(\underline{\theta})$, we consider y as a given number [28].

Denote D_y the region in K^p such that $g(\underline{\theta}) \le y$. It is possible that this region is not connected. We have

$$\{Y \le y\} = \{g(\underline{\theta}) \le y\} = \{(\underline{\theta}) \in D_y\} \tag{3.6}$$

Therefore,

$$F_Y(y) = P\{Y \le y\} = P\{(\underline{\theta}) \in D_y\} = \int \cdots \int_{D_y} f_{\underline{\theta}}(\underline{\theta}) d\underline{\theta} \tag{3.7}$$

To determine $F_Y(y)$, it suffices to find the region D_Y for every y and to evaluate the above integral. The density of Y can be determined similarly. With ΔD_y denoting the region $y \le g(\underline{\theta}) \le y + dy$, we have

$$\{y \le g(\underline{\theta}) \le y + dy\} = \{\underline{\theta} \in \Delta D_y\}. \tag{3.8}$$

Hence

$$f_Y(y) dz = P\{y \le Y \le y + dy\} = \int_{D_y} g(\underline{\theta}) d\underline{\theta}. \tag{3.9}$$

The expected value of Y is evaluated as:

$$\begin{aligned} \mu_Y &= E[Y] = E[g(\underline{\theta})] = \int_g g(\underline{\theta}) f_Y(y) dg \\ &= \int_{\theta_1} \cdots \int_{\theta_p} g(\underline{\theta}) f_{\underline{\theta}}(\underline{\theta}) d\theta_1 \cdots d\theta_p \end{aligned} \tag{3.10}$$

The variance of Y is evaluated as:

$$\begin{aligned} \sigma_Y^2 &= \int_g (g(\underline{\theta}) - \mu_Y)^2 f_Y(y) dg \\ &= \int_{\theta_1} \cdots \int_{\theta_p} (g(\underline{\theta}) - \mu_Y)^2 f_{\underline{\theta}}(\underline{\theta}) d\theta_1 \cdots d\theta_p \end{aligned} \tag{3.11}$$

3.2 Methods of Identify Important Parameters for Output Variance

Many methods have been designed to identify important parameters. [29-32] give good accounts of them. There are two types of sensitivity analysis. One is to understand how the values of the outputs change with the inputs. Another type is to study how the variance or other measures of uncertainty of the outputs change with inputs. Much study and review have been done on the first type. Here only the second type is discussed. They are local sensitivity analysis, ANOVA, linear correlation coefficient, rank correlation coefficient, Fourier Amplitude Sensitivity Test (FAST), Deterministic Equivalent Modeling Method (DEMM), and Global Sensitivity Indices. Local sensitivity analysis and ANOVA were selected because they are the most basic and widely used in spite of many limitations. The correlation methods were selected for their ease to use. The last three methods were selected for their ability to deal with non-linear and non-monotonic systems and provide global sensitivity measures. They will be discussed in detail in the following sections. Numerical examples will be used to illustrate the use of them.

3.2.1 Local Sensitivity Analysis

Assumption: function $Y = g(\underline{x}, \underline{\theta})$ is sufficiently smooth near the point $(\eta_{\underline{\theta}})$.

The variance σ_y^2 of $Y = g(\underline{x}, \underline{\theta})$ can be estimated in terms of the mean, variance, and covariance matrix of $(\underline{\theta})$:

$$\sigma_y^2 \approx \sum_{i=1}^{p} \left(\left. \frac{\partial g}{\partial \theta_i} \right|_{\eta_{\underline{\theta}}} \right)^2 \sigma_{\theta_i}^2 + \sum_{i=1}^{p} \sum_{j=1, j \neq i}^{p} \left(\left. \frac{\partial g}{\partial \theta_i} \right|_{\eta_{\underline{\theta}}} \right) \left(\left. \frac{\partial g}{\partial \theta_j} \right|_{\eta_{\underline{\theta}}} \right) r_{ij} \sigma_{\theta_i} \sigma_{\theta_j} \qquad (3.12)$$

where the function $g(\underline{x}, \underline{\theta})$ and derivatives are evaluated at $\underline{\theta} = \eta_{\underline{\theta}}$.

If θ_js are independent, the contribution of θ_i is the $\left(\left. \frac{\partial g}{\partial \theta_i} \right|_{\eta_{\underline{\theta}}} \right)^2 \sigma_{\theta_i}^2$ term. If θ_js are correlated, the contribution of θ_i is the above term plus the terms that have θ_i. Having high correlation among the inputs means the input parameters are either redundant, or they are not the fundamental causes. The models should be improved in these cases.

Note that if the function and derivatives are not evaluated at $\underline{\theta} = \eta_{\underline{\theta}}$, the above equation is not valid. This means that the sensitivity analysis can only gives the variance information around the nominal point. This is a big limitation because if the distribution of $\underline{\theta}$ is wide, the sensitivity can well change as $\underline{\theta}$ moving away from the nominal point.

3.2.2 Analysis of Variance (ANOVA)

ANOVA is a method for determining whether there is a statistical association between an output and one or more inputs. It is based on linear regression. Therefore, it is only valid for linear cases if statistics are to be employed. In ANOVA, the variance of the output is decomposed into partial variances of increasing dimensionality. For computational experiments, the relevant ANOVA is with one observation per cell. This is because for computer models, one set of inputs will only generate one set of values of outputs, disregarding the computational error of the computer. Therefore, multi-observation per cell is meaningless in this context. Because we are interested in comparing the importance of several parameters, the simplest ANOVA for this purpose is the two-way layout with one observation per cell.

We will give the assumptions and the formula of ANOVA based on an example from [33]. Consider J workers running I machines. Each of the J workers is assigned to each of the I machines which he runs for one day. Let θ_{ij} be the daily output of the jth worker when running the ith machine and let e_{ij} be his "error." His actually daily output is then an r.v. Y_{ij} such that $Y_{ij} = \theta_{ij} + e_{ij}$. Assume that θ_{ij} equal to a certain quantity μ, the grand mean, plus a contribution α_i due to the ith machine, and called the ith row effect,

plus a contribution β_j due to the jth worker, and called the jth column effect. Assumptions made here and additional ones are listed below:

Assumptions:

- Inputs and outputs have linear relationship:

$$Y_{ij} = \mu + \alpha_i + \beta_j + e_{ij} \tag{3.13}$$

or

$$Y = X'\underline{\theta} + \underline{e} \text{ with n = IJ, p = I + J + 1,} \tag{3.14}$$

where $Y = (Y_{11},...,Y_{1J};Y_{21},...,Y_{2J};...;Y_{I1},...,Y_{IJ})'$,

$\theta = (\mu;\alpha_1,...,\alpha_I;\beta_1,...,\beta_J)'$,

$e = (e_{11},...,e_{1J};e_{21},...,e_{2J};...;e_{I1},...,e_{IJ})'$,

$\sum_{i=1}^{I}\alpha_i = \sum_{j=1}^{J}\beta_j = 0$,

$$X' = \begin{bmatrix}
1 & 1 & 0 & 0 & \cdots & 0 & 1 & 0 & 0 & \cdots & 0 \\
1 & 1 & 0 & 0 & \cdots & 0 & 0 & 1 & 0 & \cdots & 0 \\
\vdots & & & & & & & & & & \\
1 & 1 & 0 & 0 & \cdots & 0 & 0 & 0 & 0 & \cdots & 1 \\
1 & 0 & 1 & 0 & \cdots & 0 & 1 & 0 & 0 & \cdots & 0 \\
1 & 0 & 1 & 0 & \cdots & 0 & 0 & 1 & 0 & \cdots & 0 \\
\vdots & & & & & & & & & & \\
1 & 0 & 1 & 0 & \cdots & 0 & 0 & 0 & 0 & \cdots & 1 \\
\vdots & & & & & & & & & & \\
\vdots & & & & & & & & & & \\
\vdots & & & & & & & & & & \\
1 & 0 & 0 & 0 & \cdots & 0 & 1 & 1 & 0 & \cdots & 0 \\
1 & 0 & 0 & 0 & \cdots & 0 & 1 & 0 & 1 & \cdots & 0 \\
\vdots & & & & & & & & & & \\
1 & 0 & 0 & 0 & \cdots & 0 & 1 & 0 & 0 & \cdots & 1
\end{bmatrix}$$

(I columns; J rows per block; J blocks)

This is a generalization of Equation (3.1) with multiple outputs.

- System satisfies the Gauss-Markov Conditions:

$$E(\mathbf{e}) = \mathbf{0},$$
$$E(\mathbf{ee'}) = \sigma^2 I.$$

Also, e_{ij} are independent.

- Therefore, Outputs are normally distributed.

Definition:

$$\bar{Y}_{..} = \frac{1}{IJ}\sum_{i=1}^{I}\sum_{j=1}^{J}Y_{ij} \tag{3.15}$$

$$Y_{\cdot j} = \frac{1}{I}\sum_{i=1}^{I} Y_{ij} \tag{3.16}$$

$$Y_{i\cdot} = \frac{1}{J}\sum_{j=1}^{J} Y_{ij} \tag{3.17}$$

We denote $S(Y,\underline{\theta})$ as S_C, where

$$S(Y,\underline{\theta}) = \left\|Y - \underline{\mu}_Y\right\|^2 = \sum_{i=1}^{I}\sum_{j=1}^{J}\left(Y_{ij} - \mu - \alpha_i - \beta_j\right)^2 .$$

The least square estimator (LSE) of μ, α_i, and β_i are obtained from taking the derivative of $S(Y,\underline{\theta})$ to μ, α_i, and β_i respectively, and set them to zero:

$$\frac{\partial S(Y,\underline{\theta})}{\partial \mu} = 0, \qquad \frac{\partial S(Y,\underline{\theta})}{\partial \alpha_i} = 0, \qquad \frac{\partial S(Y,\underline{\theta})}{\partial \beta_j} = 0.$$

$\rightarrow \hat{\mu} = Y_{\cdot\cdot}$; $\quad \hat{\alpha}_i = Y_{i\cdot} - Y_{\cdot\cdot}$, $i = 1,\ldots,I$; $\quad \hat{\beta}_j = Y_{\cdot j} - Y_{\cdot\cdot}$, $j = 1,\ldots,J$.

Hence,

$$S_C = \sum_{i=1}^{I}\sum_{j=1}^{J}\left(Y_{ij} - Y_{i\cdot} - Y_{\cdot j} + Y_{\cdot\cdot}\right)^2 . \tag{3.18}$$

Now we can turn to the testing hypotheses problems. We have $E[Y] = \underline{\mu}_Y = X'\underline{\theta} = X'(\mu;\alpha_1,\ldots,\alpha_I;\beta_1,\ldots,\beta_J)' \in V_r$, where r is the rank of X' = I + J − 1. Therefore

$$\mu_{Yj} = \sum_{i=1}^{I} x_{ij}\theta_i, \quad j = 1,\ldots,J .$$

Consider the hypothesis

$$H_A: \alpha_1 = \ldots = \alpha_I = 0,$$

which means that the factor corresponding to the row effect has no influence on the outcome. Under H_A, $\underline{\mu}_Y \in V_{r-q}$, where $r - q_A = J$, so that $q_A = I - 1$.

Under H_A again, $S(Y,\underline{\theta})$ becomes

$$S_{C_A} = \sum_{i=1}^{I}\sum_{j=1}^{J}\left(Y_{ij} - Y_{\cdot j}\right)^2 . \tag{3.19}$$

Now S_C can be rewritten as

$$\begin{aligned} S_C = SS_e &= \sum_{i=1}^{I}\sum_{j=1}^{J}\left[\left(Y_{ij} - Y_{\cdot j}\right) - \left(Y_{i\cdot} - Y_{\cdot\cdot}\right)\right]^2 \\ &= \sum_{i=1}^{I}\sum_{j=1}^{J}\left(Y_{ij} - Y_{\cdot j}\right)^2 - J\sum_{i=1}^{I}\left(Y_{i\cdot} - Y_{\cdot\cdot}\right)^2 \end{aligned} \tag{3.20}$$

Therefore

$$S_{C_A} - S_C = SS_A, \quad \text{where } SS_A = J\sum_{i=1}^{I}\hat{\alpha}_i^2 = J\sum_{i=1}^{I}Y_{i\cdot}^2 - IJY_{\cdot\cdot}^2 . \tag{3.21}$$

It follows that for testing H_A, the $\mathcal{F}$ statistic, to be denoted by $\mathcal{F}_A$, is given by

$$\mathcal{F}_A = \frac{(I-1)(J-1)}{I-1}\frac{SS_A}{SS_e} . \tag{3.22}$$

Similar for testing the hypothesis

$$H_B: \beta_1 = \ldots = \beta_j = 0,$$

we have

$$SS_B = S_{c_B} - S_C = I\sum_{i=1}^{I}\hat{\beta}_i^2 = I\sum_{j=1}^{J}Y_{\cdot j}^2 - IJY_{\cdot\cdot}^2, \tag{3.23}$$

and

$$\mathcal{F}_B = \frac{(I-1)(J-1)}{I-1}\frac{SS_B}{SS_e} \tag{3.24}$$

SS_A and SS_B are known as sums of squares of row effects and column effects.

Finally, we set

$$SS_T = \sum_{i=1}^{I}\sum_{j=1}^{J}\left(Y_{ij} - Y_{\cdot\cdot}\right)^2 = \sum_{i=1}^{I}\sum_{j=1}^{J}Y_{ij}^2 - IJY_{\cdot\cdot}^2. \tag{3.25}$$

It can be derived that

$$SS_T = SS_A + SS_B + SS_e. \tag{3.26}$$

The LSE of σ^2 is

$$\hat{\sigma}^2 = MS_e = \frac{SS_e}{(I-1)(J-1)} \tag{3.27}$$

Hence, SS_T is decomposed into SS_A, SS_B, and the residual term SS_e. SS_T can be seen as the variance of sample Y_{ij}. If SS_A is larger than SS_B, then the row factor has stronger effect on the variance of Y_{ij}, and vice versa. It is to note that since we only take one sample from each combination of (α_i, β_j), the SS_e can either be interpreted as residual sum of squares, or if strong interaction is assumed between the two factors, the interaction term SS_{AB}. Unless multiple samples are taken for each cell, SS_e and SS_{AB} term cannot co-exist.

When there are more than 2 factors, we can also generalize the above derivation in a successive manner. First, let's define some terms. Assume there are p factors. Each factor is denoted as $\theta_{i_k}^{(l)}$ where k = 1, ..., p; l = 1, ..., I_p. I_p is the number of sampling points for each factor. The grand average of Y is:

$$Y_g = \frac{1}{\prod_{i=1}^{p} I_i}\underbrace{\sum_{i_1=1}^{I_1}\cdots\sum_{i_p=1}^{I_p}\left(Y_{i_1\ldots i_p}\right)}_{p-1, I_p \neq I_k} \tag{3.28}$$

The average over all the factors except for θ_{i_k} is:

$$Y_{i_k\cdot\cdot} = \frac{1}{\prod_{i=1, i\neq k}^{p} I_i}\underbrace{\sum_{i_1=1}^{I_1}\cdots\sum_{i_p=1}^{I_p}\left(Y_{i_1\ldots i_p}\right)}_{p-1, I_p \neq I_k} \tag{3.29}$$

The average of all factors except for θ_{i_k}, ($k \in \Omega$), is:

$$Y_{i_k, k\in\Omega\cdot\cdot} = \frac{1}{\prod_{i=1, i\notin\Omega}^{p} I_i}\underbrace{\sum_{i_1=1}^{I_1}\cdots\sum_{i_p=1}^{I_p}\left(Y_{i_1\ldots i_p}\right)}_{p-m, (i_k, k\notin\Omega)} \tag{3.30}$$

where Ω is a set of integrals ranging from 1 to p, the number of integral in Ω is m. The content in the parentheses mean the summation of $Y_{i_1 \cdots i_p}$ are only over the factors θ_{i_k} which are not in Ω.

The decomposition of $Y_{i_1 \cdots i_p} - Y_g$ for one factor is just $Y_{i_1} - Y_g \equiv M_{i_1}$. For two factors, it is

$$Y_{i_1 i_2} - Y_g = \sum_{k=1}^{2} M_{i_k} + M_{i_1 i_2}. \tag{3.31}$$

Therefore,

$$M_{i_1 i_2} = Y_{i_1 i_2} - Y_g - \sum_{k=1}^{2} M_{i_k} = Y_{i_1 i_2} - Y_{i_1 \cdot} - Y_{i_2 \cdot} + Y_g. \tag{3.32}$$

For three factors, the decomposition is

$$Y_{i_1 i_2 i_3} - Y_g = \sum_{k=1}^{3} M_{i_k} + \sum_{k=1,3>j>k}^{3} M_{i_k i_j} + M_{i_1 i_2 i_3} \tag{3.33}$$

where the combination of i_k and i_j in $\sum_{k=1,3>j>k}^{3} M_{i_k i_j}$ are $i_1 i_2$, $i_1 i_3$, and $i_2 i_3$.

$$\begin{aligned} M_{i_1 i_2 i_3} &= Y_{i_1 i_2 i_3} - Y_g - \sum_{k=1}^{3} M_{i_k} - \sum_{k=1,3>j>k}^{3} M_{i_k i_j} \\ &= Y_{i_1 i_2 i_3} - Y_{i_1 i_2 \cdot} - Y_{i_1 i_3 \cdot} - Y_{i_2 i_3 \cdot} + Y_{i_1 \cdot} + Y_{i_2 \cdot} + Y_{i_3 \cdot} - Y_g \end{aligned} \tag{3.34}$$

The main effect of individual factor θ_{i_k} is

$$\prod_{j=1, j \neq i_k}^{p} I_j \sum_{i_k=1}^{I_k} M_{i_k}^{\ 2} = \prod_{j=1, j \neq i_k}^{p} I_j \sum_{i_k=1}^{I_k} \left(Y_{i_k \cdot \cdot} - Y_g \right)^2 \tag{3.35}$$

The contribution of a 2-factor interaction term $\theta_{i_k} \theta_{i_l}$ is

$$\prod_{j=1, j \neq i_k, i_l}^{p} I_j \sum_{i_k=1}^{I_k} \sum_{i_l=1}^{I_l} M_{i_k i_l} = \prod_{j=1, j \neq i_k, i_l}^{p} I_j \sum_{i_k=1}^{I_k} \sum_{i_l=1}^{I_l} \left(Y_{i_k i_l} - Y_{i_k \cdot} - Y_{i_l \cdot} + Y_g \right)^2 \sum_{i=1}^{n} X_i \tag{3.36}$$

The contribution of a 3-factor interaction term $\theta_{i_k} \theta_{i_l} \theta_{i_q}$ is

$$\begin{aligned} &\prod_{j=1, j \neq i_k, i_l, i_q}^{p} I_j \sum_{i_k=1}^{I_k} \sum_{i_l=1}^{I_l} \sum_{i_q=1}^{I_q} M_{i_k i_l} \\ &= \prod_{j=1, j \neq i_k, i_l, i_q}^{p} I_j \sum_{i_k=1}^{I_k} \sum_{i_l=1}^{I_l} \sum_{i_q=1}^{I_q} \left(Y_{i_1 i_2 i_3} - Y_{i_1 i_2 \cdot} - Y_{i_1 i_3 \cdot} - Y_{i_2 i_3 \cdot} + Y_{i_1 \cdot} + Y_{i_2 \cdot} + Y_{i_3 \cdot} - Y_g \right)^2 \end{aligned} \tag{3.37}$$

For more than 3 factors cases, the decomposition and the contributions can be obtained in this successive manner.

3.2.3 Linear Correlation Coefficient (LCC)

Assumption: in order to use LCC to correctly analyze the contribution of a factor to the variance of the output, the system needs to be linear.

LCC between θ and Y is defined as:

$$\rho_{\theta,Y} = E\left[\left(\frac{\theta-\mu_\theta}{\sigma_\theta}\right)\left(\frac{\theta-\mu_Y}{\sigma_Y}\right)\right] \tag{3.38}$$

From the Cauchy-Schwarz inequality, $\rho^2 \le 1$: that is $-1 \le \rho \le 1$, and ρ = 1 if and only if

$$Y = \mu_Y + \frac{\sigma_Y}{\sigma_\theta}(\theta-\mu_\theta) \tag{3.39}$$

with probability 1, and ρ = –1 if and only if

$$Y = \mu_Y - \frac{\sigma_Y}{\sigma_\theta}(\theta-\mu_\theta) \tag{3.40}$$

with probability 1. Therefore $\rho = \pm 1$ means X and Y are linearly related. ρ = 1 means the correlation is positive, ρ = –1 means the correlation is negative. If ρ = 0, X and Y are uncorrelated. Therefore, ρ is a measure of linear dependence between X and Y.

A correlation coefficient also shows the contribution of input parameters to the variance of the output in a linear model shown as below:

$$Y = \sum_i^p x_i\theta_i \tag{3.41}$$

The derivation is as follow:

$$\rho_{\theta_i,Y} = \frac{E\left[(\theta_i-\mu_{\theta_i})(Y-\mu_Y)\right]}{\sigma_{\theta_i}\sigma_Y} = \frac{E[\theta_i Y]-\mu_{\theta_i}\mu_Y}{\sigma_{\theta_i}\sigma_Y} \tag{3.42}$$

$$= \frac{E\left[\sum_{j\neq i} x_j\theta_j\theta_i + x_i\theta_i^2\right] - \mu_{\theta_i}\sum_j x_j\mu_{\theta_j}}{\sigma_{\theta_i}\sigma_Y}$$

$$\because\ Cov(\theta_i,\theta_j) = E[\theta_i\theta_j] - \mu_{\theta_i}\mu_{\theta_j} \tag{3.43}$$

$$\therefore\ \rho_{\theta_i,Y} = \frac{\sum_{j\neq i} x_j\left[Cov(\theta_i,\theta_j)+\mu_{\theta_j}\mu_{\theta_i}\right] + x_i\left(\sigma_{\theta_i}^2+\mu_{\theta_i}^2\right) - x_i\mu_{\theta_i}^2 - \sum_{j\neq i} x_j\mu_{\theta_j}\mu_{\theta_i}}{\sigma_{\theta_i}\sigma_Y} \tag{3.44}$$

$$= \frac{\sum_j x_j Cov(\theta_i,\theta_j) + x_i\sigma_{\theta_i}^2}{\sigma_{\theta_i}\sigma_Y}$$

$$\therefore \rho_{\theta_i,Y} = \frac{x_i\sigma_{\theta_i} + \sum_j x_j\frac{Cov(\theta_i,\theta_j)}{\sigma_{\theta_i}}}{\sigma_Y} \tag{3.45}$$

The numerator in Equation (3.45) has two terms: the first term is the contribution of θ_i alone to the standard deviation of Y; the second term is the contribution of θ_i along with other θ_js. Therefore, the correlation coefficient is the ratio of the contribution of these two terms to the standard deviation of Y. It is to note that the summation of $\rho_{\theta_i,Y}$

does not equal to 1. This is because the covariance terms are double counted in the summation.

For non-linear systems, a correlation coefficient cannot correctly capture the contribution of inputs to the variance of outputs, since it only detects the linear relationship. Nonparametric correlations are often used as an improvement of the LCC.

3.2.4 Nonparametric Correlations

We will show that there are several other important nonparametric measures that are related to spearman and how it is related to the variates.

Nonparametric statistics uses the rank of the samples of the variates rather than the value of the samples [34]. For a continuous population, rank can be established by the following manner. Suppose we draw two members x_i and x_j at random from a continuous population. We can ignore the probability that $x_i = x_j$. In testing the trend or independence between two variables Y and X, we can see these variables as two characteristics of a subject. Rank the sample values of the characteristics as R_i and S_i, respectively. An important rank measure Spearman's rank correlation coefficient (RCC) is defined as:

$$r_s = \frac{\sum(R_i - \bar{R})(S_i - \bar{S})}{\sqrt{\sum(R_i - \bar{R})^2 (S_i - \bar{S})^2}} \tag{3.46}$$

where $\bar{R} = \sum R_i / N$ and $\bar{S} = \sum S_i / N$. It is viewed as an approximate of the LCC and also related to other important rank measures, one of which is the statistic D.

D is defined as

$$D = \sum_{i=1}^{n}(T_i - i)^2 = \sum_{i=1}^{n}(S_i - R_i)^2 \tag{3.47}$$

where T_i – ranking of R_i if $S_1 = 1, \ldots, S_N = N$.
D is a measure of the trend between Y and X: the larger the D is, the stronger the downward trend is; the smaller the D is, the stronger the upward trend. The statistic D is an intuitively reasonable test statistic since if there is a upward trend between S_i and R_i, we will expect to see larger R_i associated with larger S_i. Therefore the difference $(S_i - R_i)^2$ should be small.

Expansion of Equation (3.47) shows that

$$D = \Sigma T_i^2 - 2\Sigma i T_i + \Sigma i^2$$

Since $(T_1, \ldots T_N)$ is a rearrangement of the integers $(1, \ldots, N)$, it follows that $\Sigma T_i^2 = \Sigma i^2$. So

$$D = \tfrac{1}{3}N(N+1)(2N+1) - 2\sum iT_i \tag{3.48}$$

It can easily be seen that $\bar{R} = \bar{S} = \tfrac{1}{2}(N+1)$ and

$$\sum(R_i - \bar{R})^2 = \sum(S_i - \bar{S})^2 = (N^3 - N)/12$$

Since the numerator of r_s is equal to

$$\sum R_i S_i - \bar{S}\sum R_i - \bar{R}\sum S_i + N\bar{R}\bar{S} = \sum R_i S_i - N\bar{R}\bar{S} = \sum iT_i - \tfrac{1}{4}N(N+1)^2$$

It follows that

$$r_s = 1 - \frac{6D}{N^3 - N}$$

Thus, r_s is an equivalent test statistic to D, with large values of r_s significant against the independence hypothesis.

RCC has many advantages. Its statistics is independent of the distribution of the original function because the distribution of the rank is known to be uniform. It also alleviates the influence of outliers and measurement errors since regardless how far out the outliers or the errors are, their ranks will only increase by a finite integer. The actual effect of a RCC is that it emphasizes the importance of first order effect on the expense of higher order terms [32, 35, 36]. Because the rank transformation modifies the model under analysis, its conclusion is more qualitative in terms of the relative weight of the parameters. This can also be seen in the first example of Section 3.3.2.

3.2.5 Fourier Amplitude Sensitivity Test (FAST)

The basic idea behind FAST is that rather than evaluating the multiple integration in Equation (3.10) and (3.11), a single variable search curve is used to cover the multidimensional space of the input factors in FAST, therefore only one integration needs to be evaluated. This method was established by Cukier et al [37-40] and later on advanced by McRae et al [41, 42]. This is achieved by the following transformation:

$$\theta_l = F_l(\sin \omega_l s), \quad l = 1,2,...,p \tag{3.49}$$

where F_i, i = 1, 2, ..., p, are a set of known functions;

ω_i, i = 1, 2, ..., p, are a set of frequencies;

s is a scalar variable.

This transformation permits all the parameters to be varied simultaneously by varying s. The rapidity of the variation is determined by the forms of F_i. By variation of s over the range of $-\infty \le s \le \infty$, Equation (3.49) traces out a space-filling curve in the p-dimensional space. Based on Weyl's [43] proof that one can equate the p - space integral with the s-space integral with proper choice of F_i, Equation (3.10) becomes

$$\mu_r = \lim_{T\to\infty} \frac{1}{2T} \int_{-T}^{T} g\left(\underline{x}, \underline{\theta}(s)\right) ds \,. \tag{3.50}$$

The set of frequencies $\{\omega_i\}$ should be incommensurate, meaning

$$\sum_{i=1}^{p} \gamma_i \omega_i = 0 \tag{3.51}$$

for any integer set $\{\gamma_i\}$ if and only if $\gamma_i = 0$, i = 1, 2, ..., p, in order for Equation (3.49) to be truly space-filling, i.e. it passes arbitrarily close to any point in the p-dimensional parameter space of K^p. Unfortunately, in practice, $\{\omega_i\}$ cannot be incommensurate, but rather is selected as an appropriate set of integer frequencies. This implies that parameters θ_i, i = 1, 2, ..., p, are periodic in s on the interval $(-\pi, \pi)$. Equation (3.50) then becomes

$$\mu_Y = \frac{1}{2\pi}\int_{-\pi}^{\pi} g\left(\underline{x},\underline{\theta}(s)\right)ds \,. \tag{3.52}$$

The variance of Y becomes

$$\sigma_Y^2 = \frac{1}{2\pi}\int_{-\pi}^{\pi} g^2\left(\underline{x},\underline{\theta}(s)\right)ds - \mu_Y^2 \tag{3.53}$$

Examples of search curves with $\{\omega_i\} = \{5, 11\}$ and $\{\omega_i\} = \{19, 23\}$ are shown in Figure 3.3 and Figure 3.4.

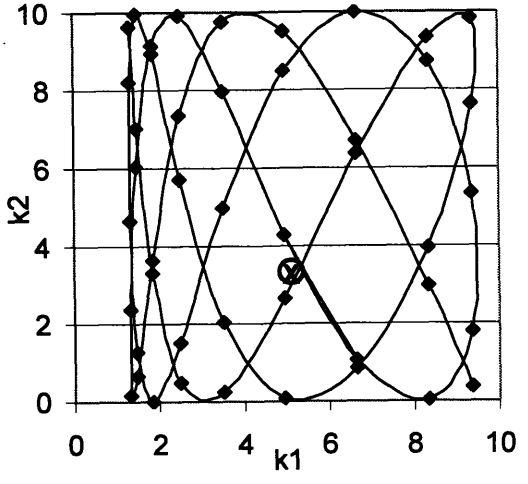

Figure 3.3 Space-Filling Search Curve for {ωi} = {5, 11} where $k_1 = 3.5\exp(\sin 5s)$ and $k_2 = 5(1+\sin 11s)$. Solid dots are the sampling points. ⊗ is the mean point.

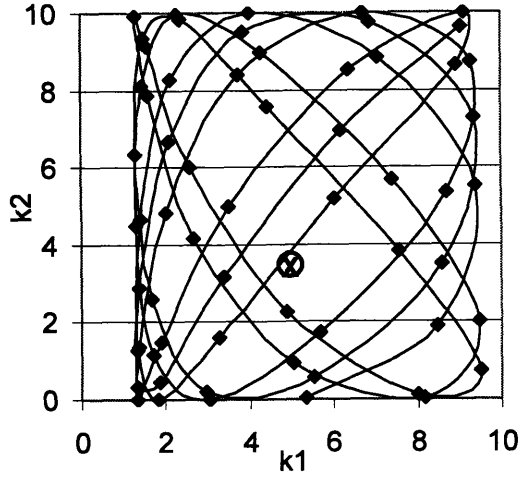

Figure 3.4 Space-Filling Search Curve for $\{\omega_i\} = \{19, 23\}$ where $k_1 = 3.5\exp(\sin 23s)$ and $k_2 = 5(1+\sin 23s)$. Solid dots are the sampling points. ⊗ is the mean point.

To know the contribution to the variance of Y by each individual factor, we can expand Y into a Fourier series:

$$Y = \sum_{i=-\infty}^{\infty} \left[A_i(\underline{x}) \cos is + B_i(\underline{x}) \sin is \right]. \tag{3.54}$$

where

$$A_i(\underline{x}) = \frac{1}{2\pi} \int_{-\pi}^{\pi} Y(\underline{x}, s) \cos is \, ds \tag{3.55}$$

$$B_i(\underline{x}) = \frac{1}{2\pi} \int_{-\pi}^{\pi} Y(\underline{x}, s) \sin is \, ds \tag{3.56}$$

Please note that this definition is slightly different from the conventional definition in terms of *i*'s range. From Parseval's theorem we have

$$\overline{Y^2} = \frac{1}{2\pi} \int_{-\pi}^{\pi} g^2(\underline{x}, s) \, ds = \sum_{i=-\infty}^{\infty} \left\{ A_i^2(\underline{x}) + B_i^2(\underline{x}) \right\}. \tag{3.57}$$

Also

$$\mu_Y^2 = A_0^2 \tag{3.58}$$

From Equation (3.53) to (3.58), we can have

$$\sigma_Y^2 = 2 \sum_{i=1}^{\infty} \left\{ A_i^2(\underline{x}) + B_i^2(\underline{x}) \right\} \tag{3.59}$$

If the Fourier coefficients are evaluated for the fundamental frequencies of the transformation (3.49) and its harmonics, i.e. i = pω$_l$, p = 1, 2, ..., the variance

$$\sigma_{\omega_l}^2 = 2 \sum_{p=1}^{\infty} \left\{ A_{p\omega_l}^2(\underline{x}) + B_{p\omega_l}^2(\underline{x}) \right\} \tag{3.60}$$

is the part of the total variance that arises from the uncertainty in the *l*th parameter. The ratio $S_{\omega_l} = \sigma_{\omega_l}^2 / \sigma_Y^2$ is the partial variance. Since it is a normalized sensitivity measure, we can use it to rank the importance of the contributions of parameters to the output uncertainty.

Since $\sigma_{\omega_l}^2$ involves only the fundamental and all harmonics of the *l*th frequency ω$_l$ while σ^2 consists of all the integer frequencies, it is readily seen that $\sum_l S_{\omega_l} \neq 1$. We can decompose σ^2 to illustrate what other components σ^2 is made of. First, we expand Y in another form of multiple Fourier series:

$$Y = \sum_{r_1} \sum_{r_2} \cdots \sum_{r_n} c_{r_1 r_2 \ldots r_n} \exp\left[-i \left(\psi_1 r_1 + \psi_2 r_2 + \cdots + \psi_n r_n \right) \right] \qquad -\infty < r_i < \infty. \tag{3.61}$$

where ψ$_l$ = ω$_l$s. Using Parseval's theorem again to expand the variance σ^2 yields [40]

$$\sigma^2 = \sum_{p_1=1}^{\infty} \sum_{p_2=1}^{\infty} \cdots \sum_{p_n=1}^{\infty} \left| c(p_1, p_2, \ldots, p_n) \right|^2. \tag{3.62}$$

If we rearrange the sum into groups of increasing dimensionality, we have

$$\sigma_i^2 = \sum_{p_i=1}^{\infty} \left| c(0, \ldots, p_i, \ldots, 0) \right|^2, \tag{3.63}$$

$$\sigma_{ij}^2 = \sum_{p_i=1}^{\infty} \sum_{p_j=1}^{\infty} \left| c(0, \ldots, p_i, \ldots, p_j, \ldots, 0) \right|^2, \tag{3.64}$$

$$\sigma_{ijk}^2 = \sum_{p_i=1}^{\infty}\sum_{p_j=1}^{\infty}\sum_{p_k=1}^{\infty}\left|c(0,\ldots,p_i,\ldots,p_j,\ldots,p_k,\ldots,0)\right|^2, \tag{3.65}$$

etc., so that

$$\sigma^2 = \sum_{i=1}^{n}\sigma_i^2 + \sum_{i=2}^{n}\sum_{j=1}^{i-1}\sigma_{ij}^2 + \sum_{i=3}^{n}\sum_{j=2}^{i-1}\sum_{k=1}^{j-1}\sigma_{ijk}^2 + \cdots. \tag{3.66}$$

The first term in Equation (3.66) represents the contributions of the parameters individually to the total variance, averaged over the uncertainties in all other parameters. Similarly, the second term can be viewed as the part of the variance arising from the interaction between two parameters; the third term as the interaction among three parameters, and so on. The second term σ_{ij}^2 can be calculated as integrating Y over all but the two parameter θ_i and θ_j. This kind of decomposition is going to be used again in another method called Global Sensitivity Index, which will be described in a later section.

The definition in Equation (3.49) naturally gives rise to the idea of exploiting the symmetric properties of the search curve to reduce the number of evaluations in Equation (3.55) and (3.56). If we choose only the frequencies to be only odd integrals, the functions $\theta_i = F_i(\sin\omega_i s)$, $l = 1,2,\ldots,p$ become symmetric about $\pm\pi/2$. We can simplify Equation (3.55) and (3.56) to

$$A_i(\underline{x}) = \begin{cases} 0, & i \text{ odd} \\ \frac{1}{\pi}\int_0^{\pi/2}\left[g(\underline{x},s) + g(\underline{x},-s)\right]\cos is\,ds, & i \text{ even} \end{cases} \tag{3.67}$$

Similarly,

$$B_i(\underline{x}) = \begin{cases} 0, & i \text{ even} \\ \frac{1}{\pi}\int_0^{\pi/2}\left[g(\underline{x},s) - g(\underline{x},-s)\right]\sin is\,ds, & i \text{ odd} \end{cases} \tag{3.68}$$

With the symmetry properties, we are able to reduce the required number of evaluations of Y by half.

In order to calculate the Fourier coefficients from Equation (3.55) and (3.56), we need to know a few things: (1) the form of $F_i(\sin\omega_i s)$, (2) the points on which Y will be evaluated, (3) the number of the harmonics to be included, and (4) the choices of frequencies ω. We will discuss each of them in turn.

The shape of the search curve is going to be determined by the transformation function $F_i(t)$. If the parameters are independent, their joint probability is the product of the probabilities of each parameter:

$$P(k_1,k_2,\ldots,k_p) = P_1(k_1)P_2(k_2)\cdots P_p(k_p). \tag{3.69}$$

In this case, it can be shown that $F_i(\sin\omega_i s)$ needs to satisfy the following relationship [37, 43]:

$$\pi\left(1-t^2\right)^{1/2} P_l\left(F_l\right)\frac{dF_l(t)}{dt}=1 \tag{3.70}$$

with the initial conditions $F_l(0) = 0$. A tabulation of four search curves functions can be found in [41]. These search curve functions differ in how much variation the function can give. Based on the uncertainty in the parameters, appropriate functions can be used accordingly.

The number of points at which the system must be evaluated can be derived from Nyquist criterion [40, 42, 44], which states that a signal must be sampled at least twice as much as the frequency of the signal in order to be able to fully reconstruct:

$$N_s \geq N\omega_{\max}+1. \tag{3.71}$$

where N_s – the number of solution points

N – an imposed even integer.

If we take N_s to be $2q + 1$ with q integer, and space s evenly between $-\pi/2$ and $\pi/2$, the points on which Equation (3.67) and (3.68) need to be evaluated are

$$s_l=\frac{\pi}{N_s}\left(\frac{2l-N_s-1}{2}\right), \quad l=1,2,...,N_s. \tag{3.72}$$

As N increases, the integrals are going to be more accurate while the computational cost will increase as well. The practitioner can choose which N to use based on the required accuracy and his/her computation power.

Since integer frequencies are used, we face the problem of interference among frequencies. There are two kinds of interferences that can happen: one happens to both the fundamental frequencies and their multiples. The other one happens when the number of Fourier coefficients N used in the summation (3.75) is greater than or equal to $\omega_{\min}$ [41]. In general, interference happens between ω_i and ω_j when

$$a\omega_i = b\omega_j\left[\mathrm{Mod}\left(N\omega_{\max}+1\right)\right] \tag{3.73}$$

where a and b are integers. To avoid the first kind of interference, we can set

$$a\omega_i \leq N\omega_{\max}+1. \tag{3.74}$$

The natural choice of a is then N. The sensitivity measure then becomes

$$S_{\omega_i}=\frac{2}{\sigma^2}\sum_{p=1}^{N}\left(A_{p\omega_i}^2+B_{p\omega_i}^2\right) \tag{3.75}$$

To avoid the second kind of interference, we can set the N to be smaller than $\omega_{\min}$ [41]. If the system is not highly non-linear and close to monotonic, we take it to be the lowest required value, which is $N = 2$. This is generally sufficient because the higher order terms in the Fourier series tend to decrease rapidly unless the system is highly non-linear or non-monotonic. More on this will be discussed at the end of this section. Now we can simplify Equation (3.75) even further. Because $B_{2\omega_i}=0$ from Equation (3.68), we have

$$S_{\omega_i}=\frac{2}{\sigma_i^2}\left(B_{1\omega_i}^2+A_{2\omega_i}^2\right) \tag{3.76}$$

To avoid the interference problem, the choice of the frequency set needs to be very careful. For example, if $\omega_1 + \omega_2 = \omega_3$, then A_{ω_3} is identical with $A_{(\omega_1+\omega_2)}$ which reflect

not only the effect of the uncertainty in the value of the parameter θ_3, but also those of θ_1 and θ_2. This is not a desired situation. Hence, we choose a linearly independent set of frequencies such that

$$\sum_{i=1}^{p} a_i \omega_i \neq 0, \quad a_i \text{ are integers,} \tag{3.77}$$

for

$$\sum_{i=1}^{p} |a_i| \leq M + 1, \tag{3.78}$$

where M is an integer. As M → ∞, ω_i become truly incommensurable. We call frequencies generated in this manner are linearly independent to the order M [40]. Tables of these frequency sets can be found in [39, 41].

The working formulas to calculate the sensitivity measure include Equation (3.76), variance σ_Y^2 as

$$\sigma_Y^2 = \frac{1}{N_s} \sum_{i=1}^{N_s} \left[g(\underline{x}, s_i) - \mu_Y \right]^2 \tag{3.79}$$

where $N_s = 2\omega_{\max} + 1$, and the mean as

$$\mu_Y = \frac{1}{N_s} \sum_{i=1}^{N_s} g(\underline{x}, s_i). \tag{3.80}$$

The Fourier coefficients are calculated using simple quadrature as

$$A_{2\omega_i} = \frac{1}{N_s} \left\{ g(\underline{x}, s_{N_0}) + \sum_{q=1}^{N_q} \left[g(\underline{x}, s_{N_0+q}) + g(\underline{x}, s_{N_0-q}) \right] \cos \frac{2\omega_i q \pi}{N_s} \right\} \tag{3.81}$$

$$B_{1\omega_i} = \frac{1}{N_s} \left\{ \sum_{q=1}^{N_q} \left[g(\underline{x}, s_{N_0+q}) - g(\underline{x}, s_{N_0-q}) \right] \sin \frac{\omega_i q \pi}{N_s} \right\} \tag{3.82}$$

where $N_q = (N_s - 1)/2$;
$N_0 = N_q + 1$;
s_j is calculated as in Equation (3.72).

To illustrate the method, we choose a simple example so that the results can be easily interpreted. Consider a hypothetical recombination reaction from

$$A + A \rightarrow X$$

with reaction rate $r = {d[A]}/{dt} = -2\kappa[A]^2$ where $\kappa = k_1 \exp(-k_2/T)$. We will examine the sensitivity of the concentration of A to variations in parameter k_1 and k_2 at T = 298 K. We arbitrarily choose the nominal values of k_1 and k_2 to be 17.9 l/mol-sec and 500 K, respectively. Their ranges of uncertainty is $8.97 \leq k_1 \leq 35.9$, $0 \leq k_2 \leq 1000$ K. The initial concentration of A is $[A_0]$ = 1 mol/l. A normalized concentration is used: $u = [A]/[A_0]$. The solution for u is $u = \left(1 + 2k_1 \exp\left(-{k_2}/{T} \right) t[A_0] \right)^{-1}$.

The frequencies are $\omega_1 = 3$, $\omega_2 = 7$ based on the table of [39, 41]. Then the transformations of the parameters are: $k_1 = \bar{k}_1 \exp \nu_1$ and $k_2 = \bar{k}_2 (1 + \nu_2)$ where

$v_1 = (\ln 2)\sin\omega_1 s$ and $v_2 = \sin\omega_2 s$. Based on ω_{max}, the number of s to be evaluated is $2\omega_{max} + 1 = 15$. Next the means and variances at different time t are calculated using Equation (3.80) and (3.79). The resulting FAST sensitivity measures are shown in Figure 3.5 along with u, the relative linear sensitivities $\bar{k}_1 \frac{\partial u}{\partial k_1} = -2u^{-2}\kappa t[A_0]$ and $\bar{k}_2 \frac{\partial u}{\partial k_2} = 2u^{-2}\kappa t[A_0]k_2/T$.

From the figure, it can be seen that the variance of u is more sensitivity to the changes in k_1 than changes in k_2. Both the linear sensitivities and the FAST measures give the same results. The sum of S_{ω_1} and S_{ω_2} is very close to 1. This means the interaction between k_1 and k_2 in the ranges of interest is small.

To test the FAST method further, we increase in the range of uncertainty in k_1 as $0 \le k_1 \le 35.9$. To take into account this change, we use the transformation $k_1 = \bar{k}_1(1+\sin\omega_1 s)$. The range and transformation of k_2 are kept the same. The results are shown in Figure 3.6. The relative sensitivities are the same in this figure because they are determined by only the nominal values, not the ranges of uncertainty. This graph shows that initially u is more sensitivity to k_2, then it becomes more sensitivity to k_1. However, this change is not shown in the regular linear sensitivities. Therefore, the FAST method can take into account of large variations in parameters. Another point to notice is that the sum of S_{ω_1} and S_{ω_2} is further away from 1 compared to the previous case. This shows that with the increase in the uncertainty in k_1, the interaction between the two parameters increases.

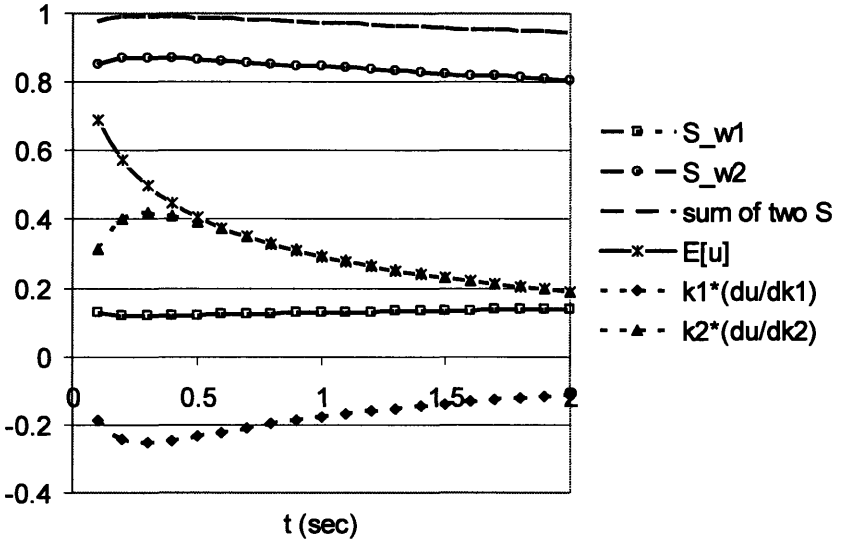

Figure 3.5 Comparison of the FAST Sensitivity Measures and Relative Linear Sensitivities of the Expected Value of $u = [A]/[A_0]$.

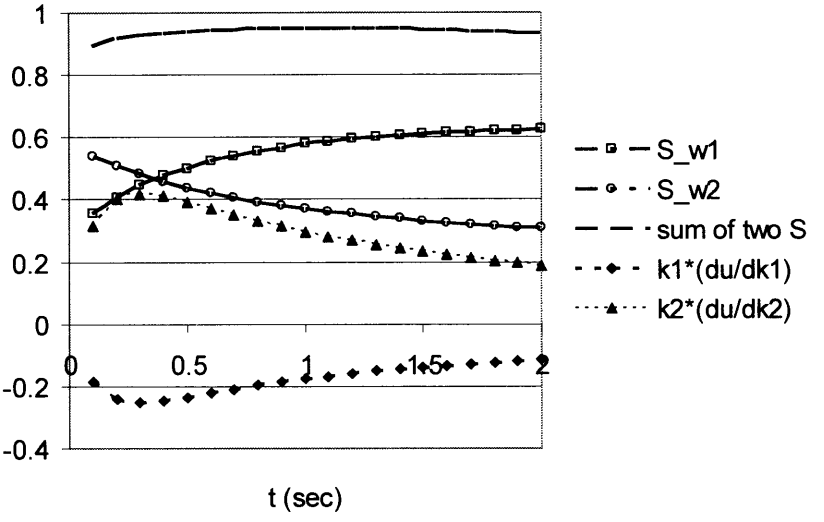

Figure 3.6 Comparison of the FAST Sensitivity Measures and Relative Linear Sensitivities of the Expected Value of $u = [A]/[A_0]$ with higher uncertainty in k_1.

If the system is highly nonlinear, such as exp(exp(k)), or highly non-monotonic, such as trigonometric functions, the first two terms FAST are not enough to account for all the contributions to the variance of Y. The number N of Fourier coefficients to be included needs to be larger than 2. For example, consider

$$Y = \sin(\theta_1) + 7\sin^2(\theta_2) \tag{3.83}$$

and

$$Y = \theta_1^2 + \exp(\exp(\theta_2)). \tag{3.84}$$

The sum of the two S_{ω_i} do not approach 1 till N = 6 or 8 as shown in Table 3.1. In these cases, the following equations should be used along with Equation (3.75):

$$A_{j\omega_i} = \frac{1}{N_s}\left\{g(\underline{x}, s_{N_0}) + \sum_{q=1}^{N_q}\left[g(\underline{x}, s_{N_0+q}) + g(\underline{x}, s_{N_0-q})\right]\cos\frac{j\omega_i q\pi}{N_s}\right\} \quad (j \text{ even}) \tag{3.85}$$

$$B_{j\omega_i} = \frac{1}{N_s}\left\{\sum_{q=1}^{N_q}\left[g(\underline{x}, s_{N_0+q}) - g(\underline{x}, s_{N_0-q})\right]\sin\frac{j\omega_i q\pi}{N_s}\right\} \quad (j \text{ odd}) \tag{3.86}$$

$$A_{j\omega_i} = 0 \quad (j \text{ odd}) \tag{3.87}$$

$$B_{j\omega_i} = 0 \quad (j \text{ even}) \tag{3.88}$$

Table 3.1 Comparison of Effects of N on the Representative of Contributions to the Variances of the Outputs by the Parameters

Sum of S_{ω_i}	N = 2	N = 4	N = 6	N = 8
Equation (3.83)	0.3184	0.7053	0.9805	0.9996
Equation (3.84)	0.2843	0.5323	0.7118	0.9676

3.2.6 Deterministic Equivalent Modeling Method (DEMM)

Rather than evaluating the expected value and variance from $g(\underline{x},\underline{\theta})$ and $f(\underline{\theta})$, the distribution of Y $f_Y(y)$ is directly approximated by a polynomial expansion. The two biggest advantages of this method are that it is computationally inexpensive, and that the explicit form of the model is not required.

The idea of DEMM will be described by an analogue to the deterministic systems. In deterministic systems, an unknown function

$$g(x)=\Theta(x)$$

can be approached by methods of weighted residuals of variation approach [45]:

$$g(\underline{x})\approx\sum_{i=1}^{N}a_i z_i(\underline{x}) \tag{3.89}$$

where $\underline{x}$ is a vector of variables, $\Theta(\underline{x})$ is a black box model, $\{a_i\}$ is a set of N unknown coefficients, $\{z_i(\underline{x})\}$ is a set of basis functions. One set of common basis functions is polynomials used in the Taylor Expansion. The error of this approximation is defined by

$$R_N(\underline{a},\underline{x})=\sum a_i z_i(\underline{x})-\Theta(\underline{x}) \tag{3.90}$$

where $\underline{a}$ is the vector of unknown coefficients. In Galerkin's approach, the residual function can be minimized by making it orthogonal to the approximation or basis function space X:

$$\int_X R_N(\underline{a},\underline{x})z_i(\underline{x})d\underline{x}=0;\quad i=1,...,N \tag{3.91}$$

This can be illustrated from the following Figure 3.7 using a two-variable model:

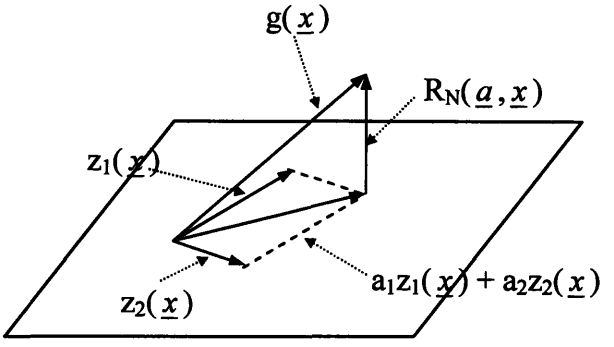

Figure 3.7 Schematic of Minimizing Error of Approximation.

In general, the methods of weighted residuals make the average of weighted residual function equal to zero [46]:

$$\int_X R_N(\underline{a},\underline{x})W_i(\underline{x})d\underline{x}=0;\quad i=1,...,N \tag{3.92}$$

where $\{W_i(\underline{x})\}$ is a sequence of N weight functions.

Similar to the idea in deterministic systems, an unknown r.v.

$$g(\underline{\theta})=\Theta(\underline{\theta})$$

can be approximated by the combination of known r.v.s:

$$\hat{g}(\underline{\theta}) = \sum_{j=1}^{N} a_j Z_j\left(\{\xi_i(\omega)\}\right) \tag{3.93}$$

where $\underline{\theta}$ is a vector of variables, $Z_j\left(\{\xi_i(\omega)\}\right)$ is the polynomial expansions, $\xi_i(\omega)$ is the basis functions, ω is an elementary r.v. $\underline{\theta}$ is to be approximated by ω as well:

$$\underline{\theta} = \underline{\theta}\left(\{\xi_i(\omega)\}\right)$$

Therefore, we have

$$R_N(\underline{a},\underline{\theta}) = \sum_{j=1}^{N} a_j Z_j\left(\{\xi_i(\omega)\}\right) - \Theta(\underline{\theta}) \tag{3.94}$$

and

$$\int_{\underline{\xi}} f_{\underline{\xi}}(\underline{\xi}) R_N(\underline{a},\underline{\theta}) Z_j\left(\{\xi_i(\omega)\}\right) d\xi_i(\omega) = 0; \quad i = 1,...,N \tag{3.95}$$

where $f_{\underline{\xi}}(\underline{\xi})$ is the joint distribution of $\underline{\xi}$. It can be shown that any square-integrable random variable can be approximated as closely as desired by a polynomial expansion [47], or polynomial chaos expansion (PCE) [48].

In practice, Zi(·) are chosen to be orthogonal. For two stochastic polynomials $\xi_1(\omega)$ and $\xi_2(\omega)$ to be orthogonal,

$$\int \xi_1(\omega)\xi_2(\omega) p_\omega(\omega) d\omega = 0. \tag{3.96}$$

There are several existing PCEs for common distributions. For example, Hermite polynomials and Legendre polynomials can be used for Gaussian and uniform distributions, respectively. The first 4 Legendre polynomials are shown in Equation (3.97):

$$\begin{aligned} L_0(\xi) &= 1, \\ L_1(\xi) &= \xi, \\ L_2(\xi) &= \tfrac{1}{2}(3\xi^2 - 1), \\ L_3(\xi) &= \tfrac{1}{2}(5\xi^3 - 3\xi). \end{aligned} \tag{3.97}$$

Problem specific polynomials, such as for truncated normal distributions, can also be generated using Gram-Schmidt orthonormalization [49].

The above description can easily be generalized to multiple stochastic parameters. For example, an M-th order PCE is written as:

$$\hat{g}(\theta_1,...,\theta_p) = g\left(\theta_1(\xi),...,\theta_p(\xi)\right) = g_0 + \underbrace{\sum_{i=1}^{p} g_{i1} L_1(\xi_i)}_{\text{linear}} + \underbrace{\sum_{i=0}^{p} g_{i2} L_2(\xi_i)}_{2^{\text{nd}}\text{ order}} + \underbrace{\sum_{i=0}^{p}\sum_{j<i} g_{i1j1} L_1(\xi_i) L_1(\xi_j)}_{\text{bilinear}} \tag{3.98}$$

$$+\underbrace{\sum_{i=0}^{p} g_{i3} L_3(\xi_i)}_{3^{\text{rd}}\text{ order}} + \underbrace{\sum_{i=0}^{p}\sum_{j=1}^{i-1} g_{i2j1} L_2(\xi_i) L_1(\xi_j)}_{2^{\text{nd}}\text{ order in }\xi_i,\ 1^{\text{st}}\text{ in }\xi_j} + \underbrace{\sum_{i=0}^{p}\sum_{j=1}^{i-1} g_{i1j2} L_1(\xi_i) L_2(\xi_j)}_{1^{\text{st}}\text{ in }\xi_i,\ 2^{\text{nd}}\text{ in }\xi_j}$$

$$+\underbrace{\sum_{i=0}^{p-2}\sum_{j=i+1}^{p-1}\sum_{k=j+1}^{p} g_{i1j1k1} L_1(\xi_i) L_1(\xi_j) L_1(\xi_k)}_{\text{trilinear}} + \text{ higher order terms}$$

There are p*M+1 coefficients of $\{g_i\}$ to be solved, which needs p*M+1 equations. For Galerkin's approach and Hermite polynomials, these p*M+1 equations can be generated by evaluating Equation (3.95) with p*M+1 $Z_j\left(\{\xi_i(\omega)\}\right)$:

$$Z_1\left(\{\xi_i(\omega)\}\right)=1$$
$$Z_2\left(\{\xi_i(\omega)\}\right)=\xi_1$$
...
$$Z_{1+p}\left(\{\xi_i(\omega)\}\right)=\xi_p$$
$$Z_{1+p+1}\left(\{\xi_i(\omega)\}\right)=\xi_1^2-1$$
...
$$Z_{1+2p}\left(\{\xi_i(\omega)\}\right)=\xi_p^2-1$$
$$Z_{1+2p+1}\left(\{\xi_i(\omega)\}\right)=\xi_1\xi_2$$
...
$$Z_{1+3p}\left(\{\xi_i(\omega)\}\right)=\xi_{p-1}\xi_p$$
...

Even though Galerkin's approach can produce an analytical solution of the PCE, it requires direct manipulation of model equations, which is often times difficult if not possible. This can be circumvented by using the collocation method, which forces the residual random variable to be deterministically zero at N specific chosen points:

$$R_N\left(\underline{a},c_j\right)=0,\ j=1,...,N \tag{3.99}$$

The collocation method can be seen as an approximation of Galerkin's approach. For an M-th order polynomial approximation, the collocation points $\{c_k\}$ are the roots of the M+1-th order polynomial. The combinations of these roots will provide M+1 equations for solving M+1 coefficients. Unless all the cross product terms as in Equation (3.98) are included, only selected collocation points will be used. The collocation points for each parameter are placed in a decreasing order of probability, e.g., $\xi_1 = c_1, c_2$; $\xi_2 = c_3, c_4$. When the probability is equal, such as in a uniform distribution, the points are organized in increasing distance from the mean. The first pair of points, which contains the most probable values for all the parameters among the collocation points (c_1, c_3), is termed the anchor point (ξ_{anchor}) [50, 51]. For increasing order of approximation, the collocation point is perturbed, such as (c_1, c_4), (c_2, c_3). If the bilinear term $L_1(\xi_1)L_1(\xi_2)$ is included, the point (c_1, c_4) will also be used in the coefficient evaluation process.

Since the approximated function is smooth and polynomial-approximable, to see the accuracy in the estimation, the truncation error can be estimated by lowest order term excluded. This is done by comparing the results from the M-th order prediction to that of the M+1-th order predication, whose collocation points are the roots of the M+2-th order polynomial . The error at each of the M+1-th order collocation points is defined as:

$$\varepsilon_i = \left\| g_i - \hat{g}_i \right\|^2 \tag{3.100}$$

Two metrics can be used — the sum square root (SSR) error and the relative sum square root (RSSR) error:

$$SSR = \sqrt{\frac{\sum_{i=1}^{m+2} f_\xi \varepsilon_i}{(m+2) f_\xi(\xi_{anchor})}}, \tag{3.19}$$

$$RSSR = \frac{SSR \text{ error}}{E(\hat{y})} \tag{3.20}$$

Since SSR is usually dependent on the magnitude of the expected value, the RSSR is a more useful measure of the error. If the error is not acceptable, higher order approximation can be used.

The procedure of DEMM usually contains the following steps:

- specify the PDF of uncertain parameters;
- generate problem-specific polynomial chaos expansions;
- approximate uncertain outputs using polynomial chaos expansion;
- find the collocation points based on the sequence of the probability of the points;
- solve the original model at the collocation points;
- solve for the coefficients of expansion from model results;
- estimate the error of approximation; and
- increase the order of approximation if necessary.

An example of applying DEMM can be shown using the following equation:

$$g = \sin(\theta) \tag{3.101}$$

where θ is uniformly distributed between $[-\pi, \pi]$. The suitable orthogonal polynomial for uniform distributions are Legrendre polynomials. θ can be represented as

$$\theta = \pi\xi$$

A 4th-order, 5-term expansion of Equation (3.101) is:

$$g \approx g_1 + g_2\xi + \tfrac{1}{2} g_3 (3\xi^2 - 1) + \tfrac{1}{2} g_4 (5\xi^3 - 3\xi) + \tfrac{1}{8} g_5 (35\xi^4 - 30\xi^2 + 3) \tag{3.102}$$

The collocation points are chosen to be the roots of the 5th polynomial

$$L_5(\xi) = \tfrac{1}{8}(63\xi^5 - 70\xi^3 + 15\xi)$$

$$P_1 = (0),\ P_2 = (0.8841),\ P_3 = (-0.8841),\ P_4 = (0.5433),\ P_5 = (-0.5433)$$

The solution for $\underline{g}$ is

$$g = [0 \quad 0.9333 \quad 0 \quad -1.1683 \quad 0]'. \tag{3.103}$$

The result of the approximation can be seen in Figure 3.8 and Table 3.2. It can be seen that the DEMM result fits well with the original PDF even at higher moments. Please note that DEMM is used to approximate the distribution, not the function of $g = \sin(\theta)$.

The coefficients of the approximation shows that θ contributes at the first and third orders.

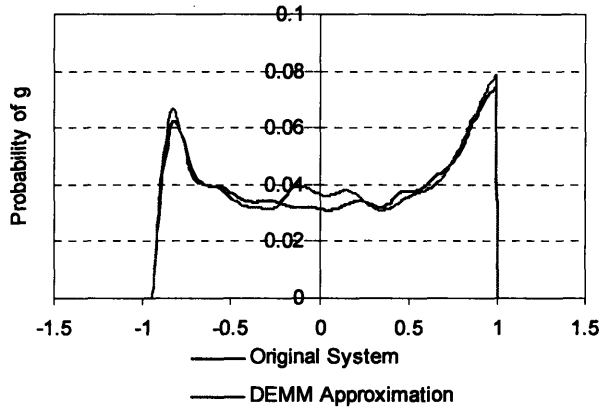

Figure 3.8 Comparison of 1 r.v. System with its 4th-order DEMM Approximation

Table 3.2 Comparison of the Moments of the Original 1 r.v. System and its DEMM Approximation

	Original System	DEMM Approximation
Mean	2.93E-05	3.23E-05
Standard Deviation	0.707	0.697
Skewness	-1.12E-04	-1.29E-04
Kurtosis	1.50	1.53

3.2.7 Global Sensitivity Indices (GSI)

To capture the effect of input parameters on the variance of the output completely, not only the first order, local terms need to be studies, higher order non-linear and cross terms also need to be considered. Some of the methods described above have the capacity of capturing global effects, such as FAST, DEMM, and the method of this subsection. Some of the methods do not have that capacity such as ANOVA. The name of the method here may be misleading in the sense that it is the only method for global sensitivity analysis. However, due to the lack of a better name for it in the literature, GSI is used.

The method described here is based on Sobol' [52] and extensions of work by [35, 53-55]. The basic idea of GSI is to decompose the variance into a expansion with increasing dimensionality. The literature assumes function $g(\underline{x},\underline{\theta})$ ($\underline{x}$ will be omitted in the future) is defined in the p-dimensional unit cube:

$$K^p = \{\underline{\theta} \mid 0 \le \theta_i \le 1; i = 1,...,p\} \tag{3.104}$$

Please note that this assumption is not necessary but only to allow the omission of the PDFs of $\underline{\theta}$. To make the method applicable to a variety of distributions, the PDFs of $\underline{\theta}$ are kept in the equations. In some equations, the integration range from 0 to 1 is kept. Let $\sum \hat{T}_{i_1 \cdots i_s}$ define the sum over all the combinations of indices in K^p

$$\sum \hat{T}_{i_1 \cdots i_2} \equiv T_0 + \sum_{i=1}^{p} T_i + \sum_{1 \le i \le p} \sum_{1 \le j \le i} T_{ij} + \cdots + T_{12 \cdots p} \tag{3.105}$$

Definition: The representation of $g(\underline{\theta})$ as a sum

$$g(\theta_1, \cdots, \theta_p) = \sum \hat{g}_{i_1 \cdots i_s}(\theta_1, \cdots, \theta_p) \tag{3.106}$$

is called a decomposition into summands of different dimensions if

$$g_0 = \text{constant} \tag{3.107}$$

and

$$\int g_{i_1 \cdots i_s}(\theta_{i_1}, \ldots, \theta_{i_s}) f_{\theta_{i_k}}(\theta_{i_k}) d\theta_{i_k} = 0, \quad \text{if} 1 \le k \le s \tag{3.108}$$

From the definition, we can get the following properties:

$$g_0 = \int_{K^p} g(\underline{\theta}) f_{\underline{\theta}}(\underline{\theta}) d\underline{\theta}. \tag{3.109}$$

For any different summands $g_{i_1 \cdots i_s}$ and $g_{j_1 \cdots j_l}$:

$$\int_{K^p} g_{i_1 \cdots i_s}(\theta_{i_1}, \ldots \theta_{i_s}) g_{j_1 \cdots j_s}(\theta_{j_1}, \ldots \theta_{j_s}) f_{\underline{\theta}}(\underline{\theta}) d\underline{\theta} = 0 \tag{3.110}$$

This is because from Equation (3.108), at lease one of the indices $i_1, \ldots, i_s, j_1, \ldots, j_s$ will not be repeated twice. This shows the orthogonality of the decomposition terms.

Theorem: The definition Equation (3.106) is unique whenever $g(\underline{\theta})$ is integrable over K^p. The terms in the decomposition can be derived as follow. g_0 is given by Equation (3.109). The one-indexed terms $g_i(\theta_i)$ are only a function of θ_i and can be obtained as:

$$\begin{aligned}
&\int_0^1 \cdots \int_0^1 g(\underline{\theta}) f_{\underline{\theta}/\theta_i}(\underline{\theta}/\theta_i) \{d\underline{\theta}/d\theta_i\} \\
&= \int_0^1 \cdots \int_0^1 g_0 f_{\underline{\theta}/\theta_i}(\underline{\theta}/\theta_i) \{d\underline{\theta}/d\theta_i\} + \int_0^1 \cdots \int_0^1 \sum_{1 \le j \le p} g_j(\theta_j) f_{\underline{\theta}/\theta_i}(\underline{\theta}/\theta_i) \{d\underline{\theta}/d\theta_i\} + \\
&\int_0^1 \cdots \int_0^1 \sum_{1 \le j \le p} \sum_{1 \le k \le j} g_{jk}(\theta_j, \theta_k) f_{\underline{\theta}/\theta_i}(\underline{\theta}/\theta_i) \{d\underline{\theta}/d\theta_i\} + \ldots + \int_0^1 \cdots \int_0^1 g_{i_1 \cdots i_s}(\underline{\theta}) f_{\underline{\theta}/\theta_i}(\underline{\theta}/\theta_i) \{d\underline{\theta}/d\theta_i\} \\
&= g_0 \int_0^1 \cdots \int_0^1 f_{\underline{\theta}/\theta_i}(\underline{\theta}/\theta_i) \{d\underline{\theta}/d\theta_i\} + \sum_{1 \le j \le p, j \ne i} \int_0^1 \cdots \int_0^1 g_j(\theta_j) f_{\underline{\theta}/\theta_i}(\underline{\theta}/\theta_i) \{d\underline{\theta}/d\theta_i\} + \\
&g_i(\theta_i) \int_0^1 \cdots \int_0^1 f_{\underline{\theta}/\theta_i}(\underline{\theta}/\theta_i) \{d\underline{\theta}/d\theta_i\} + \sum_{1 \le j \le p} \sum_{1 \le k \le j} \int_0^1 \cdots \int_0^1 g_{jk}(\theta_j, \theta_k) f_{\underline{\theta}/\theta_i}(\underline{\theta}/\theta_i) \{d\underline{\theta}/d\theta_i\} + \\
&\ldots + \int_0^1 \cdots \int_0^1 g_{i_1 \cdots i_s}(\underline{\theta}) f_{\underline{\theta}/\theta_i}(\underline{\theta}/\theta_i) \{d\underline{\theta}/d\theta_i\} \\
&= g_0 \square 1 + 0 + g_i(\theta_i) \square 1 + 0 + 0 + \ldots + 0 \\
&= g_0 + g_i(\theta_i)
\end{aligned} \tag{3.111}$$

where $d\underline{\theta}/d\theta_i$ indicates integration over all the variables except θ_i. $f_{\underline{\theta}/\theta_i}(\underline{\theta}/\theta_i)$ indicates the joint probability distribution of all $\underline{\theta}$ except for θ_i. Similarly, the two-indexed terms are:

$$\int_0^1 \cdots \int_0^1 g(\underline{\theta}) f_{\underline{\theta}/\theta_i\theta_j}(\underline{\theta}/\theta_i\theta_j)\{d\underline{\theta}/d\theta_i d\theta_j\} = g_0 + g_i(\theta_i) + g_j(\theta_j) + g_{ij}(\theta_i,\theta_j) \quad (3.112)$$

There are several points to be noted here. First, it is that the above derivation does not require the θ_i to be independent. However, when there is correlation between variables, decomposition of contribution to variance into each individual variables is impossible. Secondly, $g_{i_1\cdots i_s}(\theta_{i_1},\ldots,\theta_{i_s})$ is a r.v., not a function. Thirdly, even though in Sobol's original derivation, $\underline{\theta}$ is defined uniformly between [0,1], the method is applicable for other ranges and other types of distributions. One problem in the definition is that it does not specify whether the $\theta_{i_1,j\ldots k}$s in Equation (3.108) are going be evaluated at nominal values, expected values, or other values. In the rest of the chapter, expected value is used.

The sensitivity estimates $S_{i_1\cdots i_s}$ are defined as:

$$S_{i_1\cdots i_s} = \frac{D_{i_1\cdots i_s}}{D} \quad (3.113)$$

where

$$D = \int_{K^n} g^2(\underline{\theta}) f_{\underline{\theta}}(\underline{\theta}) d\underline{\theta} - g_0^2 \quad (3.114)$$

and

$$D_{i_1\cdots i_s} = \int_0^1 \cdots \int_0^1 g^2_{i_1\cdots i_s}(\theta_{i_1}\cdots\theta_{i_s}) f_{\theta_{i_1}\cdots\theta_{i_s}}(\theta_{i_1}\cdots\theta_{i_s}) d\theta_{i_1}\cdots d\theta_{i_s} \quad (3.115)$$

For example, in calculating D_{23} for a three-parameter system, Equation (3.112) gives,

$$g_{23} = \int\cdots\int g \cdot f_{\underline{\theta}/\theta_2\theta_3}\{d\underline{\theta}/d\theta_2 d\theta_3\} - g_0 - g_2 - g_3 .$$

Therefore,

$$D_{23} = \int g_{23}^2 f_{\theta_2} f_{\theta_3} d\theta_2 d\theta_3 = \int\left(\int\cdots\int g \cdot f_{\underline{\theta}/\theta_2\theta_3}\{d\underline{\theta}/d\theta_2 d\theta_3\}\right)^2 f_{\theta_2} f_{\theta_3} d\theta_2 d\theta_3 - D_2 - D_3 - g_0^2$$

Squaring Equation (3.106) and using the orthogonality in Equation (3.110), we can get

$$D = \sum \hat{D}_{i_1\cdots i_s} . \quad (3.116)$$

Therefore, D and $D_{i_1\cdots i_s}$ can be seen as the variances of $g(\underline{\theta})$ and $g_{i_1\cdots i_s}$, respectively. At the same time,

$$\sum \hat{S}_{i_1\cdots i_s} = 1, \quad (3.117)$$

which is a nice quality for assigning contributions of output variance to each factors. The $S_{i_1\cdots i_s}$ are true global sensitivity estimates as they give the fraction of the total variance of $g(\underline{\theta})$ by each factor both individually and collectively with other factors. Most of the time, we are interested in this combined effect, especially for non-linear systems where higher order interactions with factors are important. Therefore, we can use partition $\underline{\theta}$

into two subsets: one containing a given variable θ_i alone, the other set $\underline{\theta}_{ci}$ containing all the θ_j with $j \neq i$. Then Equation (3.112) becomes:

$$g(\underline{\theta}) = g_0 + g_i(\theta_i) + g_{ci}(\underline{\theta}_{ci}) + g_{i,ci}(\theta_i, \underline{\theta}_{ci}). \tag{3.118}$$

Therefore, Equation (3.116) becomes:

$$D = D_i + D_{ci} + D_{i,ci}. \tag{3.119}$$

The Global Sensitivity Indices (GSI) is then defined as:

$$S_{Ti} \equiv S_i + S_{i,ci} = 1 - S_{ci} \tag{3.120}$$

where S_{ci} equals the sum of all the $S_{i_1 \ldots i_s}$ terms where the index i is excluded. Hence, S_{Ti} denotes the total effect of variable θ_j, which includes the fraction of variance accounted for by θ_j alone and the fraction accounted by any combination of θ_j with the remaining variables.

Another use of GSI is to study the contribution of groups of factors [52, 56]. For example, $\underline{\theta}$ can be partitioned into two groups $\underline{\varsigma}$ and $\underline{\upsilon}$, containing factors from θ_1 to θ_t, and θ_{t+1} to θ_p, respectively. Then $g(\underline{\theta})$ can be decomposed as:

$$g(\underline{\theta}) = g_0 + g_1(\underline{\varsigma}) + g_2(\underline{\upsilon}) + g_{12}(\underline{\varsigma}, \underline{\upsilon}), \tag{3.121}$$

with

$$\int_{K^t} g_1 f_{\underline{\varsigma}}(\underline{\varsigma}) d\underline{\varsigma} = \int_{K^{p-t}} g_2 f_{\underline{\upsilon}}(\underline{\upsilon}) d\underline{\upsilon} = \int_{K^t} g_{12} f_{\underline{\varsigma}}(\underline{\varsigma}) d\underline{\varsigma} = \int_{K^{p-t}} g_{12} f_{\underline{\upsilon}}(\underline{\upsilon}) d\underline{\upsilon} = 0 \tag{3.122}$$

and

$$D_{\underline{\varsigma}} = \int_{K^t} g_1^2 f_{\underline{\varsigma}}(\underline{\varsigma}) d\underline{\varsigma}, \quad D_{\underline{\upsilon}} = \int_{K^{p-t}} g_2^2 f_{\underline{\upsilon}}(\underline{\upsilon}) d\underline{\upsilon}, \quad D_{\underline{\varsigma}\underline{\upsilon}} = \int_{K^p} g_{12}^2 f_{\underline{\varsigma}\underline{\upsilon}}(\underline{\varsigma}, \underline{\upsilon}) d\underline{\varsigma} d\underline{\upsilon}. \tag{3.123}$$

Then the GSI of $\underline{\varsigma}$ can be defined as:

$$S_{\underline{\varsigma}}^{total} = \frac{D_{\underline{\varsigma}}^{total}}{D} = \frac{D_{\underline{\varsigma}} + D_{\underline{\varsigma}\underline{\upsilon}}}{D} = \frac{D - D_{\underline{\upsilon}}}{D} \tag{3.124}$$

Computation of GSI: The estimation of $\hat{g}_0$ is straightforward using Monte Carlo simulations:

$$\hat{g}_0 \approx \frac{1}{N} \sum_{m=1}^{N} g(\underline{\theta}_m) \tag{3.125}$$

where N tends to infinity and $\underline{\theta}_m$ is a sampled point in the space K^p. For one-indexed term D_i:

$$\begin{aligned} D_i &= \int g_i^2(\theta_i) f_{\theta_i}(\theta_i) d\theta_i \\ &= -g_0^2 + \int \left(\int \cdots \int g(\underline{\alpha}, \theta_i) f_{\underline{\alpha}}(\underline{\alpha}) d\underline{\alpha} \right) \left(\int \cdots \int g(\underline{\beta}, \theta_i) f_{\underline{\beta}}(\underline{\beta}) d\underline{\beta} \right) f_{\theta_i}(\theta_i) d\theta_i \end{aligned} \tag{3.126}$$

where $\underline{\alpha}$ and $\underline{\beta}$ are projections of $\underline{\theta}$ on $K^p - 1$, which is K^p minus θ_i. The integral has dimension $2(p-1) + 1 = 2p - 1$. The Monte Carlo estimation of it is:

$$\hat{D}_i \approx \frac{1}{N} \sum_{m=1}^{N} g(\underline{\alpha}_m, \theta_{im}) g(\underline{\beta}_m, \theta_{im}) - \hat{g}_0^2. \tag{3.127}$$

The estimation of S_{ci} is:

$$S_{ci} \approx \frac{1}{D}\left[\frac{1}{N}\sum_{m=1}^{N} g(\underline{\alpha}_m, \theta_{im})\, g(\underline{\alpha}_m, \theta'_{im}) - \hat{g}_0^2\right] \tag{3.128}$$

The total number of sampling is $N \times (p-1) + N + N = N \times (p+1)$, where $N \times (p-1)$ for $\underline{\alpha}_m$, N for θ_{im}, N for θ'_{im}. g_0 can use the samples from $\underline{\alpha}_m$ and θ_{im} or θ'_{im}. Please note that there is no need to calculate all the $S_{i_1 \ldots i_s}$.

To illustrate the method, GSI was applied to comparing the life cycle global warming potential of using NF_3 and F_2 as the chamber cleaning gas for chemical vapor deposition chambers in the semiconductor manufacturing. The cleaning process is described in Chapter 5. The top three most important parameters were first identified based on rank correlation coefficients. Then the GSIs of these parameters were calculated.

Let's use the power used in the plasma generator as an example to describe the computation procedure. First, the relative global warming potential (GWP) was calculated using the model, then another relative GWP was calculated using the same model except that the power used in plasma generator was re-sampled, while all other variables were kept the same. This was achieve in Excel by setting a dummy NF3 chamber cleaning process. All the inputs of this process is the same as the real process except that the power in the generator is another r.v.. This r.v. has the same distribution as that of the real process, but is independent of the latter. Accordingly, all the parameters dependent on the power need to be recalculated.

It can be seen from Table 3.3 that the GSIs agree well with the rank correlation coefficients in terms of ranking. Because ranks strongly linearize the system, the values of the rank coefficients are only qualitative. On the other hand, GSI results can be treated quantitatively. The power to the electron temperature in the NF_3 disassociation reaction and its interaction with other terms contribute to more than one third of the total variance. Therefore, to reduce the variance of the GWP, this accuracy of this parameter should first being reduced.

Table 3.3 Top Three Parameters with the Highest Rank Correlation Coefficients of the Relative GWP of the NF_3 and F_2 Cleaning Processes and Their GSI

Parameter	Rank Correlation Coefficient	Global Sensitivity Index
Power to the Electron Temperature in the NF_3 Disassociation Reaction	-0.54	0.36
NF_3 Efficiency in NF_3 Production from NH_3 and HF	-0.46	0.22
Power Used in Plasma Generator (W)	0.40	0.15

3.3 Comparison of the Methods

3.3.1 A Non-Linear, Non-Monotonic Two-Parameter Case

Let's consider a two variable system

$$Y = g(\theta_1, \theta_2) = \sin(\theta_1) + 7\sin^2(\theta_2), \tag{3.129}$$

where both θs uniformly distributed between $[-\pi, \pi]$. θ_1 and θ_2 are independent. The contributions of θ_1 and θ_2 to the variance of Y can be solved analytically since the two terms are independent in Equation (3.129). The variance of Y is 6.6225 out of which 0.5 is from $\sin(\theta_1)$ and 6.1225 is from $7\sin^2(\theta_2)$.

Local Sensitivity Analysis

Based on Equation (3.12), the contribution of θ_1 and θ_2 can be approximated with the $\left(\left.\frac{\partial g}{\partial \theta_i}\right|_{\eta_\theta}\right)^2 \sigma_{\theta_i}^2$ term. $\left(\left.\frac{\partial g}{\partial \theta_1}\right|_{\eta_\theta}\right)^2 \sigma_{\theta_1}^2 = \frac{\pi^2}{3}$, while $\left(\left.\frac{\partial g}{\partial \theta_2}\right|_{\eta_\theta}\right)^2 \sigma_{\theta_2}^2 = 0$ because at the nominal point ($\theta_1 = 0$, $\theta_2 = 0$), $\left(\left.\frac{\partial g}{\partial \theta_2}\right|_{\eta_\theta}\right) = 14\sin\theta_2\cos\theta_2\big|_{\eta_\theta} = 0$. This is obviously incorrect representation of the contribution of θ_2 as in other points, the derivative will not be zero. This shows the limit of the local sensitivity analysis.

ANOVA

Based on ANOVA, the contributions of the two parameters can be seen from SS_A and SS_B. Using a 31×31 array, 961 samples of g were generated. $SS_A = J\sum_{i=1}^{I} Y_{i\cdot}^2 - IJY_{\cdot\cdot}^2 = 483$, while $SS_B = I\sum_{j=1}^{J} Y_{\cdot j}^2 - IJY_{\cdot\cdot}^2 = 5869$. Because ANOVA assume linear relationship between the variables, it would have worked if the parameters under study were $\sin(\theta_1)$ and $7\sin(\theta_2)^2$.

Correlation Coefficients and Rank Correlation Coefficients

Using 1000 samples of g, the correlation coefficients and rank correlation coefficients of θ_1 and θ_2 are shown in Table 3.5. The number of sampling points was chosen to be the same order as ANOVA.

FAST

First, we generate the frequencies for the two parameters. Using the table from [41], the frequencies for two-parameter systems are $\omega_1 = 3$, and $\omega_2 = 7$. They are arbitrarily assigned to θ_1 and θ_2, respectively. It is to be found later that switching the frequencies assigned to the two parameters does not affect the results. Then the transformations of the parameters are chosen based on the range of uncertainty and their

nominal values: $\theta_1 = \pi \sin \omega_1 s$ and $\theta_2 = \pi \sin \omega_2 s$. Choosing N to be 10, the number of s to be evaluated is $10\omega_{max} + 1 = 71$.

DEMM

The 3rd-order expansion has 10 terms:

$$g = g_1 + g_2\xi_1 + g_3\xi_2 + 0.5g_4(3\xi_1^2 - 1) + 0.5g_5(3\xi_2^2 - 1) + g_6\xi_1\xi_2 + 0.5g_7(5\xi_1^3 - 3\xi_1) + 0.5g_8(5\xi_2^3 - 3\xi_2) + 0.5g_9(3\xi_1^2 - 1)\xi_2 + 0.5g_{10}(3\xi_2^2 - 1)\xi_1. \quad (3.130)$$

The solution for the coefficients is

$$g = [3.9404 \quad 0.9625 \quad 0 \quad 0 \quad -4.3937 \quad 0 \quad -1.3335 \quad 0 \quad 0 \quad 0]' \quad (3.131)$$

Since the coefficients represent the contribution of the corresponding factor, we know that θ_1 contributes in the first and third order, θ_2 contributes in the second order. There is no interaction between the two variables, which is obvious from the formula.

The approximation of the distribution is shown in Figure 3.6 and Table 3.4. The SSR is 2.77. The RSSR is 0.79. It can be seen that results are less satisfactory than the one variable situation even though more terms are used. Given the same order of expansion, the number of terms increases rapidly with all the cross section terms by the order of p^m, where p is the number of variables, and m is the order of the expansion. The dimensionality problem is not as severe as that in Monte Carlo simulation, whose order of sampling increases with the order of a^p, where a is the number of samples for each variable.

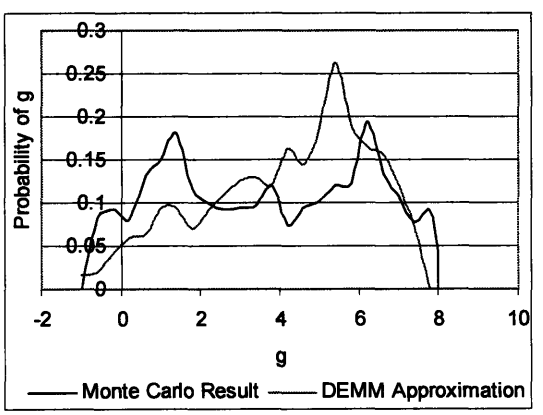

Figure 3.9 Comparison of 2 r.v. System with its 3th-order DEMM Approximation

Table 3.4 Comparison of the Moments of the Original 2 r.v. System and its DEMM Approximation

	Original System	DEMM Approximation
Mean	3.52	3.95
Standard Deviation	2.57	2.08
Skewness	-1.62E-02	-0.530E-2
Kurtosis	1.71	2.36

GSI

The expected value of g is:

$$g_0 = \int_{-\pi}^{\pi}\int_{-\pi}^{\pi}\left[\sin(\theta_1)+7\sin^2(\theta_2)\right]p_1(\theta_1)p_2(\theta_2)d\theta_1 d\theta_2 = 3.5 \tag{3.132}$$

and

$$D = \int_{-\pi}^{\pi}\int_{-\pi}^{\pi}\left[\sin(\theta_1)+7\sin^2(\theta_2)\right]^2 p_1(\theta_1)p_2(\theta_2)d\theta_1 d\theta_2 - g_0^2 = 6.6225 \tag{3.133}$$

g_1 is evaluated as

$$g_1(\theta_1) = \int_{-\pi}^{\pi}\left[\sin(\theta_1)+7\sin^2(\theta_2)\right]p_2(\theta_2)d\theta_2 - g_0 = \sin(\theta_1) \tag{3.134}$$

and

$$D_1 = \int_{-\pi}^{\pi} g_1^2(\theta_1)p_1(\theta_1)d\theta_1 = \frac{1}{2} \tag{3.135}$$

g_2 is evaluated as:

$$g_1(\theta_2) = \int_{-\pi}^{\pi}\left[\sin(\theta_1)+7\sin^2(\theta_2)\right]p_1(\theta_1)d\theta_1 - g_0 = 7\sin^2(\theta_2) - 3.5 \tag{3.136}$$

Other partial variances $D_{i_1 \ldots i_s}$ can be obtained analytically as

$$D_2 = 6.125 \tag{3.137}$$

$$D_{12} = 0 \tag{3.138}$$

The results of the above methods are summarized in Table 3.5. Because the highly non-monotonic nature of the trigonometric functions, methods that assume monotonity give very poor results, such as local sensitivity and correlation methods. ANOVA assumes linearity in the relationship of the terms, but not within the terms. Therefore it gives correct relative importance of the two terms. DEMM does not give an aggregate account of the contribution.

Table 3.5 Comparison of Results from Sensitivity Methods on A Non-Linear, Non-Monotonic Two-Parameter Case

	θ_1			θ_2			S_1/S_2*	Number of manipulations of model
Analytical Solution	0.5			6.125			12.25	N/A
Local Sensitivity	$\pi^2/3$			0			0	N/A
ANOVA	483			5869			12.15	961
Correlation Coefficients	0.222			0			0	1000
Rank Correlation Coefficients	0.231			3.78E-03			0.0161	1000
FAST**	0.0566			0.943			16.7	710
DEMM	1st order	2nd order	3rd order	1st order	2nd order	3rd order	N/A	10
	0.963	0	0	0	-4.39	-1.33		

GSI	0.0755	0.924	12.25	Determined by integration.

* S_i -- the sensitivity measures of θ_i.
** Ten terms of Fourier Coefficients are used.

3.3.2 A Non-Linear, Non-Monotonic Three-Parameter Case

An example of three variables is considered based on Ishigami & Homma [57].

$$g(\theta_1,\theta_2,\theta_3)=\sin(\theta_1)+a\sin^2(\theta_2)+b\theta_3^4\sin(\theta_1) \tag{3.139}$$

where its input probability density functions are

$$p_i(\theta_i)=\begin{cases}\dfrac{1}{2\pi}, & \text{when } -\pi\le\theta_i\le\pi\\ 0, & \text{when } \theta_i<-\pi,\ \theta_i>\pi\end{cases} \quad \text{for } i=1,2,3. \tag{3.140}$$

This example is to study how well the methods detect and represent the interaction of parameters resulted from the formula. Therefore, only FAST, DEMM, and GSI are discussed. For the following calculation, a = 7 and b = 0.1.

FAST

The frequencies are chosen to be $\underline{\omega}=\{1,9,13\}$ again based on [41]. The transformations of the parameters are the same as the previous example. The number of Fourier coefficients to be calculated are set to 10 because of the system is highly non-monotonic and non-linear. Using the same set of equations as before, the results are listed in Table 3.7 shows that the results of the three methods give agree with each other in magnitude, except that the FAST method lumps together the contributions of a parameter individually and along with other parameters. Hence, it does not show the contribution from $\theta_1\theta_3$ and the contribution of θ_1 is larger than θ_2. Saltelli et al have developed a modified FAST to calculate these contributions separately as DEMM and GSI do [58].

DEMM

Using the collocation method, a 10-term expansion is

$$g=g_1+g_2\xi_1+g_3\xi_2+g_4\xi_3+0.5g_5(3\xi_1^2-1)+0.5g_6(3\xi_2^2-1)+0.5g_7(3\xi_3^2-1)+ \\ +g_8\xi_1\xi_2+g_9\xi_2\xi_3+g_{10}\xi_1\xi_3 \tag{3.141}$$

Since there are 10 terms to be evaluated, the roots of the 2nd order Legrendre polynomial is used:

$$P_1=(0,0,0)\quad P_2=\left(\sqrt{3/5},0,0\right)\quad P_3=\left(0,\sqrt{3/5},0\right)\quad P_4=\left(0,0,\sqrt{3/5}\right)$$
$$P_5=\left(0,-\sqrt{3/5},0\right)\quad P_6=\left(0,0,-\sqrt{3/5}\right)\quad P_7=\left(-\sqrt{3/5},0,0\right)\quad P_8=\left(0,\sqrt{3/5},\sqrt{3/5}\right) \tag{3.142}$$
$$P_9=\left(\sqrt{3/5},0,\sqrt{3/5}\right)\quad P_{10}=\left(\sqrt{3/5},\sqrt{3/5},0\right)$$

The resulting deterministic equivalent model on these points becomes:

$$\begin{bmatrix} 1 & 0 & 0 & 0 & -0.5 & -0.5 & -0.5 & 0 & 0 & 0 \\ 1 & \sqrt{1/5} & 0 & 0 & 0.4 & -0.5 & -0.5 & 0 & 0 & 0 \\ 1 & 0 & \sqrt{1/5} & 0 & -0.5 & 0.4 & -0.5 & 0 & 0 & 0 \\ 1 & 0 & 0 & \sqrt{1/5} & -0.5 & -0.5 & 0.4 & 0 & 0 & 0 \\ 1 & 0 & -\sqrt{1/5} & 0 & -0.5 & 0.4 & -0.5 & 0 & 0 & 0 \\ 1 & 0 & 0 & -\sqrt{1/5} & -0.5 & -0.5 & 0.4 & 0 & 0 & 0 \\ 1 & -\sqrt{1/5} & 0 & 0 & 0.4 & -0.5 & -0.5 & 0 & 0 & 0 \\ 1 & 0 & \sqrt{1/5} & \sqrt{1/5} & -0.5 & 0.4 & 0.4 & 0 & 0.6 & 0 \\ 1 & \sqrt{1/5} & 0 & \sqrt{1/5} & 0.4 & -0.5 & 0.4 & 0 & 0 & 0.6 \\ 1 & \sqrt{1/5} & \sqrt{1/5} & 0 & 0.4 & 0.4 & -0.5 & 0.6 & 0 & 0 \end{bmatrix} \begin{bmatrix} g_1 \\ g_2 \\ g_3 \\ g_4 \\ g_5 \\ g_6 \\ g_7 \\ g_8 \\ g_9 \\ g_{10} \end{bmatrix} = \begin{bmatrix} 0 \\ 0.6504 \\ 2.9612 \\ 0 \\ 2.9612 \\ 0 \\ -0.6504 \\ 2.9612 \\ 2.9312 \\ 3.6117 \end{bmatrix} \quad (3.143)$$

The solution for this equation is

$$\underline{g} = [1.6451 \quad 0.8397 \quad 0 \quad 0 \quad 0 \quad 3.2903 \quad 0 \quad 0 \quad 0 \quad 3.8014]'. \quad (3.144)$$

The analytical solution of g_1 is 3.5. The SSR is 4.7474. The RSSR is 1.3564. This is not a very good fit, which means that a higher order expansion is needed for a better fit. However, the coefficients tell us that θ_1 contributes both at the linear and the bilinear term with θ_3. This example shows that DEMM can be applied to both non-linear and non-monotonic systems for identifying important parameters that contribute to the variance of the outputs and show their magnitude of influence.

A few points to be noted here. For multi-variable systems, care needs to be put onto the choices of the collocation points as it is possible for the matrix (3.143) to be singular. For example, for a 2-variable, 3rd-order expansion case with roots {a, -a, b, -b}, if the collocation points include (a, a), (a, -a), (-a, a), (-a, -a), (b, b), (b, -b), (-b, b), (-b, -b), then the matrix of the coefficients for g is (3.145) singular. This is can be seen from the following derivation after (3.145).

$$\begin{bmatrix} 1 & a & a & 0.5(3a^2-1) & 0.5(3a^2-1) & a^2 & 0.5(5a^3-3a) & 0.5(5a^3-3a) & 0.5(3a^2-1)a & 0.5(3a^2-1)a \\ 1 & a & -a & 0.5(3a^2-1) & 0.5(3a^2-1) & -a^2 & 0.5(5a^3-3a) & -0.5(5a^3-3a) & -0.5(3a^2-1)a & 0.5(3a^2-1)a \\ 1 & -a & a & 0.5(3a^2-1) & 0.5(3a^2-1) & -a^2 & -0.5(5a^3-3a) & 0.5(5a^3-3a) & 0.5(3a^2-1)a & -0.5(3a^2-1)a \\ 1 & -a & -a & 0.5(3a^2-1) & 0.5(3a^2-1) & a^2 & -0.5(5a^3-3a) & -0.5(5a^3-3a) & -0.5(3a^2-1)a & -0.5(3a^2-1)a \\ 1 & b & b & 0.5(3b^2-1) & 0.5(3b^2-1) & b^2 & 0.5(5b^3-3b) & 0.5(5b^3-3b) & 0.5(3b^2-1)b & 0.5(3b^2-1)b \\ 1 & b & -b & 0.5(3b^2-1) & 0.5(3b^2-1) & -b^2 & 0.5(5b^3-3b) & -0.5(5b^3-3b) & -0.5(3b^2-1)b & 0.5(3b^2-1)b \\ 1 & -b & b & 0.5(3b^2-1) & 0.5(3b^2-1) & -b^2 & -0.5(5b^3-3b) & 0.5(5b^3-3b) & 0.5(3b^2-1)b & -0.5(3b^2-1)b \\ 1 & -b & -b & 0.5(3b^2-1) & 0.5(3b^2-1) & b^2 & -0.5(5b^3-3b) & -0.5(5b^3-3b) & -0.5(3b^2-1)b & -0.5(3b^2-1)b \\ 1 & a & b & 0.5(3a^2-1) & 0.5(3b^2-1) & ab & 0.5(5a^3-3a) & 0.5(5b^3-3b) & 0.5(3a^2-1)b & 0.5(3b^2-1)a \\ 1 & b & a & 0.5(3b^2-1) & 0.5(3a^2-1) & ab & 0.5(5b^3-3b) & 0.5(5a^3-3a) & 0.5(3b^2-1)a & 0.5(3a^2-1)b \end{bmatrix} \quad (3.145)$$

$$(1)-(2)=\begin{bmatrix}0 & 0 & 2a & 0 & 0 & 2a^2 & 0 & (5a^3-3a) & (3a^2-1)a & 0\end{bmatrix},$$
$$(3)-(4)=\begin{bmatrix}0 & 0 & 2a & 0 & 0 & -2a^2 & 0 & (5a^3-3a) & (3a^2-1)a & 0\end{bmatrix},$$
$$[(1)-(2)]-[(3)-(4)]=\begin{bmatrix}0 & 0 & 0 & 0 & 0 & 4a^2 & 0 & 0 & 0 & 0\end{bmatrix},$$
$$[(5)-(6)]-[(7)-(8)]=\begin{bmatrix}0 & 0 & 0 & 0 & 0 & 4b^2 & 0 & 0 & 0 & 0\end{bmatrix},$$
$$\therefore\{[(1)-(2)]-[(3)-(4)]\}/a-\{[(5)-(6)]-[(7)-(8)]\}/b=0.$$

where (.) means the ordinary number of the row.

Singularity happens when the selected collocation points can form two hypercubes of the same shapes and centers whose vertexes are occupied by 8 collocation points each and only the length of the sides are different. For example, for a 3-variable, 3rd-order case, let's indicate the roots as ±a, ±b. If the collocation points include {(a, a, a), (a, a,-a), (a, -a, a), (-a, a, a), (-a, -a, a), (-a, a,-a), (a, -a, -a), (-a, -a, -a), (b, b, b), (b, b,-b), (b, -b, b), (-b, b, b), (-b, -b, b), (-b, b,-b), (b, -b, -b), (-b, -b, -b)}, then out of the 16 rows defined by these points, 5 of them are linearly dependent on others. Since the number of combinations of the roots is always larger than the number of terms for a p-variable, m-order expansion, it is possible to avoid the ones that give singularity.

GSI

The expected value of g is:

$$g_0=\int_{-\pi}^{\pi}\int_{-\pi}^{\pi}\int_{-\pi}^{\pi}\left[\sin(\theta_1)+a\sin^2(\theta_2)+b\theta_3^4\sin(\theta_1)\right]p_1(\theta_1)p_2(\theta_2)p_3(\theta_3)d\theta_1d\theta_2d\theta_3=\frac{a}{2} \quad (3.146)$$

and

$$D=\int_{-\pi}^{\pi}\int_{-\pi}^{\pi}\int_{-\pi}^{\pi}\left[\sin(\theta_1)+a\sin^2(\theta_2)+b\theta_3^4\sin(\theta_1)\right]^2p_1(\theta_1)p_2(\theta_2)p_3(\theta_3)d\theta_1d\theta_2d\theta_3-g_0^2$$
$$=\frac{a^2}{8}+\frac{b\pi^4}{5}+\frac{b^2\pi^8}{18}+\frac{1}{2}. \quad (3.147)$$

g1 is evaluated as

$$g_1(\theta_1)=\int_{-\pi}^{\pi}\int_{-\pi}^{\pi}\left[\sin(\theta_1)+a\sin^2(\theta_2)+b\theta_3^4\sin(\theta_1)\right]p_2(\theta_2)p_3(\theta_3)d\theta_2d\theta_3-g_0$$
$$=\frac{b\pi^4\sin(\theta_1)}{5}+\sin(\theta_1) \quad (3.148)$$

and

$$D_1=\int_{-\pi}^{\pi}g_1^2(\theta_1)p_1(\theta_1)d\theta_1$$
$$=\frac{b\pi^4}{5}+\frac{b^2\pi^8}{50}+\frac{1}{2} \quad (3.149)$$

g2 is evaluated as:

$$g_1(\theta_2)=\int_{-\pi}^{\pi}\int_{-\pi}^{\pi}\left[\sin(\theta_1)+a\sin^2(\theta_2)+b\theta_3^4\sin(\theta_1)\right]p_1(\theta_1)p_3(\theta_3)d\theta_1d\theta_3-g_0$$
$$=a\sin^2(\theta_2)-a/2 \quad (3.150)$$

Other partial variances $D_{i_1\cdots i_s}$ can be obtained analytically as

$$D_2=\frac{a^2}{8} \quad (3.151)$$

$$D_3 = D_{12} = D_{23} = D_{123} = 0 \tag{3.152}$$

$$D_{13} = \frac{8b^2\pi^8}{225} \tag{3.153}$$

The agreement of Monte Carlo method with the analytical solutions is also tested. Latin Hypercube Sampling (LHS) method was implemented in MATLAB® with 5000 and 10000 sampling points. The comparison is shown in Table 3.6. The agreement between the numerical results and the analytical results is acceptable. The convergence of the LHS method is slow. The effect of rank is to decrease the relative influence of the higher order term as the rank index S_{13} is smaller than the non-rank one, while increases the relative influence of the first order terms as the rank indices of S_1 and S_2 are both larger than the non-rank ones.

Table 3.6 Comparison of Analytical and Numerical Solutions of Sensitivity Indices

	Analytical Solution	5000 Samples	10,000 Samples	Ranks of 5000 Samples
S_1	0.314	0.290	0.333	0.311
S_2	0.443	0.434	0.445	0.511
S_3	0.000	0.006	0.009	0.008
S_{12}	0.000	0.021	0.004	0.006
S_{23}	0.000	0.021	0.004	0.019
S_{31}	0.243	0.251	0.210	0.161
S_{123}	0.000	-0.129	-0.004	-0.040

To study the convergence of the LHS method, the indices were calculated using a set of samples ranging from 100 to 10,000. The results can be seen in Figure 3.10 and Figure 3.11. It can be seen that both the mean and the standard deviation of g converge to the analytical solutions. However, the mean converges at a faster rate than the standard deviation. The square of the sampled points magnifies the errors in the sampling. The convergence rates of the sensitivity indices are similar to that of the standard deviation except for the very beginning, as can be seen in Figure 3.11. The top line is the normalized D, which is the D calculated from the samples divided by the analytical solution in Equation (3.139).

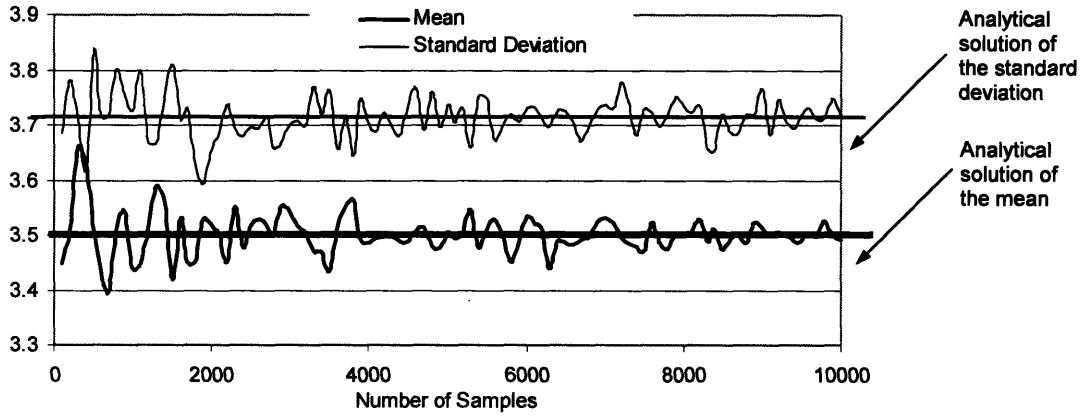

Figure 3.10 Convergence of the Mean and Standard Deviation of Equation (3.139) Using the LHS Method for GSI

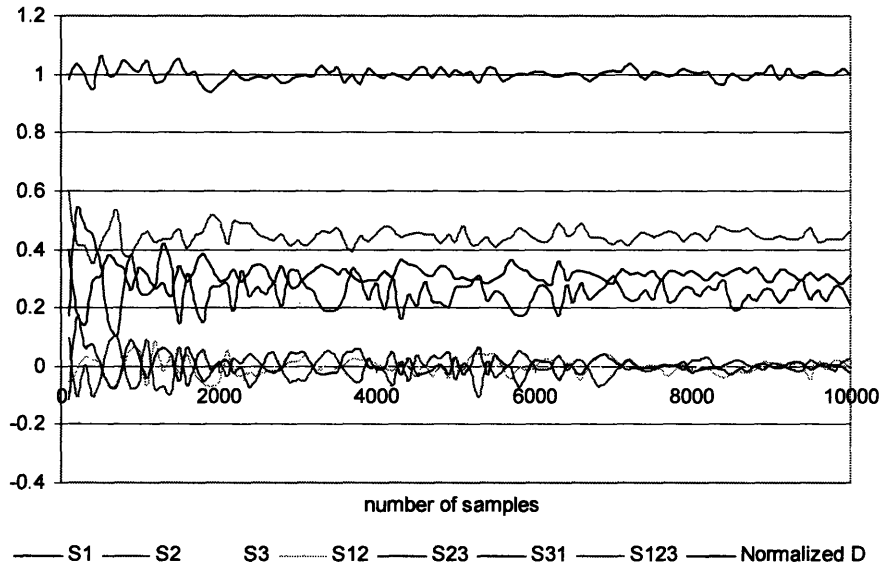

Figure 3.11 Convergence of the Sensitivity Indices of Equation (3.139) Using the LHS Method for GSI

Table 3.7 shows that the results of the three methods give agree with each other in magnitude, except that the FAST method lumps together the contributions of a parameter individually and along with other parameters. Hence, it does not show the contribution from $\theta_1\theta_3$ and the contribution of θ_1 is larger than θ_2. It has been developed to calculate these contributions separately as DEMM and GSI [58].

Table 3.7 Comparison of Sensitivity Methods on a Non-Linear, Non-Monotonic Three-Parameter Case

	θ_1	θ_2	θ_3	$\theta_1\theta_3$
FAST	0.425	0.376	1.37E-14	N/A
DEMM	0.840	3.29*	0	3.80
GSI	0.314	0.443	0	0.243

* This is the contribution of θ_2 at the 2nd order. See Equation (3.144).

3.3.3 Comparison of the Methods

- Relationship among the Methods

Even though starting from very different setting, correlation ratios, ANOVA, importance measures, Sobol' and the first order sensitivity indices of FAST arrive at the same quantity $Var_\theta[E(Y|\theta)]$ [53]. We can think of the above quality in this way: the goal of our sensitivity analysis is to find a parameter θ_i that if fixed, reduces the variance in Y $Var(Y|\theta_i = \theta_i^*)$ the most. However, since we do not know the true value of θ_i we do not know where to fix θ_i. At the same time, for non-linear models, it is possible that $Var(Y|\theta_i = \theta_i^*) \geq Var(Y)$. This problem can be overcome by averaging this measure over the distribution of the uncertain factors to obtain $E_{\theta i}[Var_{\theta -i}(Y|\theta_i)]$. The subscripts mean that the average is over all the possible values of θ_i, while the variance is over all the possible values of $\theta_{j,\, j\neq i}$ while θ_i is fixed. Because

$$E[Var(Y \mid \theta_i)] + Var(E[Y \mid \theta_i]) = Var(Y) \tag{3.154}$$

the smaller $E[Var(Y|\theta_i)]$ is, the better θ_i is in reducing Var(Y). It is the same as saying that the larger $Var(E[Y|\theta_i])$ is, the better θ_i is in reducing Var(Y). $Var(E[Y|\theta_i])$ is called the first order effect of θ_i on Y.

Table 3.8 compares the sensitivity methods from various aspects. It can be seen that FAST, DEMM, and GSI share many of the same properties. This is because they all express the variance of the output as a summation of contributions from each individual inputs and their interaction terms. The difference is how they come up with the summation.

- Assumptions of the Methods

The accuracy of the sensitivity analysis results depends on whether the key assumptions of the methods are satisfied or not. Hence when applying the methods, care needs to be taken for checking the validity of the assumptions. These assumptions are listed in Table 3.8. It can be seen that variance based methods FAST, DEMM, and GSI require the least amount of assumptions, therefore they are most applicable to different systems. However, this comes at a computational cost compared to the simpler methods.

- Representation of Sensitivity

Each sensitivity method has its own measure of sensitivity. Local sensitivity analysis only gives the gradients of the outputs to the inputs at local points. The FAST, DEMM, and GSI methods can clearly apportion the output variance to the variance in inputs. If the linearity and other assumptions are satisfied, linear correlation coefficients

and ANOVA can do the same. When apportioning the variance, DEMM gives the contribution at different orders such as the 1st order, the 2nd order, the joint 2nd order, while the other methods can give an aggregate contribution to variance.

- Computational Issues

Large complex systems can be computationally intensive. Therefore, there are incentives to identify sensitivity methods that do not entail significant additional computation requirements. In this aspect, DEMM requires the least amount of manipulation of the original model. Only p·M+1 evaluations are needed, where p is the number of uncertain input parameters and M is the order of polynomial chaos expansion. Unless the system is highly non-linear and non-monotonic, the 3rd to 4th order of expansion is sufficient. For a similar system, the number of evaluations of the model for FAST increases almost linearly with the number of the parameters. Based on the data provided in [39], the regressed formula is $N = 241p - 1449$, which is one or two orders of magnitude larger than that of DEMM. For GSI, the number of evaluations is determined by the integration of equations such as Equation (3.108). Its orders of magnitude is similar to a Monte Carlo simulation, which is much larger than DEMM and FAST. ANOVA and correlation methods can use the results of a Monte Carlo analysis for generating mean and variance without additional model runs.

Table 3.8 Comparison of Sensitivity Methods

		Local Sensitivity	ANOVA	Linear Correlation Coefficient	Rank Correlation Coefficient	FAST	DEMM	GSI
Requirements on Model	Deterministic or Probabilistic	D*	P*	P	P	P	P	P
	Linear	Y	Y	Y	N	N	N	N
	Monotonic	Y	Y	Y	Y	N	N	N
	Outputs Normally Distributed	N	Y	N	N	N	N	N
	Tolerate Correlation in Inputs	N	Y	Y	Y	N		Y
	Discrete Systems	N	Y	Y	Y	N	N	N
Method Capacity	Model Dependent	Y	N	N	N	N	N	N
	Local Method or Global Method	L**	G**	G	G	G	G	G
	Arbitrarily Large Variation in Inputs	N	Y	Y	Y	Y	Y	Y
	Simultaneous Variations in Inputs	N	Y	Y	Y	Y	Y	Y
	Generate Moments	N	N	N	N	Y	Y	Y
	Generate Distributions	N	N	N	N	N	Y	N
Representation of Sensitivity	Apportion Variance to Variance in Inputs	N	Y	Y	N	Y	Y	Y

* D – Deterministic, P – Probabilistic. ** L – Local Method, G – Global Method

For systems with differential equations, the common linearized methods requires p sensitivity coefficients $\partial Y / \partial \theta_i$, i = 1, 2, ..., p to be calculated in addition to the original Equation (3.1). The FAST method requires Equation (3.1) to be evaluated at N_s points. For a system that does not involve differential equations, such as the one described in this paper, the advantages in computational time saving using FAST is not as obvious. However, for a system with m differential equations and p parameters, the linearized method requires the one-time solution of mp differential equations in addition to the original m differential equations; while the FAST method requires N_s solutions of the original set of m differential equations.

Another side of the computational issue is how easily can the methods be implemented once the evaluations of the model are done. The correlation methods require minimum calculations and programming, while all other methods' implementation in computer codes is non-trivial.

3.4 Conclusion

Seven sensitivity analysis methods have been reviewed and compared here. Each of them has its assumptions and limitations, advantages and disadvantages. The choice of the method(s) should be determined by the nature of the system under study, the need of the sensitivity analysis, and the computation power. For example, some of the methods described here can not only give measures of the sensitivity, but also generate the moments or the approximated probability distributions of the system. DEMM is capable of both, while GSI and FAST can only generate the moments. Once a approximated distribution is available, other sensitivity methods can be applied to this simplified model, therefore reduce the computation requirements. Therefore, if a study requires the distribution of the outputs with limited computational power, DEMM is a good method.

Because RCC can indicate the first order effect of the parameters on the outputs' variance, and has been implemented in @Risk, it was used as a first cut for all the more than 400 parameters in the LCA models. Given its limitation, other more sophisticated method such as FAST can be used for the top 10 most important parameters to obtain a more precise magnitude of the contribution accounting for the higher order non-linear effects.

It is important to define the setting of the problem prior to the analysis. A sensitivity analysis should not focus on the model output itself, but on the answer the models is supposed to provide for the decision [55]. In the decision context of this thesis, the environmental and process models are used to distinguish alternative technologies. As long as the relative ratios of the criteria, such as the global warming potential, exceed certain value with certain confidence level, the accuracy of the analysis is satisfactory. Therefore, reducing the variance, which can increase the confidence level, is a proper setting of the problem.

Chapter 4 Evaluation Models & a Case Study on Cu CVD

In this chapter, the environmental and economical evaluation models will be described. Even though the main topic of the thesis is on comparison alternative technologies, for the ease of understanding the evaluation models, a case study on the Cu chemical vapor deposition (CVD) process alone will be used to illustrate the models. Because of the importance of understanding the process under study, the Cu CVD process will be described here in details. In a later chapter, how much information is needed for a meaningful comparison will be discussed.

4.1 The Cu CVD Process and its Modeling

For the metallization of future ultra-large scale integrated devices, copper has been considered a promising material to replace aluminum due to its lower electrical resistivity and higher electromigration resistance. These superior properties promise the improvement of the speed and reliability of devices.

There are four ways to deposit copper onto a silicon wafer, namely physical vapor deposition (sputtering), electroless deposition, electroplating, and CVD [59]. CVD "is a method of forming thin solid film on a substrate by the reaction of vapor phase chemicals which contain the required constituents." [60] At the device level in a microprocessor, the dimensions of the metal interconnect can fall below 0.1 microns. This requires the copper metallization technique to ensure a perfect filling of surface etched trenches and vias, whose aspect ratio exceed 10:1. With its inherently conformal deposition, CVD offers the ability to achieve either void free full fill, or create ultra-thin 'seed' copper layers for further void free full fill.

Currently the most commonly used precursors is CupraSelct™. The chemical formula is Cu^{I}(trimethylvinylsilane)(hexafluoroacetylaceonate), or Cu^{I}(tmvs)(hfac) ($C_{10}H_{13}CuF_6O_2Si$). The formulas for tmvs and hfac are $C_5H_{12}Si$ and $C_5HF_6O_2$, respectively. The carrier gas can be hydrogen, argon, and other gases depending on the company. At room temperature, the precursor is liquid. It is heated up to gas phase and mixed with carrier gas before entering the deposition chamber.

4.1.1 Process Model

The following description of the Cu CVD process is based on a Cu CVD Unit Process model developed by University of Maryland [61]. The model assumes the reactor as homogenous and isothermal. No side reactions are considered either. There is also no deposit of Cu on the inner chamber wall.

- **Reaction Mechanism of Cu CVD**

The Cu CVD reaction can be described as a sequence of steps, which is shown in Figure 4.1:

a. The precursor transports onto the surface of the substrate,
b. The precursor adsorbs onto the surface of the substrate,
c. The adsorbed species undergo a chemical reaction to form the Cu film,
d. The reaction by-products desorb from the substrate surface,
e. The reaction by-products transport out of the reaction chamber.

The surface reaction is:

$$2\ Cu^{I}(tmvs)(hfac) \rightarrow Cu^{0} + Cu^{II}(hfac)_2 + 2\ tmvs$$

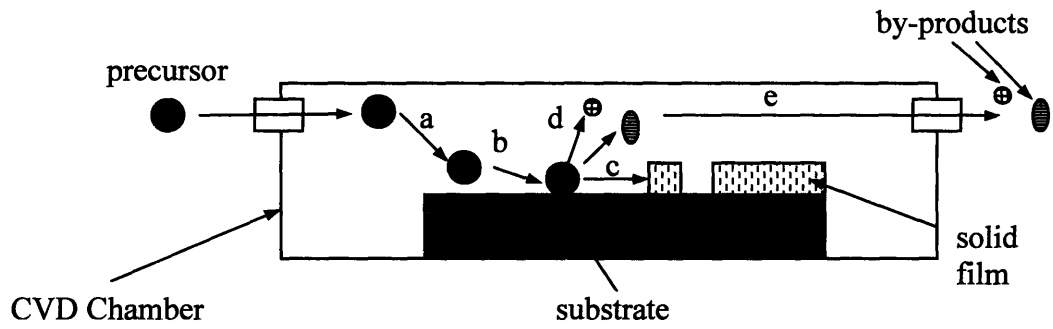

Figure 4.1 Schematic Picture for the CVD Reaction

The overall film growth rate is proportional to the effective surface reaction rate.

$$R_g = \frac{0.5 \times R_e \times V_{RI} \times MW}{\rho \times A} \times 10^8 \qquad (4.1)$$

where R_g – Film growth rate, A/sec;
R_e – Effective surface reaction rate, mol/l-sec;
V_{RI} – Reactor volume, l;
MW – Molecule weight of the film, g/mol;
ρ – Film density, g/cm^3;
A – Wafer area, cm^2.

The effective surface reaction rate is controlled by all the above steps, with the slowest step determining the final growth rate. The Cu CVD Unit Process assumes that steps (b), (d), and (e) are relatively fast comparing to steps (a) and (c), so the film growth rate is only determined by the transport rate and surface reaction rate, which is shown below.

$$R_e = \frac{1}{\frac{1}{R_t} + \frac{1}{R_s}} \qquad (4.2)$$

where R_t – Transport rate, mol/l-sec;
R_s – Surface reaction rate, mol/l-sec.

The transport rate is determined as follow:

$$R_t = k_t \cdot (C_g - C_s) \tag{4.3}$$

where k_t – transport rate coefficient, which was set to be 0.388506 sec^{-1} in the model; This implicitly assumed that the transport rate coefficient does not change with temperature.

C_g – Precursor concentration in the gas phase, mol/l;

C_s -- Precursor concentration on the substrate surface, mol/l.

The surface reaction rate is determined by the surface precursor concentration and the surface reaction coefficient:

$$R_s = k_s \cdot C_s \tag{4.4}$$

where k_s – Surface reaction coefficient, sec^{-1}.

$$k_s = A \cdot e^{-\frac{E_a}{RT}} \tag{4.5}$$

where A – Surface reaction rate constant, which is set to $1.16 * 10^{-8}$ sec^{-1};

E_a – Activation energy, which is set to $8.1 * 10^4$ J;

R – Molar gas constant, which is 8.314 J/mol-K;

T – Wafer temperature, K;

The gas phase precursor concentration is calculated as follow:

$$C_g = 760 \cdot 22.4 \cdot P_p \tag{4.5}$$

where P_p – Precursor pressure, torr.

It is assumed that the system is at steady state, hence the transport rate equals the reaction rate. Equate Equation (4.3) and (4.4), the surface precursor concentration is be solved as:

$$C_s = \frac{C_g}{1 + \frac{k_s}{k_t}} \tag{4.6}$$

- **Cu CVD Process Flow Diagram**

The process model developed by the University of Maryland [61] enables the real time calculation and monitoring of the parameters mentioned above. Its schematic diagram is shown below in Figure 4.2. It was realized in VisSim™. The model assumes that there is no reactant gas in the chamber initially. Inside the chamber, the wafer substrate is positioned on a heater. The model also assumes that before the reaction gas enters the chamber, the substrate has been heated up to a pre-set temperature. The unreacted reactant is pumped out into the exhaust by a downstream pump. After the film thickness reaches the desired value, the valves to the precursor cylinder and hydrogen cylinder is turned off. The downstream pump is still on until the residue gas is pumped out. In the model, a wafer temperature stabilization time of 10 seconds and a wafer load/unload time of 50 seconds are added to the process time to give the elapsed cycle time.

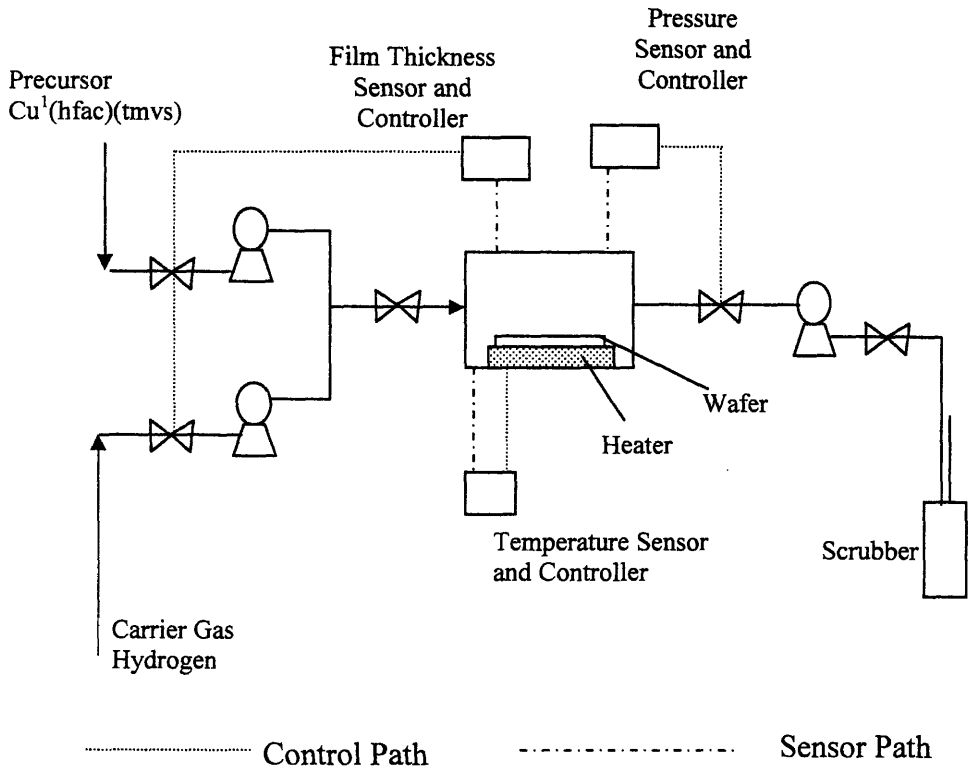

Figure 4.2 Schematic Diagram of the Cu CVD Process

4.1.3 Examples of Applying the Cu CVD Model

Two series of simulations were performed using the VisSim™ model to study the Cu CVD system's response to its inputs. In the first series, the chamber pressure, the precursor flow rate, and the carrier gas flow rate were set to constants, while the substrate temperature varied from 150 °C to 250 °C. The results are shown in Figure 4.3, which shows that as the temperature increases, both the total process time and the energy consumption decrease, and the utilization percentage increases. This is because the high the temperature is, the faster surface reaction rate is. In lower temperature range, where the surface reaction is the limiting step, the increase of surface reaction rate leads to the increase of overall reaction rate. Even though the power for maintaining the substrate temperature increases, the reduction of process time leads to the reduction of the total energy consumption. However, as the temperature increases to a certain point, around 210°C, the reaction becomes transport limiting. The increase of overall reaction is minimum. This can be seen from the graph that the total time approaches a plateau after 210°C. In this area, the effect of the power for maintaining the substrate temperature takes over the effect of reduced process time, which results in the increase of the energy consumption.

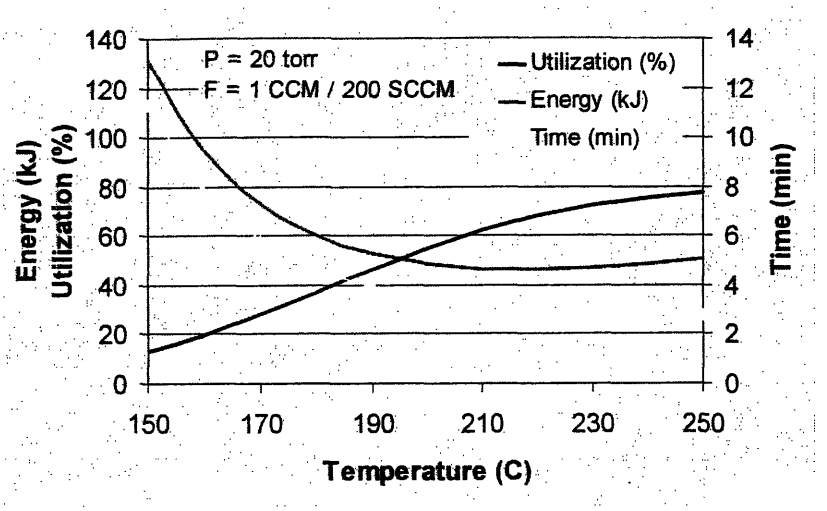

Figure 4.3 Model Responses of the Energy Consumption and the Utilization Percentage to the Change of Temperature with P = 20 torr, F_p = 1 ccm, and F_{cg} = 200 sccm

In the second series, the chamber pressure, the substrate temperature, and the precursor flow rate over the carrier gas flow rate ratio were set to be constant, while the precursor flow rate varied from 0.5 to 2.5 ccm. The results are shown in Figure 4.4, which shows that as the precursor flow rate increases, the process time decreases, which also leads to the decrease of the energy consumption. However, the precursor utilization percentage decreases. This is because the high flow rate keeps the high gas phase precursor concentration, which leads to higher transport rate and faster reaction. At the same time, it also means that a gas phase with high precursor concentrations be pumped out, which results lower precursor utilization percentage.

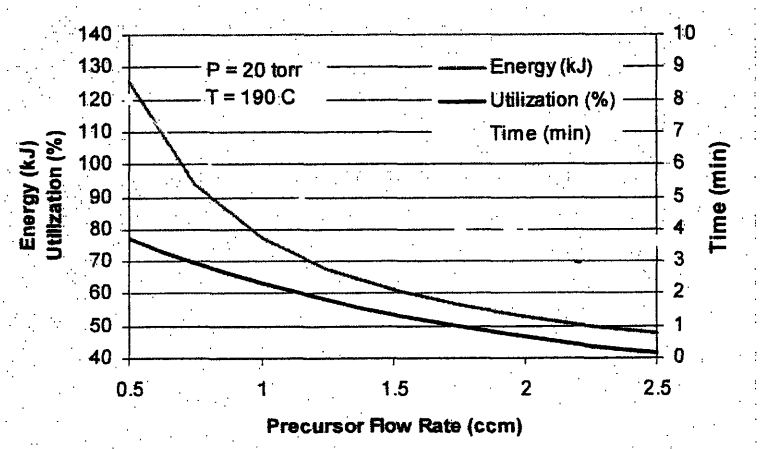

Figure 4.4 Model Responses of the Energy Consumption and the Utilization Percentage to the Change of the Precursor Flow Rate

4.2 Process by Product Input-Output Life Cycle Assessment (PIO-LCA)

The development of technology has linked the world together. Environmental issues are no longer local. Provision of raw materials, production, and disposal of waste can happen at different locations. Hence, it is more reasonable for engineers to consider not only the environmental impacts directly generated in the processes they design, but also those associated with the provision of input materials for the processes, and downstream disposal. LCA is a procedure that satisfies this purpose [62]. Figure 4.5 shows selected upstream processes of the Cu CVD process.

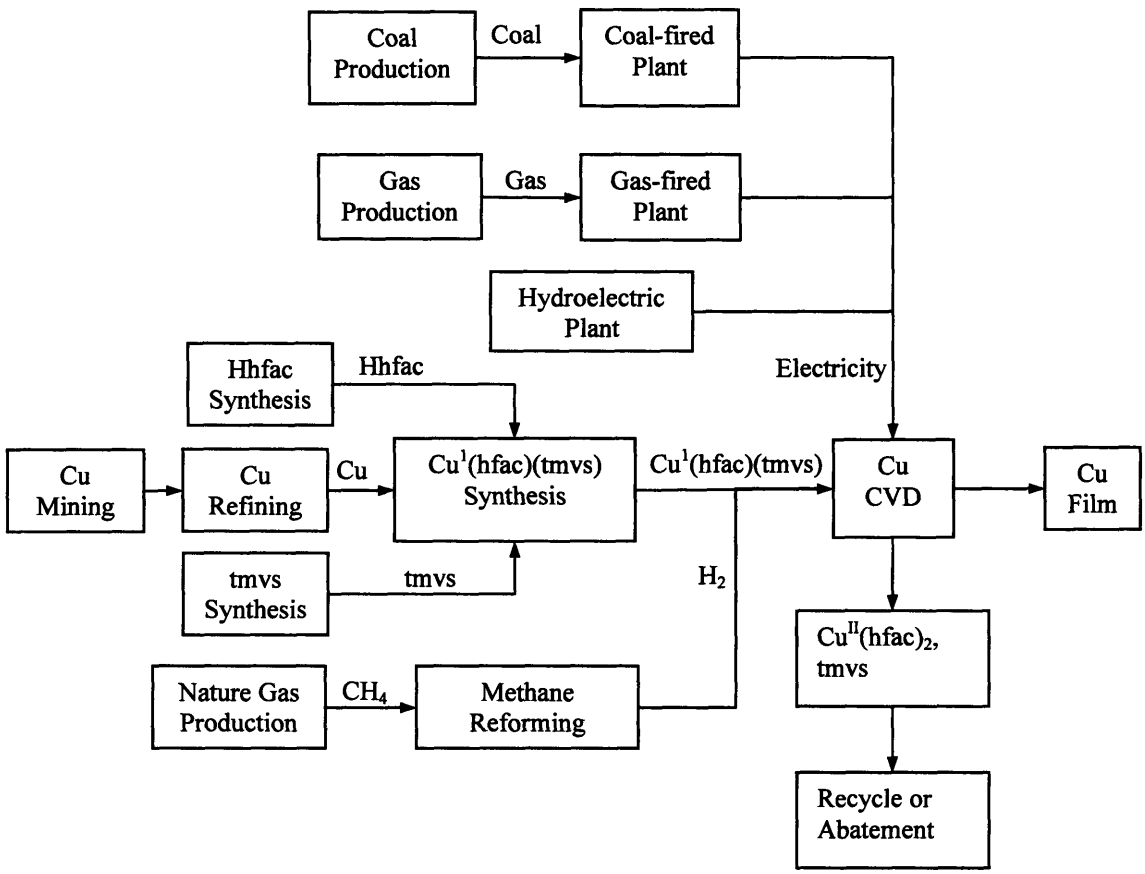

Figure 4.5 Selected Upstream Processes of the Cu CVD Process

The PIO-LCA method [12] was built on the methodology of Economic Input-Output LCA. It allows investigation at the process level rather than only at the industry level[12]. PIO-LCA represents the production of a product as a network. Unlike most LCA software which represents the production in a tree-like representation, the network representation is able to describe feedback loops and relationships among products produced in multi-product processes, as well as represent more clearly an input common to many processes. Mathematically, the network is realized in matrixes, which makes the calculation and analysis of the production network very straightforward. Upstream data

of the national averages were used. The calculation was done on an application based on Access® and Excel® [63]. The PIO-LCA method was originally developed by Cano-Ruiz [12] and is summarized below using the matrix format to describe its inputs and calculations.

4.2.1 Method Description

- **Input data**

The processes and products involved in the evaluation are organized in two matrixes: a "usage matrix" (B) and a "fabrication matrix"(C). Columns in each matrix correspond to processes, while rows correspond to products. Products here refer to any product in the common sense and service of economic value. Data regarding emissions are organized into a matrix of direct environmental exchanges (E).

The existence of multi-product processes and products being produced by different technologies makes it necessary to establish accounting rules to correctly allocate process throughputs to product demands to avoid double counting. The first rule is to allocate the amount of throughput of process that is attributed to one unit of the product made in that process. A 'Market share' matrix (F) and 'product price' vector (p) are needed for the first rule. Prices are combined with the fabrication matrix to build an 'allocation matrix' (G):

$$G_{ji} = \begin{cases} \dfrac{p_i}{\sum_{i'} C_{i'j} p_{i'}} & \forall C_{ij} \neq 0 \\ 0 & \forall C_{ij} \neq 0 \end{cases} \tag{4.7}$$

where the subscripts i and i' correspond to the product and the subscript j to the process. The value G_{ji} gives the amount of throughput of process j that is attributed to one unit of the product i made in that process. Another accounting rule is to allocate the demand for a product among the different processes that produce it based on market share. The allocation matrix is combined with the market share matrix to generate a process-by-product throughput matrix (D):

$$D_{ji} = F_{ji} G_{ji} \tag{4.8}$$

The entry D_{ji} gives the amount of throughput of process j that is attributable to the generation of one unit of product i at the current prices and prevailing process supply mix.

The inputs matrixes and their relationship can be seen in Figure 4.6.

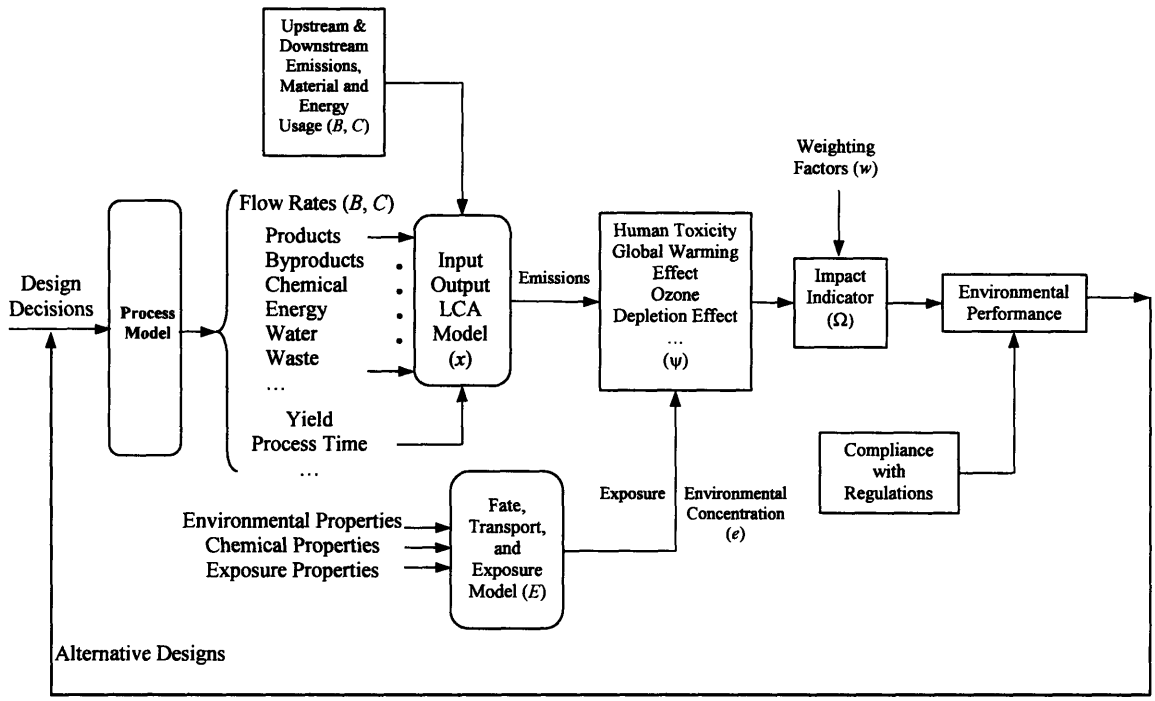

Figure 4.6 Components of an Environmental Evaluation Model

- **Inventory analysis**

In the inventory analysis stage, the life-cycle environmental exchanges are obtained for each product or process. Because feedback loops exist in production chains, a vector of total product requirements (q) (including direct and indirect product requirements) is needed:

$$q=(I+A_{prod}+A_{prod}\cdot A_{prod}+...)\cdot d=(I-A_{prod})^{-1}\cdot d \tag{4.9}$$

where I – Identity matrix.

$A_{prod} = B\cdot D$, which is the product-by-product direct requirements matrix.

To calculate the environmental exchanges, the total process throughputs are calculated as:

$$x = D\cdot q = D\cdot (I - A_{prod})^{-1}\cdot d. \tag{4.10}$$

The total throughput requirements vectors gives the amount of process activity associated with the provision not only of the products specified in the demand vector, but also with the provision of all the necessary raw materials.

The vector of life cycle environmental exchanges can be calculated as:

$$e = E\cdot x = E\cdot D\cdot (I - A_{prod})^{-1}\cdot d \tag{4.11}$$

- **Impact analysis**

In life cycle assessments, it is usually assumed that contributions due to the process or product of interest to the designer are small enough compared to the total world output. Hence the marginal increase in environmental impacts can be considered linear. The characterization factors for the exchanges can be stored in a "characterization

matrix" (H). The vector of impact category environmental indicators ψ is obtained by multiplying the transpose of matrix H:

$$\psi = H^T \cdot e = H^T \cdot E \cdot x = H^T \cdot E \cdot D \cdot (I - A_{prod})^{-1} \cdot d \quad (4.12)$$

The vector ψ can be then be multiplied with the transpose of vector w, which stores the valuation factors for each impact categories, to generate an overall index of environmental impact Ω:

$$\Omega = w^T \cdot \psi = w^T \cdot H^T \cdot e = w^T \cdot H^T \cdot E \cdot x = w^T \cdot H^T \cdot E \cdot D(I - A_{prod})^{-1} \cdot d \quad (4.13)$$

Both the characterization factors and the valuation factors are subject to large uncertainties, which can be of 3~6 orders of magnitude. The qualification of uncertainties and the inclusion of them in analysis are therefore necessary.

To understand the sources of the impacts, it is useful to decompose the overall impact indicator based on each process or product. For example, the decomposition used in this work is $\text{Diag}(x) \cdot E^T \cdot H$, which generates the matrix of contributions of process throughputs to impact category scores.

- **Improvement Analysis**

In order to evaluate the tradeoffs between alternative technologies, it is desirable to have a set of unit indicators that reflect the changing of the outputs with the changing of the inputs. The designer also needs to know what factors drive the indicator to identify improvement opportunities. An example for such a sensitivity analysis is the total impact of each unit of process throughput within each impact category given by:

$$\psi \cdot x = (I - D \cdot B)^{-1} \cdot E^T \cdot H \quad (4.14)$$

This study considered 7 environmental and health impacts. The global warming potential (GWP), which the semiconductor industry has been working hard to curb, is analyzed extensively. Other impacts can be studied in a similar manner.

4.2.2 Environmental Evaluation Database

A crucial component of any environmental evaluation besides the methodology is the database it uses. The database should store the necessary data in a transparent and comprehensive manner. It should also be able to be easily updated as new information becomes available. The database used in this work contains 31 tables. Input data and evaluation factors mentioned in the previous section can be obtained from the database.

The database can be used to store and explore data for multiple case studies. The tables that are related to defining the case study are organized in Table 4.1. Also listed are tables for storage of the economic information, chemical properties, and evaluation information. The table that stores the case studies names is Case Studies. The final products of interest for each case study are stored in Table Case Studies (products). The evaluation method for each case study is stored in Table Case Study (valuation). The processes and the products of all the processes that involve in the case study are stored in Table Processes and Table Products, respectively. The evaluation method treats data as uncertain and uses probability distributions to represent the uncertainty. The descriptions of the distributions are stored in Table Distribution. There are also some

tables documenting the process of the construction of the database. Their names start with 'Documentation'. The content of other tables can be easily concluded from their names, so they will not be explained here.

The User's Manual in the Appendix D explains the procedure of creating a new case study using the EnvEvalTool. After the case study is created, related data can be exported to Excel spreadsheets, which will then be used in the evaluation calculation.

Table 4.1 Classification of Tables in EnvEvalTool Database

Classification	Table Name
Defining the Case Study	Case Studies
	Case Studies (products)
	Case Studies (valuation)
Input-Output Data	Make Coefficient
	Use Coefficient
	Emission Factors
Economic Data	Market Shares
	Prices
Chemical Properties	Chemical Classifications
	Chemical Group Membership
	Chemical Groups
	Chemical Information
	Chemical Names
Valuation Data	CF to CF Correlations
	CF to VF Correlations
	Characterization Factors (CF)
	Exposure Factor Distributions
	Exposure Factors
	Impact Categories
	Valuation Factors (VF)
	Valuation Methods
	VF to VF Correlations
Universal Information	Distributions
	Documentation Dependencies
	Documentation Design Changes
	Documentation Objects
	References
	Sources of Characterization Factors
	Sources of Emission Factors
	Sources of Exposure Factors
	Source of Input-Output Data

4.2.3 Application of the PIO-LCA Method on the Cu CVD Process

Due to the limitation of data, the evaluation was done in a small scale. Only the environmental impacts of generating energy and hydrogen as the carrier gas are considered. As more information becomes available, the evaluation can be easily updated by adding corresponding columns and/or rows in the input matrices.

The block format of the distribution overall environmental impact indicator is shown in Figure 4.7. The very left bar, left end of the box, the middle line of the box, the right end of the box, and the very right bar of the indicator are the 5%, 25%, 50%, 75%, and 95% level, respectively. For example, 50% means there is less than 50% of possibility that the indicator of the Cu CVD will fall below $8.5 per deposition, which is where the number 50% stands. Because purpose of this case study is not to compare alternative technologies, but more to demonstrate the application of the EnvEvalTool, the absolute value of the result is not very important. More emphasis is placed onto interpreting the results from different aspects. Here are some questions that we can ask: which factors contribute most to the impact? Figure 4.7 shows that there is a large uncertainty in the upper bound of the indicator. Now the questions to be answered are: which factors contribute to this uncertainty, what are the improvement opportunities?

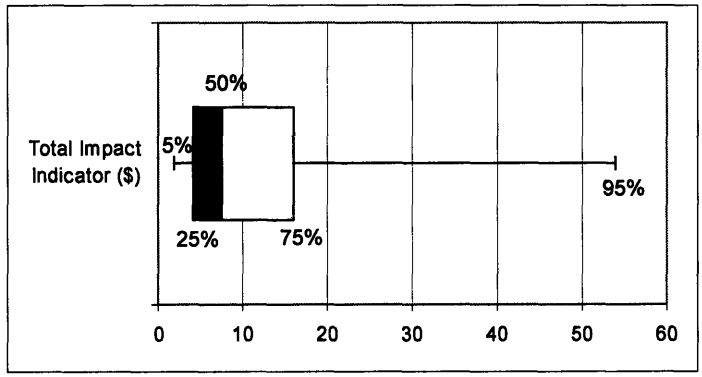

Figure 4.7 Distribution of the Overall Environmental Impact Indicator

- **Main Impact Contributors**

To answer the first question, we need to break down the overall indicator to its components. There are several ways of breaking down the indicator to individual components, as mentioned in the previous section. Let's start with the processes. The contribution of each process i can be calculated as:

$$f_{\text{proc,i}} = (E^{\text{T}} \cdot H \cdot w)_{\text{i}} \cdot x_{\text{i}} / \Omega \qquad (4.15)$$

Figure 4.8 shows the important processes that contribute to the impact indicator. It can be seen that the coal-fired power plant contributes the most, followed by diesel engine. The oil-fired power plant has certain possibility of contributing more than 20% to the indicator.

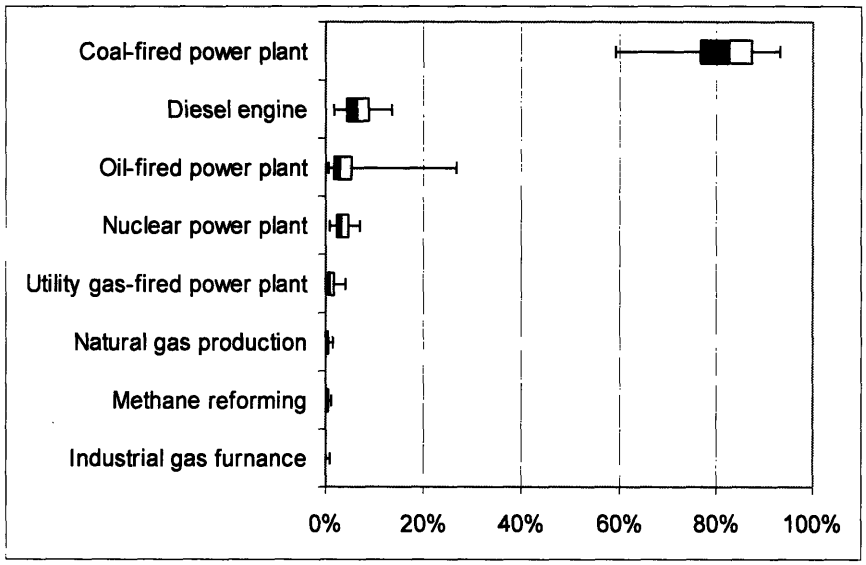

Figure 4.8 Percentage Contributions of Processes to Total Impact Indicator

By breaking down the overall impact indicator into each impact, we are able to see which effect contributes the most to the impact of coal-fired power plant. The matrix for this purpose is $\text{Diag}(x) \cdot E^{T} \cdot H \cdot \text{Diag}(w)$. The important effects are shown in Figure 4.9. These results are in consistent with the breaking down of the overall impact indicator by individual impact, which can be calculated as:

$$f_{\text{effect,j}} = w_k \cdot \psi_k / \Omega \tag{4.16}$$

Figure 4.10 shows the important effects that contribute to the impact indicator.

Even though the nominal values of human cancer toxicity potential and human non-cancer toxicity potential are relatively small, they have the potential of accounting for a large fraction of the impact. In particular, the human non-cancer toxicity potential category contributes to 30% of the impact in 10% of the Monte Carlo simulation iterations. In contrast, photochemical oxidants creation potential, eutrophication potential, and ozone depletion potential have virtually no significant chance of having a significant contribution to the total impact in this case study.

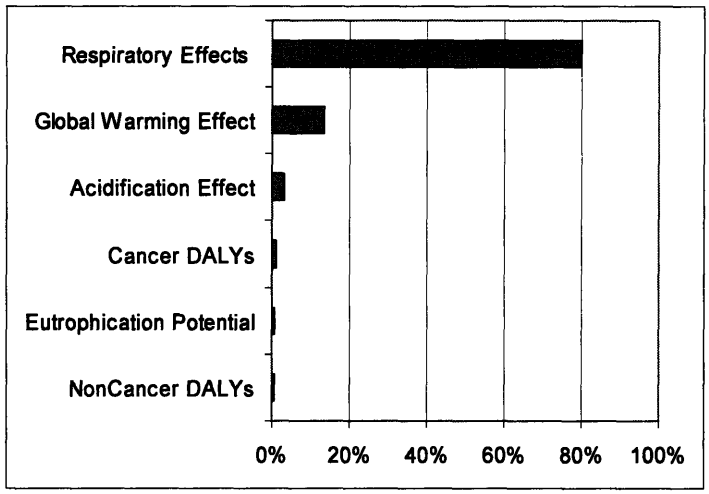

Figure 4.9 Percentage Contributions of Adverse Effects to the Impact of Coal-fired Power Plant

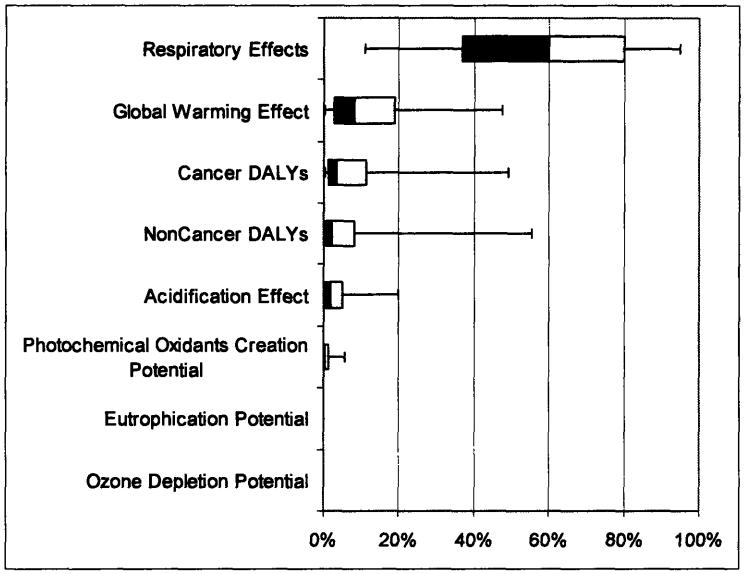

Figure 4.10 Percentage Contributions of Adverse Effects to Total Impact Indicator

Distributions for the main contributions of individual chemical emissions to the impact indicator are shown in Figure 4.11. They are calculated as:

$$f_{ex,j} = (H \cdot w)_i \cdot e_i / \Omega \qquad (4.17)$$

The nominal values show that PM10 contributes the largest impact. However, sulfur dioxide, carbon dioxide, and NOx also have significant chance to contribute more than one third of the impact. An interesting point raised by Figure 4.11 is that in almost 10% of the iterations the effects of sulfur dioxide were valued to be beneficial. This happened when the valuation factor for global warming was sampled at a high end of the distribution and the valuation factor for respiratory effects of particulate matter was sampled at a low end of the distribution. Sulfate aerosols reflect sunlight and thus have a negative contribution to radiative forcing [64]. Unfortunately they are also quite

damaging to human health, so in most of the model iterations the total impact of sulfur dioxide is judged to be adverse.

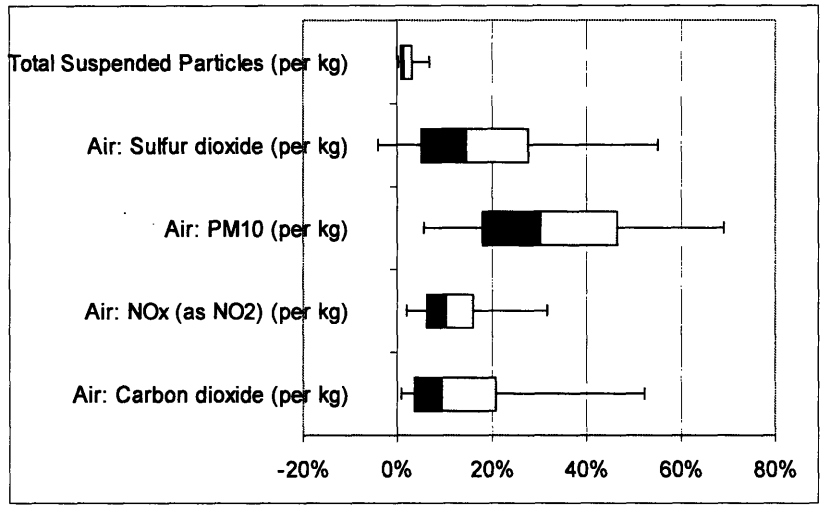

Figure 4.11 Percentage Contributions of Emissions to Total Impact Indicator

One thing to noted is that in the evaluation, a large number of environmental exchanges, processes, and ESH impacts are considered, the ones that turn out to have the probabilities of non-negligible contribution to the overall impact indicator are few. This suggests that at the beginning of the analysis, only order of magnitude estimates for emissions and characterization factors are needed. After the first analysis, the factors that cannot be neglected can be investigated with more care.

- **Improvement Opportunities**

The evaluation can also be used to for identifying improvement opportunities. For example, it can be used to identify which electricity source is more environmentally benign. As mentioned before, the coal-fired power plant contributes to around 85% of total impact. The large percentages of coal-fired power plant come from both the large market share of coal-fired power plant in generating electricity (57%) and the low thermal energy generation efficiency of coal furnace. Compared to oil furnace, which provides thermal energy for oil-fired power plant and has a unit throughput of 1055 MJ thermal energy, coal furnace has only 29.6 MJ thermal energy throughput. Thus even though the impact per unit process throughput for coal furnace is much smaller than that of the oil furnace ($0.58 compared to $11.8), to produce the same amount of electricity, using coal-fired power plant will have more impact than using oil-fired power plant. This analysis can be seen in Figure 4.12 and Figure 4.13. There is also another way to compare these two types of plant. By combing the market share matrix and the "valuation by process" matrix, we can see that coal-fired power plant consists of around 85% of impact with 57% market share, while oil-fired power plant consists of only 3% of impact with 3% market share. Per market share wise, coal-fired power plant has more impact than oil-fired plant. This means, by switching from coal-fired power plant to oil-fired power plant as the electricity source, the life cycle impact of the Cu CVD case will decrease.

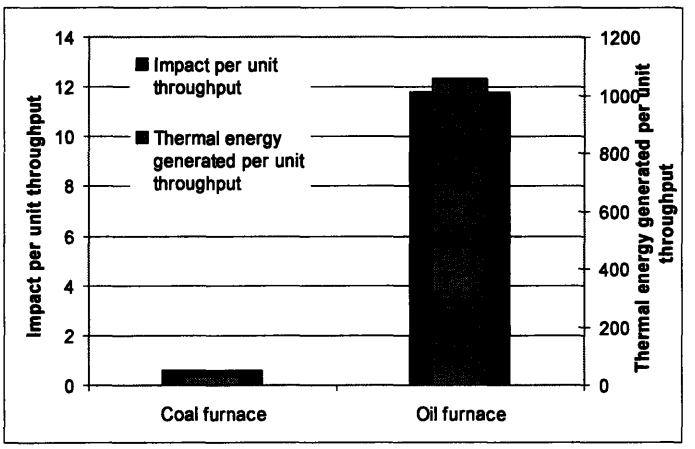

Figure 4.12 Comparison of Coal Furnace and Oil Furnace in Terms of Impact per Unit Throughput and Thermal Energy Generated per Unit Throughput

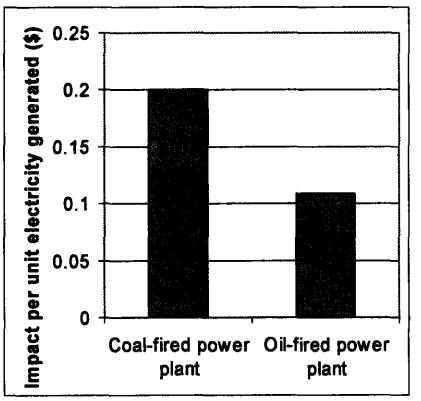

Figure 4.13 Comparison of Coal-fired Power Plant and Oil-fired Power Plant in Terms of Impact per Unit Electricity Generated

4.3 Cost-of-Ownership (COO) Analysis

The COO was designed to capture the costs of acquiring, installing, operating, and decommissioning a processing system in a factory environment {Dance, 1998 #77;Gomei, 1998 #52;Gomei, 2001 #53;SEMI, 1995 #78}. In order to represent its calculation in a comparable set-up as the PIO-LCA model, the COO model is recounted here in a matrix format. Its components can be seen in Figure 4.14.

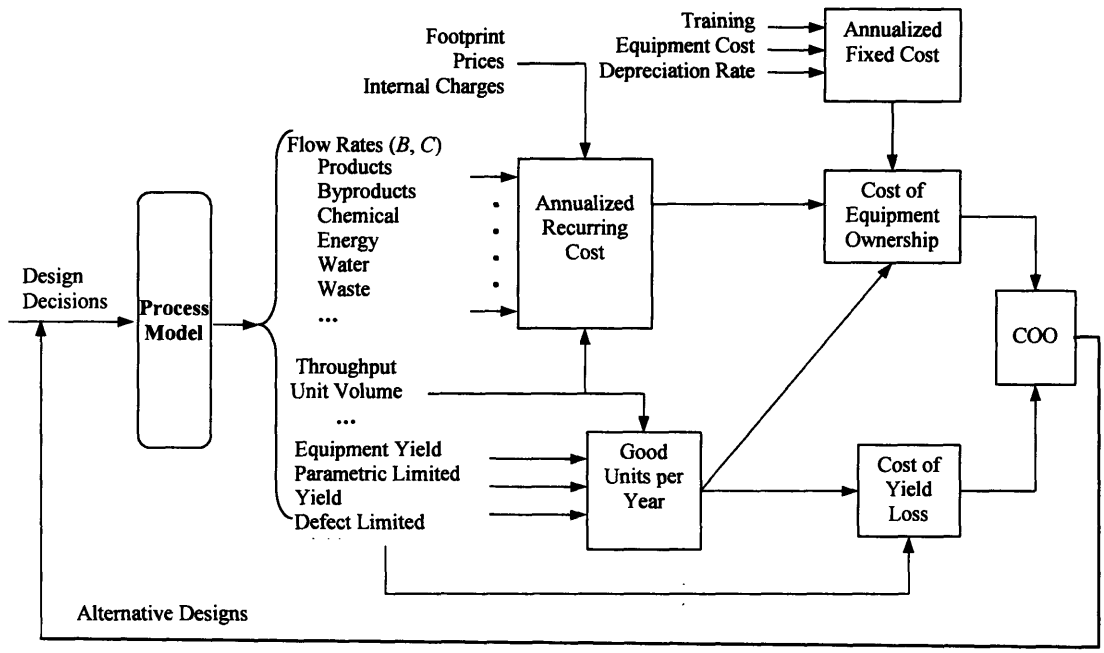

Figure 4.14 Components of an Economic Evaluation Model

4.3.1 COO Model Description

- **Input Data**

The unit usages of recurring items are stored in vector *Ur*, such as consumables, test wafers, supplies. The unit costs of these items are stored in vector *Pr*. The yields are stored in vector *Y*. Recurring cost can be classified as material, consumables, maintenance, labor, support personnel, scrap, and support service. Each of these classes can be further divided into smaller classes.

Cost of Equipment Ownership (CEO)

$$CEO = (F + R)\ (SR / GU) \tag{4.18}$$

where R – recurring cost
F – fixed cost
SR – volume required per system
GU – good unit per year

$$R = \mathrm{Pr} \cdot \mathrm{Ur}^{-1} \tag{4.19}$$

The process model provides the elements in the material, consumable, and utilities. Using the NF_3 chamber cleaning case, when R is written out, it becomes:

$$R = \left[P_{NF_3}\ \ P_{N_2}\ \ P_{Ar}\ \ P_{Energy}\ \ P_{Water}\ \ P_{WasteDispal}\ \ P_{Lbm}\ \ \ldots\ \ P_{Sp}\ \ P_{Sc}\right] \times \left[U_{NF_3}\ \ U_{N_2}\ \ U_{Ar}\ \ U_{Energy}\ \ U_{Water}\ \ U_{WasteDispal}\ \ U_{Lbm}\ \ \ldots\ \ U_{Sp}\ \ U_{Sc}\right]^T \tag{4.20}$$

where P – unit price, \$/unit;
U – unit usage.
The unit follows the subscript as below:

NF_3, N_2, Ar – example chemicals used in the process, g;
Energy – energy used in the process, Kw-h;
WasteDisposal – waste generated in the process, kg;
Lbm – labor for maintenance, hour;
Sp – support personnel, hour;
Ss – support service, hour.

$$SR = V / (TU) \tag{4.21}$$

where V – volume required, unit
T – tool throughput, wafers/year;
U – equipment utilization, dimensionless

$$U = 1 - (SM + USM + A + S + Q + E) / H \tag{4.22}$$

where SM – scheduled maintenance, hrs/week;
USM – unscheduled maintenance, hrs/week;
A – assist time, hrs/week;
S – standby time, hrs/week;
Q – production qualification time, hrs/week;
E – process engineering time, hrs/week;
H – total number of production hours scheduled per week, hrs/week.

$$GU = LTYU \tag{4.23}$$

where Y – composite yield, dimensionless;
L – useful lifetime of equipment, year;

Cost of Yield Loss (CYL)

$$CYL = (A_{ey} + A_{dy} + A_{py}) / GU \tag{4.24}$$

where A_{ey} – annualized cost of wafers lost due to equipment yield. Equipment yield is the percentage of units received by the equipment that can be passed to the next step based on any criteria such as damaged material, or material determined to be defective by inspection or test. For test equipment, validly rejected material is scrap, not a component of equipment yield.

A_{dy} – annualized attributed cost of wafers lost due to defect yield. Defect yield (DY) is the percentage of equivalent wafers that are not lost due to electrical malfunctions caused by particulate defects.

$$DY = \frac{1}{1 + (A_a DP)} \tag{4.25}$$

where A_a – activate area of the device, cm^2;
D – defect density, $/cm^2$;
P – probability that a defect will be fatal.
A_{py} – annualized attributed cost of wafers lost due to parametric yield. Parametric yield is the percentage of equivalent wafers that are not lost due to electrical malfunction caused by device parameters being outside the required range.

Cost of Ownership (COO)

COO is the sum of the cost of equipment ownership and cost of yield loss.

$$COO = CEO + CYL \tag{4.26}$$

Please note that a large part of the data in the vector Ur overlaps with the ones used in environmental valuations, such as the amounts of utility usages, waster disposal, and

consumables. An integrated modeling environment that clearly links the two sets of inputs and can present how they affect decision criteria will be very beneficial. This modeling environment will be discussed in Chapter 6.

4.3.2 Application of Modified COO on the Cu CVD Process and its Uncertainty Analysis

- **Calculation of COO of Cu CVD Process**

A COO model was built for the Cu CVD process to find the cost of putting down one layer of copper film for 300 mm wafers. The purpose of this model is not to provide a detailed analysis for the economic performance of Cu CVD, but rather to demonstrate the application of the COO analysis and applying the uncertainty analysis to a system. In addition, due to the limitation of data, many terms in the complete model were omitted, except for the ones that have proven to be important through experience such as throughput, and the ones that are unique to the Cu CVD process such as the ones related to the Cu precursor. The values of these data were mainly estimated or from similar processes. Another way to look at the simplification is to treat the purpose of the COO analysis as comparing alternative tools. The assumption is that elements, such as training, repair parts, are the same for these alternatives and can be omitted in the comparison. As well as for the simplification purpose, COO is only calculated for one year without considering the future cost.

The elements considered in the fixed cost are the deposition tool cluster cost, the abatement system cost, floor space, operation cost, and maintenance cost:

$$F = Cd + Ca + Cf + Co + Cm \tag{4.27}$$

where F – fixed cost, $/tool-yr
Cd – Deposit tool cost, $/tool-yr;
Ca – Abatement tool cost, $/tool-yr;
Cf – Floor space cost, $/tool-yr;
Co – Operation cost, $/tool-yr;
Cm – Maintenance cost, $/tool-yr;

$$Cd = Pd \cdot D \tag{4.28}$$

where Pd – Price of the deposit tool, $/tool;
D – Deprecation rate, /yr.

$$Ca = Pa \cdot D \tag{4.29}$$

where Pa – Price of the abatement tool, $/tool;

$$Cf = Pf \cdot Af \tag{4.30}$$

where Pf – Price of the clean room floor space, $/ft2-yr;
Af – Area of the tool, ft2.

It is assumed that one person can maintain two tools at $30/hr rate.

$$Co = Nl \cdot Rl \cdot H \tag{4.31}$$

where Nl – Number of labor required for the tool, /tool;
Rl – Labor rate, $/hr;
H – Yearly operating hours, hr/yr.

The maintenance cost is assumed to be 5% of the labor cost based on the case in lithography [65].

$$Cm = O / M \cdot Co \tag{4.32}$$

where O / M – Maintenance over operating labor ratio, dimensionless;

The elements in the recurring cost are: the cost of the precursor, the carrier gas, and the energy for heating the wafer and pumping. Energy for other usage such as for robot arms, preheating the precursor is not considered for simplification. Water cost is not considered because through experience water cost is not significant in the overall cost; also no available information was available.

$$R = Cp + Cc + Ce \tag{4.33}$$

where R – Reoccurring cost, $/layer;
Cp – Cost of precursor per layer of film, $/layer;
Cc – Cost of carrier gas per layer of film, $/layer;
Ce – Cost of energy per layer of film, $/layer.

$$Cp = Mp \cdot Pp \tag{4.34}$$

where Mp – Usage of precursor per layer of film, g/layer;
Pp – Price of precursor, $/g.

$$Cc = Mc \cdot Pc \tag{4.35}$$

where Mc – Usage of carrier gas per layer of film, g/layer;
Pc – Price of carrier gas, $/g.

$$Ce = We \cdot Pe \tag{4.36}$$

where We – Usage of electricity per layer of film, kW-h/layer;
Pp – Price of electricity, $/kW-h.

$$We = Wh + Wpump \tag{4.37}$$

where Wh – Usage of electricity for heating the substrate, kW-h/layer;
Wpump – Usage of electricity for pumping, kW-h/layer.

The reason why the unit of recurring cost is chosen as $/layer instead of $/yr as in the SEMI standard is that the unit of final cost is $/layer. Since the information for calculate the cost per layer of film is readily available, it would not make sense to convert it to yearly cost, then convert it back to per layer cost.

For a single process step, the yield is usually around 98%. If the yield of one step is far below 99%, it will not be accepted in the production line. In order to calculate the yield loss cost, the value of the wafer up to the steps before Cu CVD is needed. Due to the lack of the information and the yield rates are close to one, the yield of Cu CVD was assumed one. When more information is available, yield can be easily incorporated into the cost model.

$$CEO = F / (Tp \cdot H) + R \tag{4.38}$$

where Tp – Throughput, layer-film/hr;
H – Yearly working hours, hr/yr.

$$Tp = 60 / t \tag{4.39}$$

where t – total process time, min/layer-film;

Table 4.2 summarizes the input data. It is reasonable to assume that these variables are independent of each other. The correlation among the variables is important for uncertainty analysis because it affects the variance of the results. Not only the

nominal values are included, but also the distributions of these data. In this way, the uncertainty in the values can be directly addressed. For simplification, only the Guassian distribution is used.

Table 4.2 Summarization of the Input Data for the COO of Cu CVD Process

Parameter	Unit	Mean, μ	Standard Deviation, σ
Deposition Tool Cluster Price, Pd	$/tool	2,000,000	1,000,000
Abatement Cluster Price, Pa	$/tool	500,000	10,000
Energy Price	$/kW-h	0.1	0.01
Precursor Price	$/g	1.65	0.5
Carrier Gas Price	$/g	0.127	0.4
Floor Space Price, Pf	$/ft2-yr	600	100
Footprint of the Tools, Af	ft2	250	50
Labor Rate, Rl	$/hr	30	5
Number of Labor Needed for the Tool, Nl	/tool	0.5	0.2
Maintenance over Operation Ratio, O/M		5%	0.2%
Yearly Working Hours, H	Hr/yr	8400	300
Precursor Flow Rate, F	ccm	2	0.2
Substrate Temperature, T	oC	190	2

It is important to note that many of the parameters mentioned here are determined by the process itself. For example, the throughput, the precursor and carrier gas usage, and the energy usage are all dependent on the precursor flow rate and the substrate temperature. The values for the process parameters are from experience. The derived data are:

$$Mp = (0.02147 + 0.00103 \cdot (F - 2) / 0.2 - 0.00906 \cdot (T - 190) / 2) \cdot 370.83,$$
$$Mc = (0.0517 + 0.0025 \cdot (F - 2) / 0.2 - 0.0022 \cdot (T - 190) / 2) \cdot 2,$$
$$Eh = 53.13 - 2.57 \cdot (F - 2) / 0.2 - 1.17 \cdot (T - 190) / 2,$$
$$Ep = (0.5 \cdot 55 \cdot (7.5 - 6.4) + 6.4 \cdot 55 + 6.3 \cdot (t \cdot 60 - 60)) \cdot 3 \wedge 0.5 \cdot 230 / 1000,$$
$$t = 3.9255 - 0.1135 \cdot (F - 2) / 0.2 - 0.111 \cdot (T - 190) / 2 - 1.$$

The calculation gives the COO as $17.1/lay-film for a 300 mm wafer.

- **Uncertainty Analysis of the COO Model**

The Cu CVD process was a new process without much commercial activity. The values in the analysis were mainly estimated. How much confidence can we put into the results given these uncertainties in the data? If we find it is necessary to improve the accuracy of the analysis to make sound decisions, the accuracy of which data should be increased? To answer these questions, uncertainty analysis is performed on the cost model using @Risk®. Because of the short time to run the cost model and the small number of uncertain parameters, Latin Hypercube sampling method is used. The iteration number is 2000. The output is first selected as the total cost COO.

Figure 4.16 shows the histogram of the COO. The mean of COO is $17.7 /layer-film. Its standard deviation is 7.26 $/layer-film. This is a rather large value compared to the mean. The numbers in **Error! Reference source not found.** show the confidence interval of the COO. Which variables contribute most to this large uncertainty?

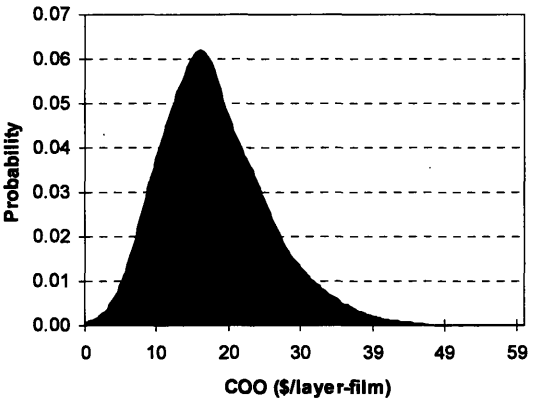

Figure 4.15 Density Plot of the Probability Distribution of COO for the Cu CVD Process

To identify the variables that contribute the most to the COO, a simple sensitivity analysis was performed on the cost model. The inputs in Table 4.2 were perturbed for 10% except for the substrate temperature. Because the acceptable temperature range is only 190 ± 2 °C, it is only perturbed for 1%. Figure 4.16 shows the percentage change in the COO to the change in the inputs. The percentage change in temperature has an significant effect. The COO is also sensitivity to the precursor price, precursor flow rate, and the yearly working hours. The sensitivity of COO to the precursor-related term comes from the dominating position the precursor cost has in the cost model. Based on the assumptions in the model, the precursor cost accounts for 74% of the total COO.

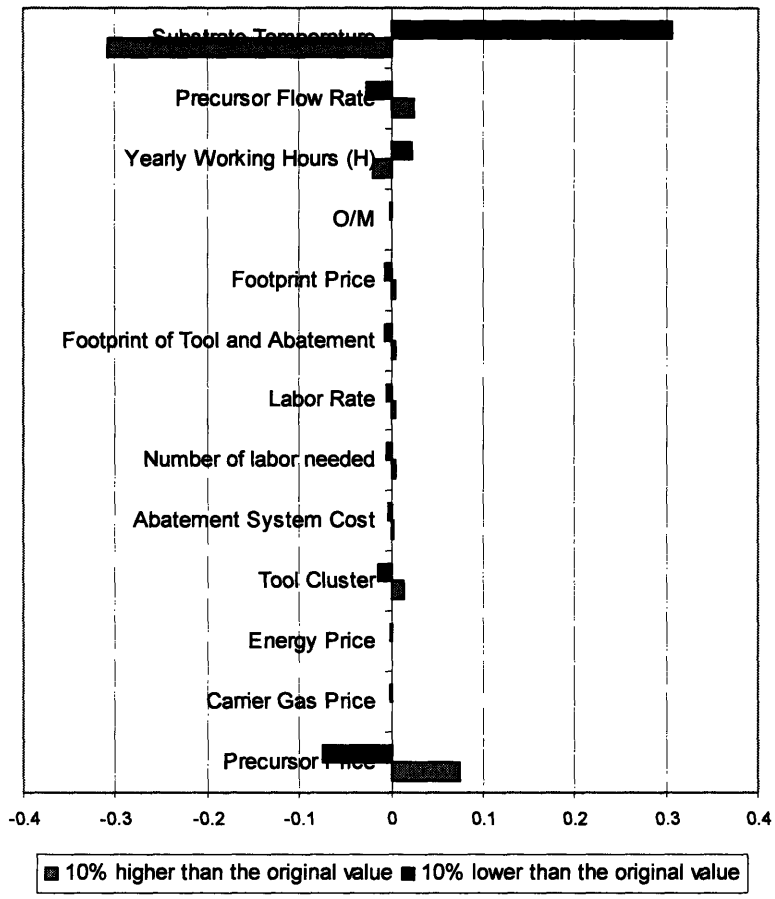

Figure 4.16 Comparison of the Variables' Effect on the COO of Cu CVD

Figure 4.17 shows the rank correlation coefficient between the uncertainty in the overall COO and the uncertainties in the variables using the @Risk Monte Carlo simulation add-on for Excel. It can be seen that the uncertainty of the substrate temperature and the precursor price dominate. This is in consistent with the sensitivity results. Their signs are the opposite. This indicates a negative correlation between the COO and the substrate temperature T, and a positive correlation between the COO and the precursor price. The increase of T has several effects: decreasing the process time, increasing the energy for heating the substrate, decreasing the energy for pumping during the deposition due to the decrease of the deposition time, decreasing the usage of the precursor and the carrier gas. Which one of these effects is most important?

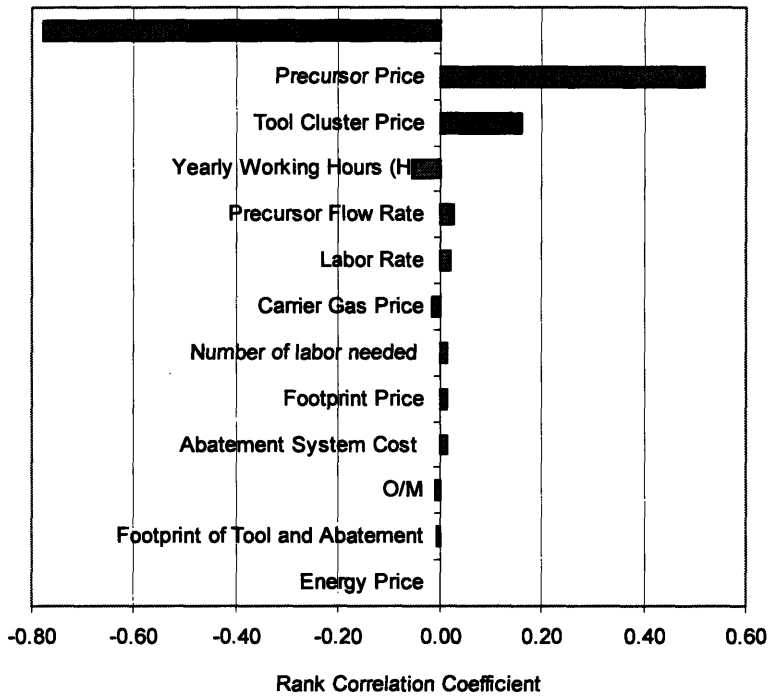

Figure 4.17 Rank Correlation Coefficients for the Uncertainty in the COO of the Cu CVD Process

Figure 4.18 shows the rank correlation coefficients between the absolute value of the COO and related variables. It can be seen that the COO is mostly dependent on the precursor usage, then to the carrier gas usage. Because the energy for pumping during the deposition is proportional to the process time, their effects on the COO are the same. It can also be seen that even though the increase in substrate temperature increase the energy consumption for heating the substrate, this increased energy consumption does not affect the COO much.

Do these analyses give direction on what to do for the industry? Yes. If we have enough confidence in the results, we can conclude that given the assumption in this cost model, the most effective way to reduce the COO is to increase the substrate temperature. If we do not have enough confidence in the results, we need to narrow down the standard deviation of the COO before we can make sound decisions. To reduce the volatility of the COO, the most effective way is to reduce the variance of the substrate temperature. The analyses also tell us that the substrate temperature affects the COO through the precursor and the carrier gas usage, and the process time. Thus if the values of these variables can be reduced by other means, they should also be effective.

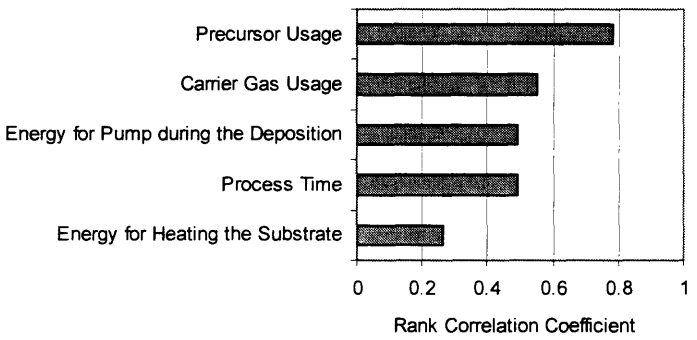

Figure 4.18 Rank Correlation Coefficients of COO in the Cu CVD Process

In order to see if these directions are correct or not, we use two methods to reduce the uncertainty of COO. One is to reduce the standard deviation of the substrate temperature by 50%, i.e., from 2 °C to 1 °C; the other one is to reduce the coefficient that relates the substrate temperature to energy for heating the substrate by 50%, i.e., from 1.17 to 0.585.

The box plots of the probability density of the two cases are plot together with the original case in Figure 4.19. For the first case, the standard deviation of COO drops to 5.23 $/layer-film, which is a 28% decrease. For the second case, the standard deviation of COO becomes 7.24 $/layer-film, which is a 0.3% decrease. This means that uncertainty analysis is able to give the design a good direction in making informed and optimal decisions.

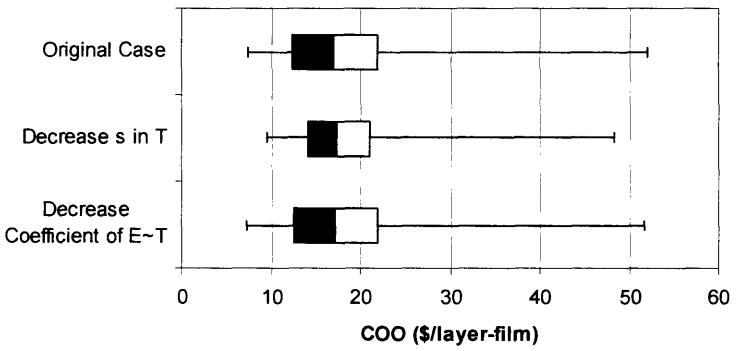

Figure 4.19 Comparison of the Probability Density of Different Methods to Reduce the Uncertainty of COO of the Cu CVD Process

We can also study the uncertainty in the sensitivity analysis. Figure 4.20 shows the percentage contributions of the important components. It can be seen that even though there is a relatively large uncertainty for the percentage of the material cost, it still consists the largest portion of the COO.

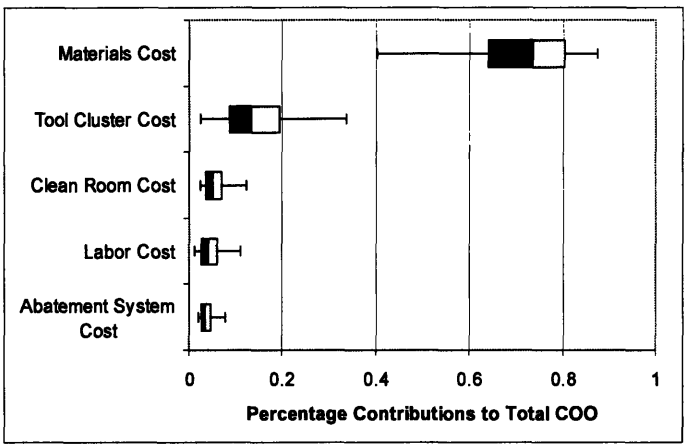

Figure 4.20 Percentage Contributions of the Subcomponents to the Total COO

Chapter 5 Framework and Tools for Integrated Technology Evaluations under Uncertainty

5.1 Decision Framework and Tools

The decision framework for integrated technology evaluations is shown in Figure 5.1. The decision context is to choose between alternative technologies. The framework starts with modeling the alternative technologies. The process model links the ESH and COO models together by providing common process parameters to both models. The effects of changes in the process parameters on both COO and ESH impacts can therefore be analyzed simultaneously, along with the tradeoffs between COO and ESH impacts. The inputs of the models are probability distributions rather than deterministic values to capture the uncertainty and variability of the parameters. Models are constructed hierarchically: first simple models are built with less accurate data and estimations. Uncertainty analysis generates the range of expected outcomes of the models. The company's risk attitude towards worker safety and health, regulatory, financial, and technical issue determines whether the resolution of the analysis is sufficient or not. If the higher accuracy is required, sensitivity analysis can identify parameters that contribute the most to the uncertainty of the outcomes. Given that it is costly to collect information, this cost should be justified by the value that the additional data provides for the decision outcomes. If the value is higher than the cost, data collection and model refining efforts then focus on the important parameters identified above. The new data are put into the process, COO, and ESH models for the next round of analysis. If the accuracy of the first round analysis is adequate, or the cost of new information is higher than its value, a decision can be made without further analysis. Because framework starts the analysis with rough estimations and simple calculations and stops at the least amount of necessary information, the first two rounds of analysis can usually be done within a short time frame.

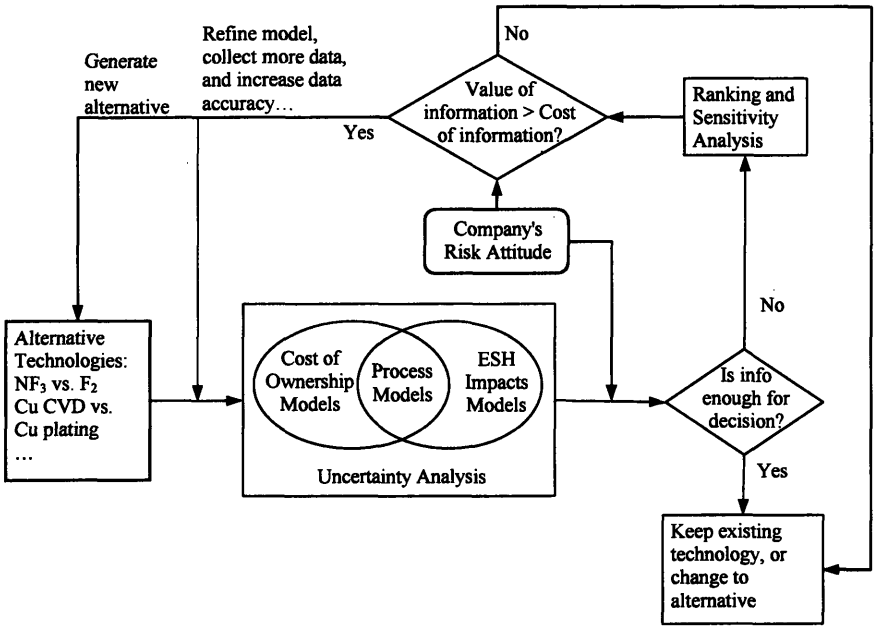

Figure 5.1 Framework for Integrated Technology Evaluation under Uncertainty

5.1.1 Hierarchical Modeling

Decision makers always face the limited time and resources for any analysis and uncertainties imbedded in inputs. To speed up the analysis and conserve resources, we can start the analysis with rough estimation and simple models. Confidence levels (CLs) in the outputs need to be quantified. Once presented the CLs, the decision maker needs to judge whether further information is warranted by the value it provides given its cost, which entails assessing the value of information. If additional information is needed, the analysis is performed in more details. This iterative process starting from simple and move up in sophistication is called hierarchical modeling.

The concept of hierarchical modeling is illustrated here through an imaginary example. The decision context is to decide whether the fluorine utilization efficiency of a chamber cleaning condition is within the acceptable limits. The reaction is

$$SiO_2 + 4F\cdot \rightarrow SiF_4 + O_2 .$$

The efficiency is defined as

$$F\% = 4N_{SiF_4}/N_{F\cdot}\cdot 100\%$$

where F% is the fluorine utilization efficiency, and N is the mole amount of gases fed into or emitted from one cleaning.

To prevent unnecessary waste of etch gas, the lower efficiency limit is set to be 10%. The upper limit is 50%. When the efficiency is higher than 50%, etch rates are

usually too slow for practical implementations. This efficiency was first estimated from a back-of-envelop calculation. Let us call it Model Level 1, as shown in

Figure **5.2**. The definition of an efficiency means it cannot be lower than 0%, which gives the lower bound. The 60% upper bound is estimated from experience. The bounds given by this model level do not fall into the requirements. However, this is mostly likely due to the simplicity of the model, not the nature of the efficiency itself. To verify this, a model with simple kinetics was built, noted as Model Level 2. This level gave satisfactory limits. Once both bounds were within the acceptable ranges, there was no need for further refining of the model or measurements. Therefore, Model Level 3 with transport and detailed kinetics was unnecessary.

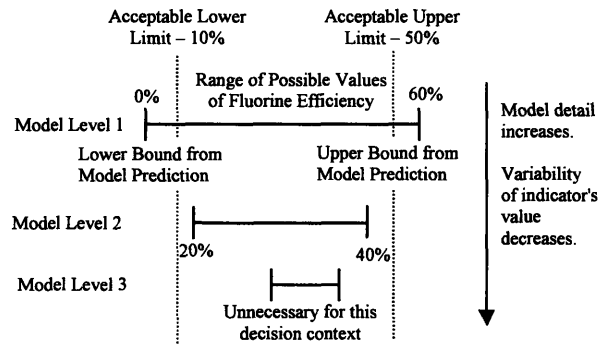

Figure 5.2 Schematic of Hierarchical Modeling for Assessing whether Fluorine Utilization Efficiency in Chamber Cleaning Falls into Acceptable Limits

The cost of Model Level 1 is very small, as it can be completed within minutes. The knowledge it provides is very limited as well. The accuracy of Model Level 2 may require a few day's effort. The effort for Model Level 3 may be of the order of weeks or months. As the model detail increases, the required resources and the accuracy of the results both increase. The optimal level can be determined by the value of information, which will be discussed later.

Figure 5.3 shows an example of applying the hierarchical method to compare two alternative technologies T1 and T2. At Model Level 1, if not all of the possible values of T1 and T2 are within the acceptable ranges, then regardless of whether the ranges of the two technologies overlap or not, the ranges need to be tightened with a more detailed model. If at Model Level 2, the ranges of both technologies fall within the acceptable ranges, but the decision maker considers there is too much overlapping of the two ranges, an even higher level of modeling is required. If at Model Level 3, the ranges are within the acceptable range and either do not overlap or only overlap to the extent with which the decision maker is comfortable, then the modeling effort is adequate.

The examples show that hierarchical modeling can avoid wasting excess resources on unnecessary details, while providing sufficient knowledge for the decision context. To achieve this, one needs to first quantify the uncertainty of the model predictions to judge whether the information is adequate, then decide whether the new

information to be collected is worth the effort. These two tasks will be discussed in the following sections.

The case study in this paper considered two levels at the process modeling and three levels at the system boundary modeling. The first process modeling level is merely based on the estimation on the fluorine efficiency and energy efficiency. The second level consists of simple kinetics.

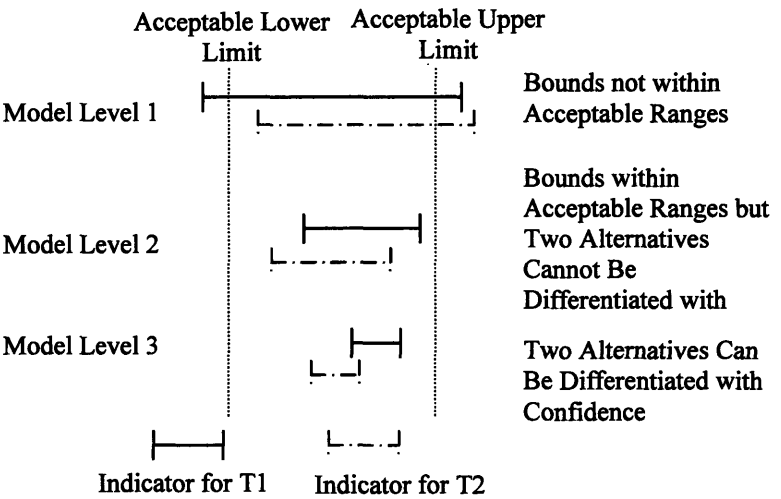

Figure 5.3 Applying Hierarchical Modeling into Differentiating Two Alternative Technologies

5.1.2 Qualification of Uncertainties in Input Data

Decision makers always face uncertainties imbedded in input data, such as the reaction rate coefficients and the market demand of a chemical. In some cases, these parameters may be single-valued, deterministic, and constant, but their values are not perfectly known at the decision time. In other cases, the values of these parameters may be constantly fluctuating, with random patterns, or with imperfectly known variability. For instance, due to limited understanding of the environmental impacts of many chemicals and their multimedia fate, transport, and exposure to human, the quality of the LCA characterization factors that relate chemical quantity with degree of adverse impacts usually varies in orders of magnitude, even though the factors themselves are single-valued. When the 95% confidence intervals for the cancer toxicity indicators are three orders of magnitude apart [12], it is inappropriate to use a single nominal value to represent the parameter while neglecting the large probability that it may take other values. Besides parametric uncertainty, the model structure itself is also subject to uncertainties. Hierarchical modeling addresses some of the latter, although it deserves further study. Chapter 3 discusses the method of uncertainty analysis. Here only the qualification of input data is discussed.

The first step in uncertainty analysis is to quantify uncertainties. There are several techniques to quantitatively represent uncertainties such as probabilistic description, interval mathematics, and fuzzy set theory. The probabilistic representation

is the most common one and was chosen for this study. The parameters are treated as random variables, which can take up values at different probabilities. The probability distribution functions (PDFs) are used to describe the data, rather than nominal values or extreme values. A commonly used PDF is normal distribution, which has a PDF of

$$f_x(x) = \Phi(x) = \frac{1}{\sqrt{2\pi}\sigma} e^{-\frac{1}{2}\frac{(x-\mu)^2}{\sigma^2}}$$

where μ is the mean and σ is the standard deviation.

The PDFs of process parameters can be generated based on physical and chemical principals, and the precision of process control. When selecting the PDFs, it should be noted that the maximum and minimum values that the PDFs may take need to be physically and chemically meaningful. For example, flow rates and the activation energy of an reaction should not take negative values. Distributions such as triangular, beta, truncated normal, or lognormal are useful in this situation. When no information other than the extreme values is available, uniform distributions can be used. When data are represented by single/nominal values or with confidence levels, this representation also needs to be converted into PDFs for further analysis. These distributions are the basis of uncertainty analysis.

The area where data are most lacking is the ESH area. There are data sources such as the Environmental Protection Agency, the Dutch Ministry of Housing, Spatial Planning and Environment, Environmental Defense Fund that have information on a similar set of data but using different measuring or assessment methods to produce the information. The data from these sources have different qualities. To take advantage of all the available information from these sources without diluting the high quality ones, an environmental information management system EnvEvalTool was developed by Cano [12, 66] to store toxicological and fate and transport data obtained from the above data sources, as well as calculated using a fate and transport model [12]. The ESH information of this work is mainly from the EnvEvalTool. The data sources are ranked based on the quality of their data. For a parameter whose value is available from multiple sources, the value will be extracted from the source with the highest data quality. When high-quality data are not available, estimates are obtained based on lower-preference quantitative, semi-quantitative or even qualitative information. The distributions of data from the lower-quality sources are generated in the following manner: lognormal distributions are used unless the parameters can take negative values, in which case other PDFs such as normal distributions are used. The most likely values of the lognormal distributions are set to be the nominal values published in the consulted source, while the variances of the distributions are derived from the correlations between data from the source and data from the highest-quality sources for that type of data element.

One point to be noted is that even though there are large uncertainties in the ESH data, they do not necessarily affect the decision outcome the most. This will be seen from the case study.

5.1.3 Value of Information(VOI)

The concept of VOI can be illustrated with an example that is often faced by decision makers: A chemical X has been used in production. The decision maker is presented with an alternative chemical Y which may bring benefits to the company. The benefits can be saving money, increasing production yield, or reducing environmental compliance cost. Some initial study has been done on Y. Right now the decision maker needs to decide whether to (1) devote more resources into further research on Y, or (2) continue with the chemical X and ignore Y, or (3) switch to Y right away. There is also the possibility to study Y in the future. For simplicity, this option is not considered here, but the same principle can be applied to it. There are uncertainties associated with the problem. The issues needed to be considered here include (1) potential economic benefit from cost saving or higher revenue, (2) future regulations on the use of the current and the new chemical and their environmental and health effects, (3) the technical performance of the new chemical, (4) the uncertainties associated with all the factors mentioned above, and (5) the risk preference of the decision maker of these factor. Because of these uncertainties and the fact that new information can influence the decision maker's choices, there is value in obtaining more information. At the same time, there is also cost of obtaining the information. Let us term it the cost of information.

The value of information (VOI) can then be defined as the additional value (or reduced cost) of the project that the new information brings compared to the value (or cost) of the project without the new information. Given the cost of collecting new information, the net VOI is the value of information minus the cost of information. Conventionally people refer to the NET VOI simply as the VOI. In the rest of the work, the conventional terminology is used. The value (or cost) can be in monetary terms or utility terms such as how much the decision maker values the reduction of one unit of global warming potentials. This value (or cost) results from the decision maker making a better choice with reduced uncertainty of the situation which leads to higher value (or lower cost) in the project.

The decision tree of the chemical example is shown in Figure 5.4. Without new information, the decision maker can only choose between the first two branches in Figure 5.4, which results in certain financial and environmental values and costs. If the decision maker chooses the third branch, it will lead to other values and costs (cost of research included). The VOI of further research equals to the best net value out of the first two branches minus the best value out of the third branch. If the VOI is greater than zero, then it is worthy to carry out more research.

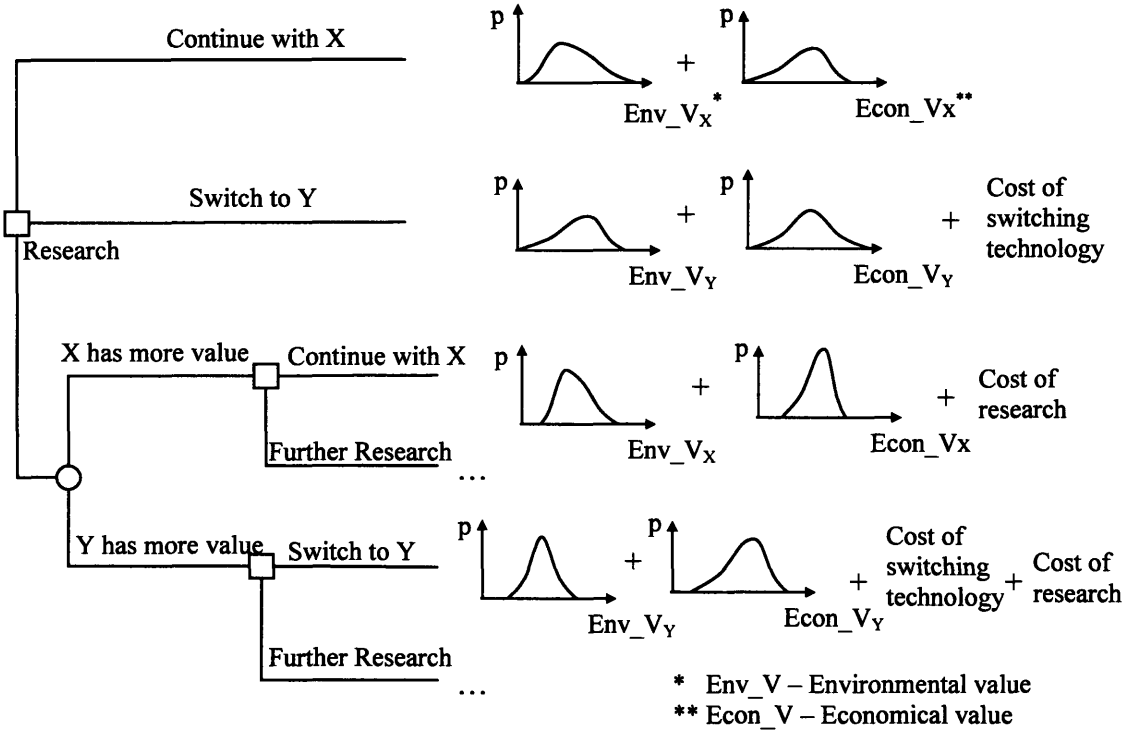

Figure 5.4 The Decision Scenario of the Chamber Cleaning Case Study

To calculate the net VOI, we need to know (1) input factors to be refined in the new research. Obviously, these factors should be the ones that contribute the most to either the uncertainty of the output or the value of the output, depending on the decision context. This is done in the sensitivity analysis. (2) The outcome of each decision path and random event. Since when VOI is calculated we do not know exactly what they will be after the research, the outcomes can only be estimated based on current knowledge. (3) The likelihood of each random event taking place. This can also only be estimated. (4) The risk attitude of the decision maker, which determines the expected utility (EU) function of the outcomes. (5) The cost of collecting the new information.

If the decision maker is assumed to be risk-averse, which is quite common, then the exponential EU function can be used to describe the utility of an outcome. The outcome can be either desirable or negative:

$$U = 1 - e^{-x} / R$$

where U – the EU of the decision outcome,

R – risk tolerance, a constant which represents the risk preference of the decision maker,

x – the decision outcome.

When the decision outcome is expressed in costs or negative effects, as x tends to infinity, U tends to one. This derives from the fact that a company only has limited resources to mitigate adverse impacts. The worst scenario is the company goes bankrupt where the financial loss is still finite. For the rest of the paper, the decision outcome is measured in

cost. Therefore, the lower the U is, the better the outcome is. There are other utility curves that can describe risk-averseness. For simplicity, this paper uses the exponential EU function. In reality, the utility curve may have other shape or even be discontinuous. For simplicity, the exponential curve is used here. A risk-seeking or risk-neutral attitude can also been described with different utility functions.

If we use the NF3 example, the risk tolerance can be determined as follow: consider the gamble

Reduce Y kg CO_2 equivalent emission with probability of 0.5,
Gain Y/2 kg CO_2 equivalent emission with probability of 0.5.

CO_2 equivalent is the unit of GWP. Please note that for the NF_3 vs. F_2 case discussed here, the EU is defined to be environmental cost because GWP is negative in its natural. As an example, the GWP of CH_4 is 21 kg CO_2 equivalent means that the GWP effect of 1kg of CH_4 is the same as 21 kg of CO_2. The largest value of Y that the decision maker would prefer to take the gamble rather than not to take it is approximately equal to his/her risk tolerance. To give some perspective, let's assume that there are 200,000 cleanings per year in a medium size fab, with a 5-year horizon, there are 1×10^6 cleanings total. The median of GWP of the NF_3 process is 1.7×10^5 kg CO_2 equivalent. It can be seen that the smaller the risk tolerance is, the more risk averse the decision maker is. In this case, two cases are considered: Y = 1×10^6 kg CO_2 equivalent, Y = 5×10^5 kg CO_2 equivalent.

The effect of the risk preference R on decision can be seen from the example below. Assume the utility functions of two decision makers D1 and D2 are $U_1 = 1-e^{-x/R_1}$ and $U_2 = 1-e^{-x/R_2}$. There are two alternative choices A1 and A2. Their outcomes are x1 and x2. Alternative A1 is currently in use. The cost of switching to Alternative A2 is y. For decision maker D1, the overall utilities of using A1 and A2 are $U_{1\_A_1} = 1-e^{-x_1/R_1}$ and $U_{1\_A_2} = 1-e^{-x_2/R_1} - y$, respectively. For decision maker D2, the total utilities are $U_{2\_A_1} = 1-e^{-x_1/R_2}$ and $U_{2\_A_2} = 1-e^{-x_2/R_2} - y$. It can be seen from Figure 5.5 that Because of the difference in R1 and R2, it is possible for $U_{1\_A_1} > U_{1\_A_2}$ while $U_{2\_A_1} < U_{2\_A_2}$.

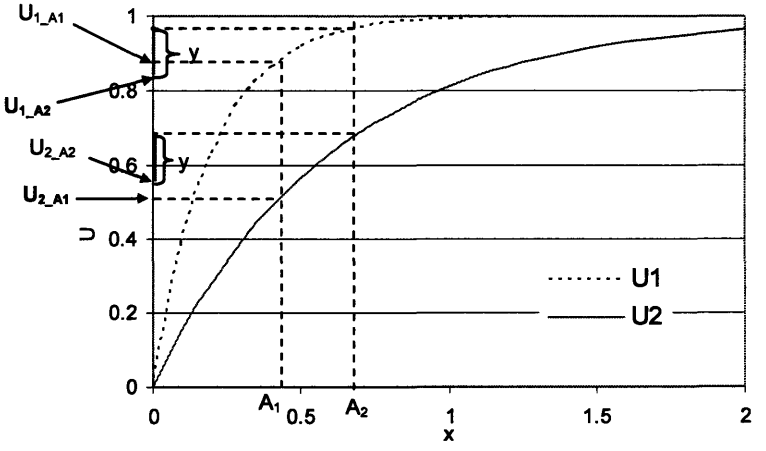

Figure 5.5 Illustration of Effect of Risk Preference on Decision Outcomes

5.1.4 Procedure of Using The Decision Framework and Tools

1. Describe the technologies and their downstream and upstream processes under consideration with simple models, such as stoichiometric equations. Calculate the mass and energy balances. Many of the factors in the process models will have large uncertainties. They should be described using probability distribution functions. When there is scarce information for upstream or downstream processes, focus more on energy consumptions and less on material usages because the former tend to generate more ESH impacts.
2. Feed the process-specific data generated above in the form of probability distributions into the PIO-LCA model and COO model. The uncertain factors in the COO model will also be described by PDFs.
3. Propagate the uncertainties through the LCA and COO models to produce the distributions of the environmental impacts and COO.
4. Convert the technical performance, LCA, and COO outcomes of the alternatives into EU using utility functions.
5. Compare the distributions of EU of the alternatives. If the confidence levels of the EUs satisfy the decision context, no further analysis is required. Otherwise, go to the next step.
6. Use sensitivity analysis to identify important parameters that contribute the most to the uncertainty of the EUs.
7. Calculate the VOI of further research. If VOI is larger than zero, go to the next step. Otherwise, revisit whether the utility functions represent the risk preference of the decision maker properly. If yes, then stop here. Otherwise, revise the functions and go back to Step 4.
8. Refine the models, collect more data, or perform further experiments to reduce the uncertainty in the important parameters.
9. Go back to Step 2.

A case study of comparing NF_3 and F_2 as the chamber cleaning gas is used to illustrate the procedure.

5.2 Case Study: Comparison of NF_3 and F_2 as Chamber Cleaning Gas

5.2.1 Background on Chamber Cleaning and Past Work of its ESH Studies

The case study used in this work is the chamber cleaning process. It has been identified as one of the processes in semiconductor manufacturing to have significant environmental impacts. It is widely used in fabs to remove the film formed during the chemical vapor deposition step on the chamber wall. This removal is necessary to reduce the particle contamination in the following steps. In the past, perfluorocompounds (PFCs) have been used to convert silicon in the film into volatile SiF_4, which can then be pumped out of the chamber. Due to the high global warming potentials (GWP) of the

PFCs, the World Semiconductor Council has agreed to a 10% reduction in global-warming PFC emissions by 2010 with a 1995 baseline [67]. Since then, the semiconductor industry has investigated several methods to achieve this goal. Using NF_3 to substitute for C_2F_6 is one of them. Even though NF_3 is still a global warming gas, it has very high disassociation rates in the plasma and higher gas utilization ratios (~99%) compared to carbonfluorine cleaning, thus leaving little NF_3 in the exhaust. Other exhausts from the cleaning include SiF_4, F_2, N_2, O_2, which are not global warming gases. Studies on NF_3 as chamber etching and cleaning gas have shown that using NF_3 can lower chamber clean time by over 30% while reducing global warming emissions by over 90% relative to a C_2F_6-based process of record before disposal [68]. When the downstream disposal of global warming gases and hazardous chemicals are considered for NF_3 and C_2F_6, NF_3 still has better overall environmental performance than C_2F_6 [19]. Other merits of NF_3 include shorter cleaning time, low toxicity, and the easy abatement of unreacted NF_3. The shortcoming of NF_3 is its high cost. The F_2 gas has been proposed as a much less expensive alternative.

This work compares the NF_3 and F_2 gases in terms of their economical and environmental performance. A typical chamber cleaning situation, i.e. the etching of silicon dioxide film deposited from tetraethylorthosilicate in a 300 mm wafer chamber was studied: plasma is generated remotely, followed by the etching in the cleaning chamber. The effluents from the chamber is treated in the downstream. The schematic picture of a cleaning process using NF_3 as the cleaning gas is shown in Figure 5.6.

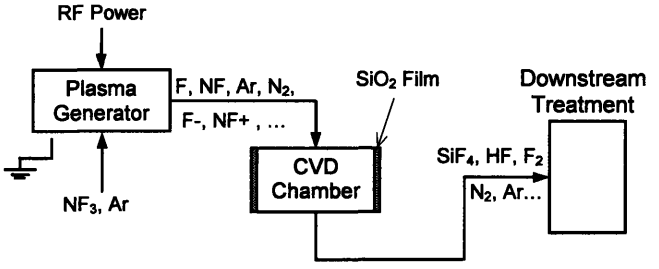

Figure 5.6 Schematic Picture of NF_3 Chamber Cleaning Process

The industry has studied the chamber cleaning processes at different system boundaries. The first boundary is around the tool, which consists of the plasma generator and the chamber, or just the chamber for in-situ plasma generation cases. This is a commonly used boundary in ESH analyses [68-74]. The second boundary includes the on-site downstream disposal system, which converts emissions from manufacturing processes to less hazardous chemicals or reduces the concentrations of the chemicals to acceptable ranges before emitting to the environment. This boundary has started to be used more widely in evaluating the ESH impacts of processes [17, 19, 75-77]. There have also been several "gate-to-gate" life-cycle inventory studies whose boundaries are around the fab [78-80]. The largest system boundary comprises the upstream production of materials and energy used in the fab and the downstream disposal. This is an LCA boundary, which has just started to gain recognition in the semiconductor industry [81, 82]. Ideally, this boundary requires knowledge on all the processes involved in upstream and end-of-life recycle or disposal. Due to the large amount of processes and products

involved, in practice only limited processes are considered. Even so, its economic cost and time are still prohibitive for carrying out a conventional LCA in a regular basis for process/equipment designs. The decision framework and tools developed in this work aim at shortening the analysis time while still providing useful information for decision-making. The system boundary of the comparison, which is the Boundary III, is shown in Figure 5.7.

To decide if F_2 is a viable alternative, criteria other than cost need to be considered. The comparison criterion is the life cycle impacts of the two processes given the same cleaning performance. The base line for the comparison was that both processes have the same cleaning time for a fixed film thickness. Therefore, the cost associated with the non-production time of the chamber is the same. This simplified the comparison in COO. Assuming the technical performance to be the same, the outcomes of the decision will be the costs of running the cleaning process including ensuring worker safety and health, and the LCA environmental impacts caused by the selected process. These values are uncertain even when the recipes of the cleaning process and downstream treatment are set constant, which is the result of the lack of perfect knowledge in the external environment and upstream processes. However, the uncertainty from the external areas turned out to be not important in making the selection of the two gases.

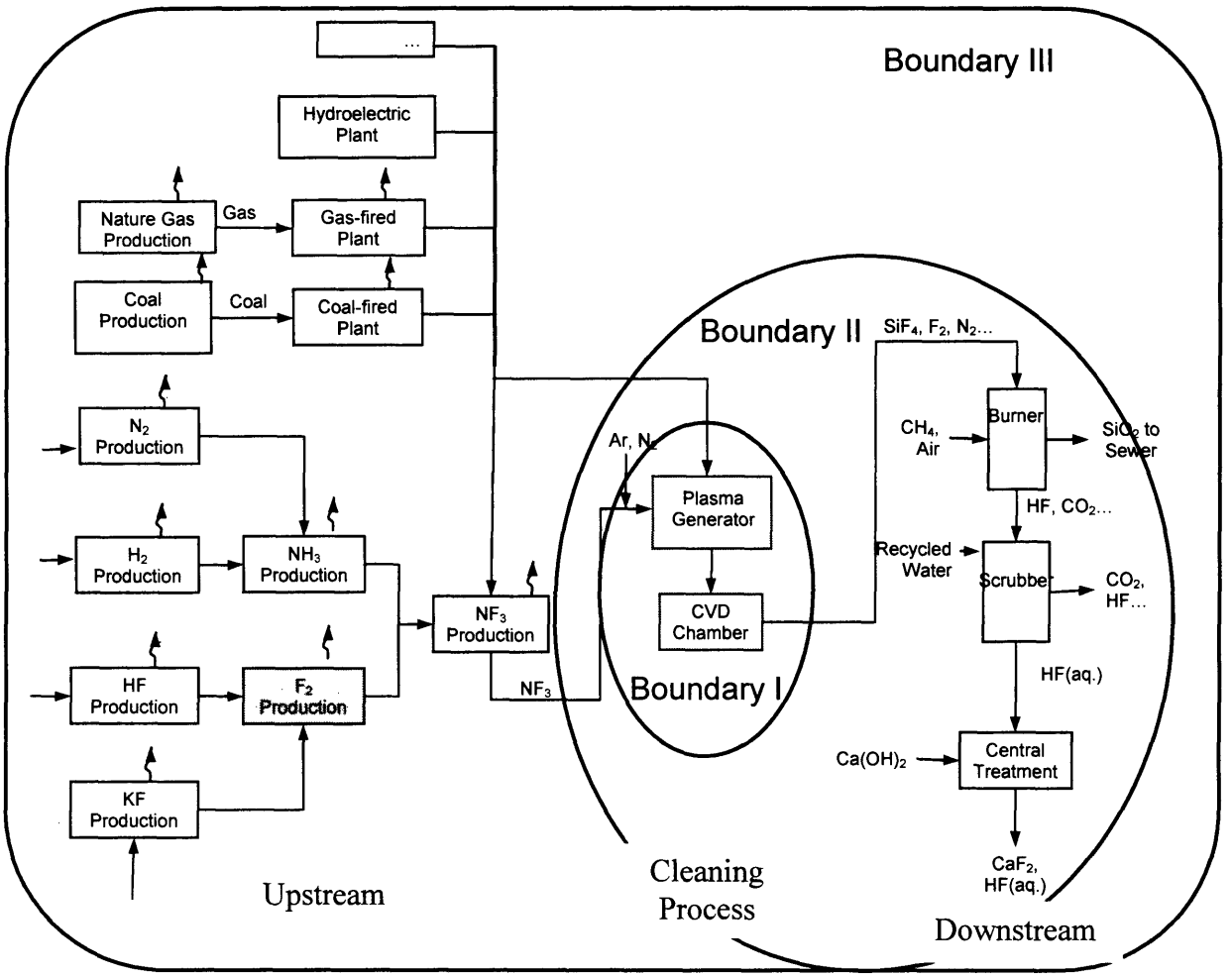

Figure 5.7 System Boundaries Considered in Comparing NF_3 and F_2 as Chamber Cleaning Gas

5.2.2 The First Round of Comparison

The process for the F_2 cleaning is similar to the one shown in Figure 5.6 except that the inlet gas should be F2, and that in the outlet gas there is no N_2.

- **Modeling of the Chamber Cleaning Process**

Since there were no experimental data available for the F_2 cleaning at the time of the study, a process model needed to be built to describe it. To study how the NF_3 process behaviors given the same conditions as those of the F_2 process, both processes were described using the same model structure. At the very beginning stage of this case study, little information was available on the two processes. Direct comparison of the performance and resource consumption was impossible. Since F_2 is one of the raw materials NF_3 production, if the energy and cleaning gas consumptions are the same for the two processes under the same cleaning rate, the NF_3 cleaning will lead to higher overall environmental impacts due to the longer upstream chain compared to the F_2

cleaning. Hence, it is necessary to study whether the difference in the operating conditions of the two processes can change this conclusion. If not, there is no need for further analysis. If yes, a quick judgment is required on where to allocate finite resources to collect the most valuable information.

Environmental impacts are driven by the mass and energy flows. Assuming that the only useful product is SiF_4, the cleaning time, the fluorine utilization efficiencies and the energy efficiencies were used to estimate the usages of the cleaning gases and energy:

$$N_{NF_3} = \frac{4N_{SiO_2}}{3F\%_{NF_3}},\ N_{F_2} = \frac{2N_{SiO_2}}{F\%_{F_2}} \tag{5.1}$$

$$E_{NF_3} = \frac{N_{SiO_2}E_{b\_NF_3}}{F\%_{NF_3}\xi_{E\_NF_3}} + tP_{plasma},\ E_{F_2} = \frac{N_{SiO_2}E_{b\_F_2}}{F\%_{F_2}\xi_{E\_NF_3}} + tP_{plasma} \tag{5.2}$$

where N_{SiO2} – amount of SiO_2 that needs to be cleaned, mole;

N_{NF3}, N_{F2} – amount of cleaning gas needed to clean N_{SiO2} of SiO_2, mole;

E_b – amount of energy needed to break the cleaning gas into radicals, J. For the NF_3 cleaning, E_b is the sum of the bond energies of NF_2-F, NF-F, and N-F. For the F_2 cleaning, E_b is the bond energy of F-F;

ξ_E – energy efficiency;

t – time needed for the cleaning, s;

P_{plasma} – power needed to sustain the plasma, W.

Strictly speaking, given no available information on the process, the lower bounds of the F% and ξ_E should be zero, and the PDFs of them should be uniform. The upper bounds of the PDFs were chosen based on practical experience. As the former case is not acceptable when F% and ξ_E are denominators, the following probability distributions were used for F%, ξ_E, and t:

$$f(F\%) = \frac{1}{0.6 - 10^{-5}} \tag{5.3}$$

$$f(\xi_E) = \frac{1}{0.6 - 10^{-10}} \tag{5.4}$$

$$f(t) = \frac{1}{1200 - 6\times10^{-4}} \tag{5.5}$$

In reality, the fluorine efficiencies, the energy efficiencies, and the cleaning time are not independent. However, since no further information was available at this stage, these factors were assumed to be independent. This assumption led to wider distributions of the cleaning gas usages, the energy usages, and the environmental impacts.

- **Modeling of the Downstream Treatment System**

The emissions from the two processes were treated with a BOC Edwards thermal processing unit (TPU). The schematic of the TPU is shown in Figure 5.8. The TPU is composed of an inward burner using natural gas and air to convert unreacted cleaning gas and F_2 into HF. Following the burner, there is a counter-current scrubber using recycled water from the fab to scrub HF from the gas phase into the aqueous phase. The aqueous

phase is then sent to the central treatment where HF is precipitated to CaF_2 by $Ca(OH)_2$. N_2 is used in purging the cleaning chamber.

Based on studies on the effectiveness of TPU [83, 84], it was concluded that the fluorine contents of the emissions from both cleaning processes can be sufficiently treated by the default burner operating settings. Hence, the operating conditions of the burner for the NF_3 cleaning and the F_2 cleaning were considered the same. The amount of water needed to treat the exhaust from the burner was calculated by modeling the scrubber as a packed-bed with countercurrent flow. A thin film model was used to describe the system.

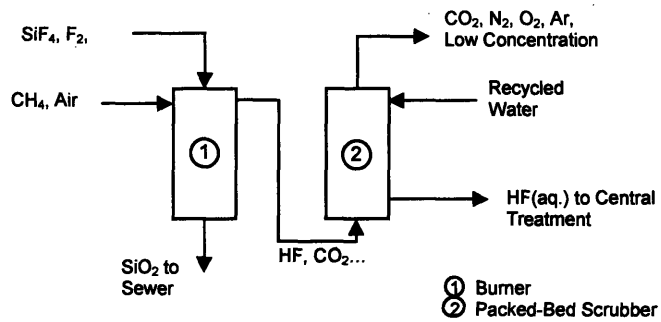

Figure 5.8 Schematic of Thermal Processing Unit

- **Modeling of the Upstream Processes**

The schematic of the system boundaries for the NF_3 cleaning is shown in Figure 5.7. The system boundaries for the F_2 cleaning are similar to those of NF_3, except that its upstream chain is shorter. As a demonstration of the Tools, the upstream inventory for the NF_3 cleaning case only included the energy usage in the production of NF_3, F_2, NH_3, and HF, with a rather complete inventory of energy generation. The energy usage of the processes were from [85, 86]. These factors are modeled as normal distributions whose standard deviations are 20% of the mean values. The material and energy usage and emissions of the two cleaning processes were used as inputs for the PIO-LCA model.

- **Modeling of the Cost-of-Ownership**

The information on the commercial F_2 cleaning was not available to the public at the time of this study. Therefore, the data used in this COO analysis were from literature of similar processes. To incorporate the uncertainty in data, PDFs were used to describe the parameters. The fixed costs of the two processes were of the plasma source and pumps, which were assumed to be the same for both processes. The fluorine Point-of-Use (POU) generator cost was included in the unit price of the fluorine gas. Therefore, only recurring costs were compared, which include the costs of the inlet gases, labor, electricity, and water for downstream disposal. It was also assumed that the POU fluorine generator depreciate linearly in 5 years, and that cleanings are done 200,000 times per year. The added value compared to wet cleanings, which comes from the lower down time of the chamber system by using NF_3 and potentially F_2 as the cleaning gas, was not considered.

Variables such as the generator price, footprint, generator capacity, unit price of the fluorine gas generated from a POU unit were from {MicroGenTM, #141}. The usage of the gases were obtained from the process model. The labor and support personnel cost for system qualification and training were from [87]. The upper bounds of the cost components of the F_2 cleaning were 10 to 100 times larger than those of the NF_3 cleaning to represent the higher risk with the F_2 cleaning, which was lesser known.

5.2.3 Results of First Round of Comparison

There are more than ten lifecycle environmental and health impacts calculated in this study. The global warming potential (GWP) is chosen as a representative impact to be discussed here. It is an impact that the semiconductor industry is familiar with and cares much about. The lifecycle GWP refers to the GWP generated not only from the exhausts of the cleaning processes, but also from the upstream and downstream processes such as burning coal to generate power. This kind of GWP is induced by the cleaning processes, therefore the cleaning processes should be held responsible for it. The same case applies for other impacts as well. Monte Carlo simulations generated the distributions of the lifecycle GWPs of the two processes as well as the confidence levels of the corresponding values, shown in Figure 5.9. The unit CO_2 equivalent is the unit of the GWP. As an example, the GWP of CH_4 is 21 kg CO_2 equivalent means that the global warming effect of 1kg of CH_4 is the same as 21 kg of CO_2. If only the two GWPs are compared, the conclusion may be since there is too much overlapping of the ranges of the two GWPS, the processes cannot be distinguished. However, the ratio of the GWPs shown in Figure 5.10 indicates that there is only about 15% possibility that the NF_3 cleaning have a lower GWP than the F_2 cleaning. Therefore, in comparison of two processes, the relative ratio rather than the absolute value should be studied.

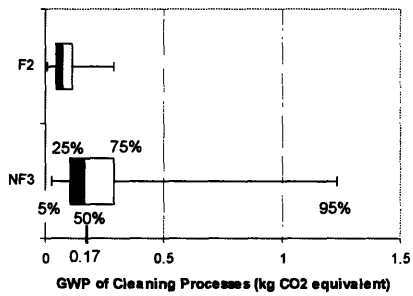

Figure 5.9 Comparison of the GWP Effect of the Two Cleaning Processes at the First Process Modeling Level

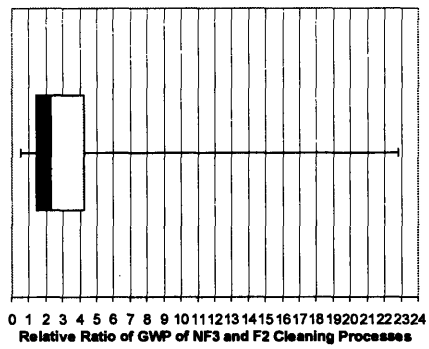

Figure 5.10 Distribution of Relative GWP of the Two Cleaning Processes at the First Process Modeling Level

The distributions of the costs per clean for the NF_3 process and the F_2 process are shown in Figure 5.11, along with the ratio of the cost of the NF_3 process over the F_2 process. There is less than 25% of possibility that the ratio is less than 1, which means that there is less than 25% that the F_2 cleaning will be more costly than the NF_3 cleaning.

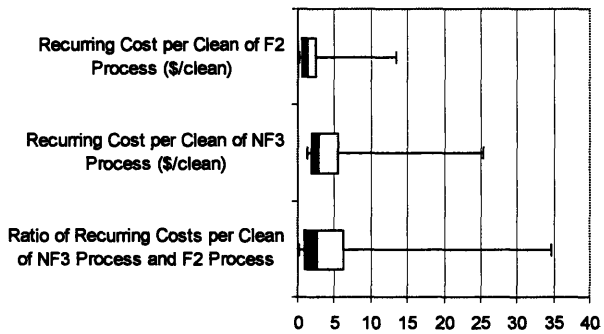

Figure 5.11 Probability Distributions of the Costs per Clean for the NF_3 Process and the F_2 Process, and the Ratio of the Cost of the NF_3 Process over the F_2 Process at the 1st

The very simple estimation of the process models provides 85% of confidence in distinguishing the two processes using the GWP and 75% of confidence using the COO. Is it still necessary to carry out further analysis? If the decision maker is unsatisfied with the confidence levels, then the value of information from further analysis can be studied to see whether it is worthy to perform further research.

Because the additional value and cost of gathering more information on different parameters are different, the VOI of a study depends on which parameters are going to be refined. Naturally, they should be the main contributors to the uncertainty in the outputs. Table 5.1 lists the five factors that have the largest absolute value of the Spearman rank correlation coefficients of the relative GWP of the two processes. They are the ones that contribute the most to the uncertainty in the relative ratio. The correlation coefficients being negative means that the corresponding factors negatively correlate with the GWP: the larger the factor values are, the smaller the GWP is. All of these five parameters are of the process model. Therefore, better models for the processes should be investigated before improving the models for the upstream processes and the ESH data in the LCA.

Table 5.1 Parameters with the Highest Rank Correlation Coefficients of the Relative GWP of the NF_3 and F_2 Cleaning Processes at the First Process Modeling Level

Parameter	Rank Correlation Coefficient
Fluorine Utilization Rate in NF_3 Cleaning	-0.64
Fluorine Utilization Rate in F_2 Cleaning	0.46
Cleaning Time t (s)	-0.28
Energy Utilization Rate in NF_3 Cleaning	-0.20
Energy Utilization Rate in F_2 Cleaning	0.12

It is also informative to see what the important factors are for the absolute value of the GWP of a single process alone. Table 5.2 lists the top 5 factors for the NF_3 case. Even though one factor of the process model still ranks the first, the characterization factors of many important global warming gases have large effects on the uncertainty of the GWP. These gases are the major pollutants from power generation. Because the intense power consumption in the plasma generator, power generation amounts to be the process that generate the biggest LCA impacts. The difference between Table 5.1 and Table 5.2 comes from the fact that even though the possible values for the GWP effect of a global warming gas range widely, when the Monte Carlo simulation picked a value for it, regardless large or small, the same value was used for evaluating the impact of both NF_3 cleaning and F_2 cleaning. Thus, the absolute uncertainty in the GWP effect of SO_2 does not affect the uncertainty of the relative ratio.

Table 5.2 Parameters with the Highest Rank Correlation Coefficients of the GWP of the NF_3 Cleaning Processes at the First Process Modeling Level

Name	Rank Correlation Coefficient
Fluorine Utilization Rate in NF_3 Cleaning	-0.64
GWP of SO_2 (kg CO_2 equivalent/kg)	-0.35
GWP of H_2S (kg CO_2 equivalent/kg)	-0.35
GWP of PM10 (kg CO_2 equivalent/kg)	-0.33
GWP of HF (kg CO_2 equivalent/kg)	-0.32

Similar to the sensitivity results on the GWP, the most important parameters for the ratio of the recurring costs of the two processes are of the process models, as can be seen in Table 5.3.

Table 5.3 Parameters with the Highest Rank Correlation Coefficients of the Ratio of the Recurring Costs of the Two Processes at the First Process Modeling Level

Name	Rank Correlation Coefficient
Fluorine Utilization Rate in NF_3 Cleaning	-0.54
Fluorine Utilization Rate in F_2 Cleaning	0.53
Price of Anhydrous HF ($/kg)	-0.50

5.2.4 The VOI of Further Analysis

- **Calculation of VOI**

The decision scenarios faced by the decision maker at this stage can be captured in Figure 5.12. The goal of further research is to better distinguish the two technologies. After the first modeling level, the conclusion was that the confidence level (CL) of F_2 having a lower lifecycle GWP than NF_3 is 85%. The utility should be assigned to the underlying GWP, rather than the CL. The reason behind this choice can be illustrated by the following example. Let us assume that there are two decisions. One concerns of \$10 and the other one concerns of \$10,000. The current knowledge of the two decision contexts both leads to 85% of CL in the decision outcome. It is obvious that the values of increasing the CL to 95% for the two decision contexts are very different due to the absolute dollar amounts involved.

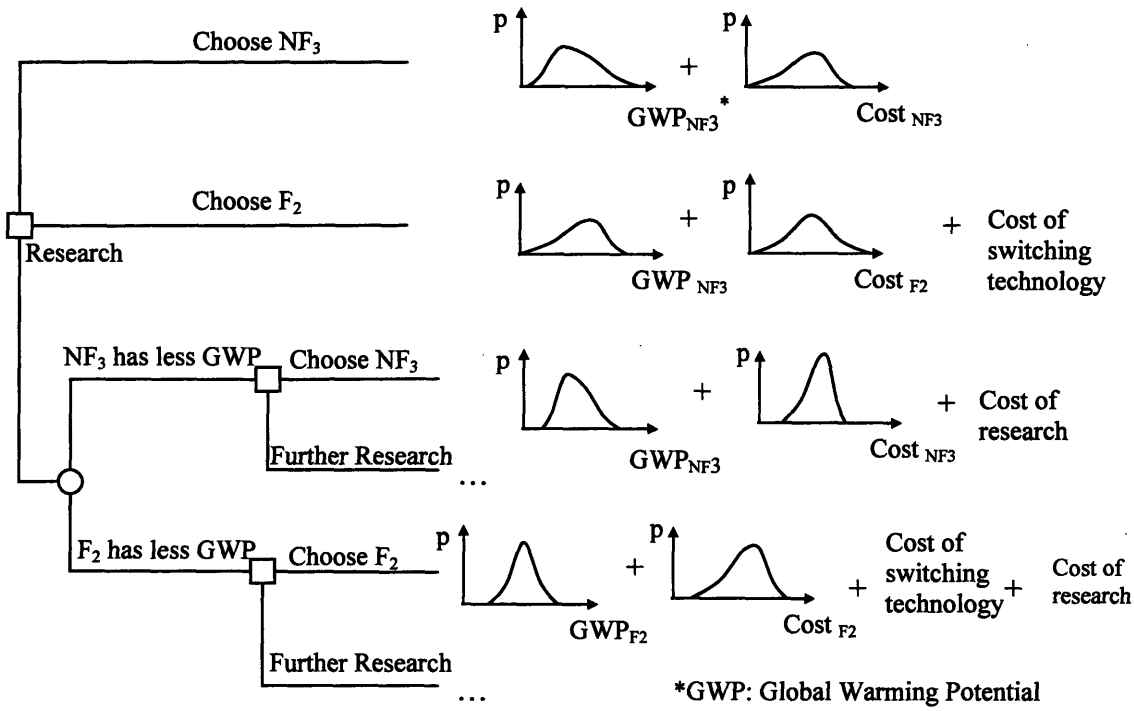

Figure 5.12 The Decision Scenarios of the Chamber Cleaning Case Study

Another piece of information needed is the cost of obtaining information. Cost can come from various sources: monetary, personnel, opportunity cost, and etc. To simplify the problem, given that only modeling is involved in the analysis but no experiments, only personnel cost in the form of salary was considered. For a \$100,000 salary of an engineer, the cost to the company was of the order of magnitude of \$250,000.

The steps of calculating the VOI were:

1. The fluorine yields, cleaning time, and the energy yields of the NF_3 and F_2 processes were identified as the most important parameters for the relative GWP.
2. Based on past experience, it was assumed that the standard deviations of the fluorine yields would be reduced by 40% at the 2nd modeling level.

3. The PIO-LCA model is run again to generate the distributions of the GWP for each process.
4. The utilities of the GWPs were calculated using the utility function. Two risk tolerances were compared here: R_1 = 1×10^6 kg CO_2 equivalent, R_2 = 5×10^5 kg CO_2 equivalent.
5. The cost of switching the technology from NF_3 to F_2 was assumed to be \$1,000,000 for the life time of the technologies. The time value of money was not considered in this study given the delay is short, and that the choice of the cleaning gas will not hold off other manufacturing processes. Therefore, the EU of money was \$1,000,000 / \$6,000,000 ≈ 0.167. This EU was added into the total outcome of each path.
6. The EUs (i.e. environmental cost) of the processes at the 1st level and the projected EUs at 2nd level were calculated using the Monte Carlo simulations. The latter was calculated as: for each Monte Carlo simulation, the EU of the two processes were obtained. If the EU of F_2 plus the EU of the switching cost was still smaller than the EU of NF_3, then the decision was to choose F_2. The EU of this simulation was the EU of F_2 plus the EU of the switching cost. Otherwise, the EU of this simulation was the EU of the NF_3 process. Then, the average of the EUs of all the simulations was the projected EU of modeling at the 2nd level.
7. The variable costs of using the two gases were also included in the analysis. The same monetary utility function was used.

The results of the simulation is shown in Figure 5.13. Research above the 2nd level is not considered at this point. EUs of switching technology were included.

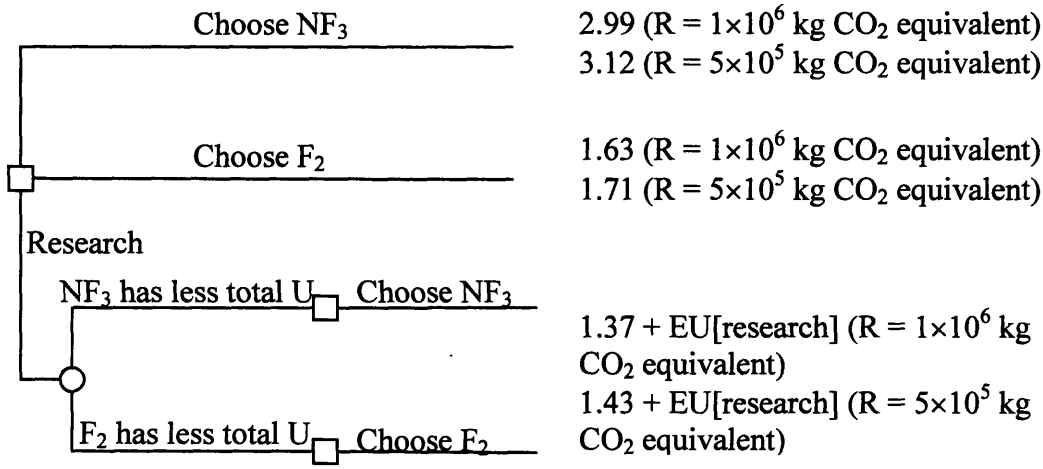

Figure 5.13 Outcomes of Decision Paths in the Comparison

Based on the 1st level result, between the NF_3 and F_2 processes, the latter should be chosen. If the research branch is also considered, the expected value of information of decision maker D_1 with R_1 = 1×10^6 kg CO_2 equivalent is:

$$EU[VOI]_{D1} = 1.63 - 1.37 = 0.26$$

Therefore, when the cost of research, i.e. EU[research] is less than 0.26, models at the 2nd level should be built. Similarly, EU[VOI] of decision maker D_2 with R_2 = 5×10^5 kg CO_2 equivalent is 0.28. The corresponding costs of research in these two scenarios are \$1,560,000 and \$1,680,000, respectively. If 0.26 < EU[research] < 0.28, then D_1 would perform the research while D_2 would not but rather choose the F2 process right away.

- **Discussion**

This case was constructed to illustrate the concept of VOI and the methodology of calculating it. The numbers in the report are not necessarily the best representations of the real world. For example, based on the GWP utility curve, changing from the annual aggregate 1.7×10^5 kg CO_2 equivalent GWP of the NF_3 process to 7×10^4 kg CO_2 equivalent GWP of the F_2 process, the utility is 0.088. This is equivalent to a change of \$532,000 based on the monetary utility curve. That is to say that the decision maker is willing to trade off 1×10^5 kg CO_2 equivalent for \$532,000, which means that the price of CO_2 is about \$5/kg CO_2. The price for the CO_2 trading market is around much less than that: the price in the EU is ~ 7 Euro/ton CO_2. For the trades based on the Kyoto Protocol, it is about \$5/ton CO_2. The market price in the US right now is about \$1/ton CO_2 [88].

If the decision maker prefers not to convert the utilities of the GWP and money into the same unit, Pareto optimality can be used. In a multiple-criteria scenario, a solution can be considered Pareto optimal if there is no other solution that performs at least as well on every criteria and strictly better on at least one criteria. That is, a Pareto-optimal solution cannot be improved without hurting at least one of the criteria. For this case, there are three possible outcomes: choosing NF_3 directly, choosing F_2 directly, and carrying out research and choosing according to the results of the research. They are plotted in Figure 5.14.

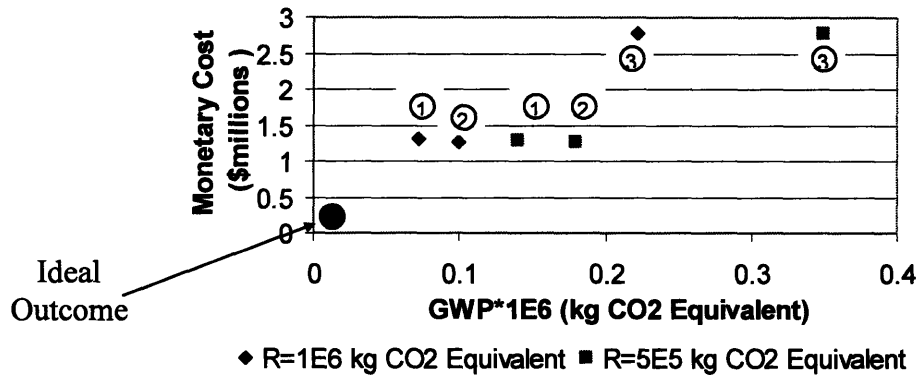

Figure 5.14 Comparison of Outcomes of Monetary Costs and GWP of Different Decision Path with Two Risk Tolerances. 1 – Research Path, 2—Directly switching to F_2, 3 – Continuing with NF_3. The red dot shows the ideal outcome which is not achievable.

Because both axes are costs, the closer the outcomes are to the origin, the better the outcomes are. Obviously, the ideal outcome denoted by the red dot is not achievable. The dots denoted by 3 are the dominated by Dots 1 and 2 with both risk tolerances. Both

in terms of GWP and monetary costs the formers are worse. For Dots 1 and 2, Dot 1 has a lower GWP but a higher monetary cost than Dot 2 with both risk tolerances. To go from Dot 1 to Dot 2 or from Dot 2 to Dot 1, one of the criteria will be hurt for the other one to be improved. Therefore, Dots 1 and 2 are the Pareto optimal.

For the cost of information, in a university or even in the industry, research at the 2nd modeling level would hardly cost more than two months. The salary cost during this time frame is around $50,000. This is much lower than the cost of research beyond which the research will not be carried out. Therefore, given this salary situation, the 2nd level research should be performed for both risk tolerances.

5.2.5 Second Round of Comparison

Since it is worthwhile to conduct further research based on the VOI result, and that the important parameters are of the cleaning process models, the two processes are modeled in a more detailed level. At the second modeling level, most of the cleaning operating parameters, such as chamber pressures, chamber temperatures, were set to be the same for both processes. The plasma powers were chosen so that the disassociation rates of the cleaning gases are larger than 90%. The cleaning gas flow rate for the NF_3 cleaning was chosen from literature [89], while that of F_2 was solved to achieve the same cleaning rate of the NF_3 cleaning.

- **Modeling of Plasma Generator and CVD Chamber**

The generator was modeled as a continuous stirred tank reactor (CSTR). The "startup" time when the gas is just pumped into the chamber is neglected because the residence times of both cleaning cases are 5 orders of magnitude smaller than the cleaning time. Therefore the amount of SiO_2 that is reacted during the startup time is negligible, hence the system can be viewed as at steady state. The schematic of the generator and CVD chamber is the same as in Figure 5.6.

$$NF_3 + e \text{ --> } NF_2 + F + e$$

$$k_3 = 2.06 \times 10^{-17} T_e^{1.7} \exp\left(-37274/T_e\right) \tag{5.5}$$

$$NF_2 + e \text{ --> } NF + F + e$$

$$k_2 = 1.57 \times 10^{-17} T_e^{1.8} \exp\left(-27565/T_e\right) \tag{5.6}$$

$$NF + e \text{ --> } N + F + e$$

$$k_1 = 1.57 \times 10^{-17} T_e^{1.8} \exp\left(-27565/T_e\right) \tag{5.7}$$

where k_i – reaction rate coefficient for reaction i, cm^3/molecular-s

T_e – electron temperature, K.

The mass balances of species NF_3, NF_2 radical, NF radical, and F radicals of the NF_3 cleaning are:

$$Q_{out} n_F = k_3 n_{NF_3} n_{e.a} V + k_2 n_{NF_2} n_{e.a} V + k_1 n_{NF} n_{e.a} V \tag{5.8}$$

$$Q_{out} n_{NF_3} - Q_{in} n^{i}_{NF_3} = -k_3 n_{NF_3} n_{e.a} V \tag{5.9}$$

$$Q_{out} n_{NF_2} = k_3 n_{NF_3} n_{e.a} V - k_2 n_{NF_2} n_{e.a} V$$

$$Q_{out} n_{NF} = k_2 n_{NF_2} n_{e.a} V - k_1 n_{NF} n_{e.a} V$$

(5.10)

(5.11)

where Q_{out} – outlet flow rate of gas leaving the generator, cm^3/s,
Q_{in} – outlet flow rate of gas entering the generator, cm^3/s.
V – volume of the generator, cm^3,
$n_{e,a}$ – average molecular concentration of electrons, cm^{-3},
n_{NF3} – outlet molecular concentration of NF_3, cm^{-3},
n^i_{NF3} – inlet molecular concentration of NF_3, cm^{-3},
n_{NF2} – outlet molecular concentration of NF_2, cm^{-3},
n_{NF} – outlet molecular concentration of NF, cm^{-3}.

The reaction in the plasma source of the F_2 the cleaning is [90]:

$$F_2 + e \text{ --> } F + F^-$$

$$k_F = 1.02 \times 10^{-5} T_e^{-0.9} \exp\left(-1081.8/T_e\right) \tag{5.12}$$

where k_F – reaction rate coefficient, cm^3/s

The fluorine anions undergo the following reaction to become fluorine radicals [90]:

$$F^- + Ar^+ \text{ --> } F + Ar$$

$$k_{F\text{-}Ar} = 1.00E\text{-}8 \tag{5.13}$$

The overall mass balances for F_2 and F are:

$$Q_{out} n_F = k_F n_{F_2} n_{e,a} V + k_{F-Ar} n_{F^-} n_{Ar^+} V \tag{5.14}$$

$$Q_{out} n_{F_2} - Q_{in} n^i_{F_2} = -k_F n_{F_2} n_{e,a} V \tag{5.15}$$

where n_F – outlet molecular concentration of fluorine radical, cm^{-3},
n_{F2} – outlet molecular concentration of F_2, cm^{-3},
n_{Ar+} – outlet molecular concentration of Ar^+, cm^{-3},
n_{F-} – outlet molecular concentration of F^-, cm^{-3},
n^i_{F2} – inlet molecular concentration of F_2, cm^{-3}.

Since [90] does not provide their uncertainties, the rate coefficients of the decomposing reactions were all assumed to have a normal distribution with the standard deviation being 10% of the nominal value. Truncated normal distributions were used where the factors have physical limits, such as the activation energies in the Arrehenuis formulas should not be less than zero.

Ions are also generated inside the plasma generator. However, as they travel through the transport tube from the generator to the cleaning chamber, they mostly collide with the tube wall and form stable molecules. As a result, the ions do not play an important role in etching the residual on the chamber wall. The neutrals are assumed to be pumped out of the generator and chamber with no reactions with the SiO_2 film.

The etching gas is distributed by a shower-head before entering the cleaning chamber. The chamber was modeled as a PSTR as well given its lower gas density. The chamber pressure, the surface and gas temperature were set to be the same for both cleanings. The etch rate of SiO_2 was correlated to the n_F and the surface temperature in an Arrehenuis form based on experimental data [91]:

$$r = (8.97 \pm 0.82) \times 10^{-13} n_F T_s^{1/2} \exp\left(-0.163eV/kT_s\right)$$

(5.16)

where r – etch rate, Å/min,
eV – energy of an electron, 1.6E-19 J,
k – Boltzmann constant, 1.38E-23 m^2 kg s^{-2} K^{-1},
T_s – surface temperature, K.

Based on the gas conditions in the generator and the chamber, assuming no radical loss on the walls, the F radical density in the chamber for NF_3 cleaning was calculated, so as the etch rate from Equation (5.16). For F_2 to achieve the same etch rate, the F radical density in the chamber for the F_2 cleaning needs to be the same as that of the NF_3 cleaning. Based on this requirement, the F_2 inlet flow rate was solved.

From the gas flow rate and the amount of SiO_2 deposited in the chamber, the material used in the process and the emissions were calculated. The energy consumption considered in this work was only that of the plasma generation but not including pumping, cooling, and etc because it is the main energy consumption process in the chamber cleaning process [92].

- **Results of Second Round of Comparison**

Results of Cleaning Processes

Properties that were not able to be predicted in the first round could be described at this round of comparison. The distributions of the etch rate of the SiO_2 film and the fluorine utilization efficiencies F% of the NF_3 cleaning are shown in Figure 5.15 and Figure 5.16. The modeling results of the etch rate, fluorine utilization efficiency, and NF_3 decompose rates are slightly higher than industrial data due to the assumption of no radical loss in the etch chamber. As the purpose of this study is to distinguish the two cleaning technologies, this assumption affects the results of both cases in the same direction, and does not affect the conclusion of the analysis. The fluorine efficiency of the F_2 cleaning and the ratio of the two efficiencies are also shown in Figure 5.16. Compared to the distributions of Equation (5.1) and Equation (5.2), the distributions in Figure 5.16 are narrower, which can be seen clearer in Figure 5.17. Figure 5.17 shows the distributions corresponding to the two modeling levels for the NF_3 cleaning. The two straight lines represent the acceptable limits. The distribution noted by the dash line is a uniform distribution between 0 and 60%, as there is no other information available. The solid line is the same distribution as in Figure 5.16 but in a histogram format. With 3 chemical reactions, the distribution has been narrowed.

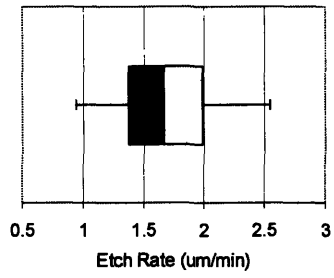

Figure 5.15 Distribution of SiO_2 Etch Rate at the Second Process Modeling Level

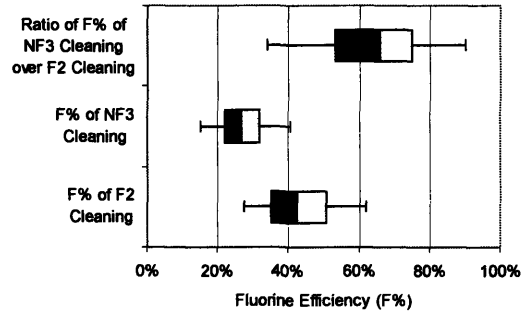

Figure 5.16 Distribution of Fluorine Utilization Efficiencies F% of NF_3 and F_2 Cleaning, and Ratio of These Two Efficiencies at the Second Process Modeling Level

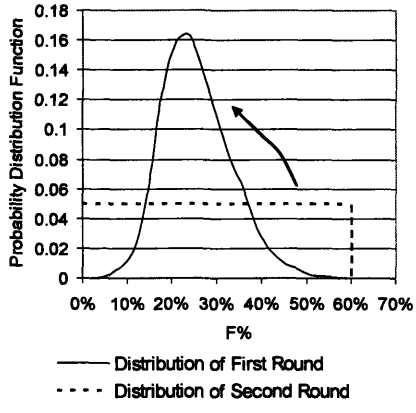

Figure 5.17 Distributions of Fluorine Efficiency F% of the NF_3 Cleaning at Different Modeling Levels

The F_2 gas flow rate distribution to achieve the same etch rate as 600 sccm NF_3 is shown in Figure 5.18. The wide spread of the value comes from the uncertainty in the disassociation reaction coefficients, the etch rate coefficients, and the plasma modeling.

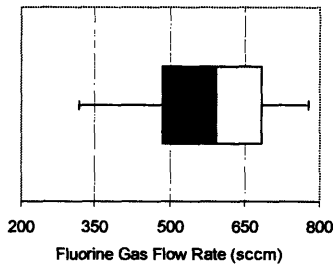

Figure 5.18 Distribution of the F_2 Gas Flow Rate at the Second Process Modeling Level

Results of Life Cycle Impacts

The LCA impacts of the two cleaning processes are compared in Figure 5.19. The units are listed below each categories. Please note that these units are different. Therefore, it is incorrect to say that the ozone depletion potential is less severe than the global warming potential, as the severity depends on how one unit of the adverse effect is valued. Since the valuation factors of these impacts vary greatly depending on the decision-maker, they were not weighted and summed up to one unit here. It can be seen that for all the categories, the NF_3 cleaning has larger impacts than those of the F_2 cleaning. It should also be noted that in this case, only the impacts induced by the energy consumption of the NF_3 production and limited upstream processes are considered, but not the emissions from these processes themselves. If they had also been considered, the difference between the impacts would have been even larger because the upstream of F_2 is a subset of that of NF_3.

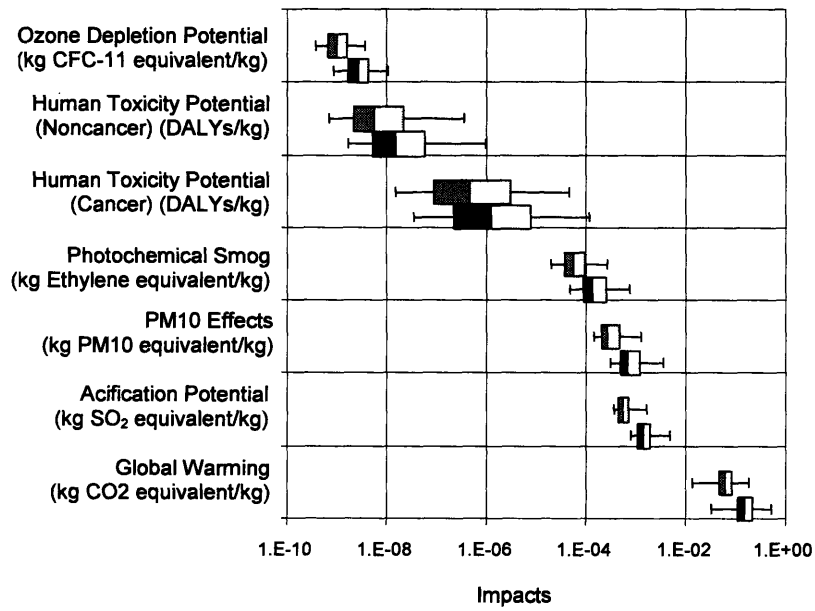

Figure 5.19 Comparison of the Environmental Impacts of the NF_3 and F_2 Chamber Cleaning Processes under Uncertainty at the Second Process Modeling Level

The comparison of the relative GWP of the NF_3 process over the F_2 process is shown in Figure 5.20. It can be clearly seen that less than 5% of the time, the GWP of the

NF_3 process will be less than 1.9 times larger than that of the F_2 process. Even though there is much uncertainty in the inputs, by directly addressing the uncertainty and using relative ratio, these two processes can be clearly differentiated. The decrease in uncertainty, or the increase in the information content has significantly increases the confidence level from the first process modeling level to the second one. However, the increase of the available information does not change the judgment that the NF_3 process has higher impacts than the F_2 process. For a decision maker who is satisfied with the 85% confidence level provided by the first modeling level, the extra effort at the second level does not add much value. This means that the amount of information needed for an analysis depends closely on the decision context.

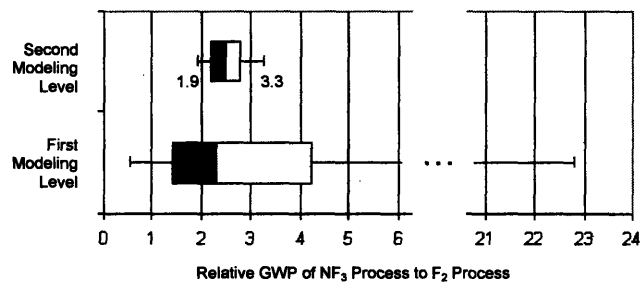

Figure 5.20 Uncertainty of the Relative GWP of the NF_3 Cleaning to the F_2 Cleaning at the Second Process Modeling Level

The higher environmental impacts of the NF_3 cleaning compared to the F_2 cleaning come from the higher power consumption in the plasma generator, the water needed to clean up the waste stream, and the longer upstream production chain. The comparison of the energy usage of the two cleaning processes with different system boundary is in Figure 5.21. Even though in this case the inclusion of the energy used outside the fab does not change the comparison result at the second process modeling level, the fact that 50% of the total energy consumption of the NF_3 cleaning is from outside the fab is still significant.

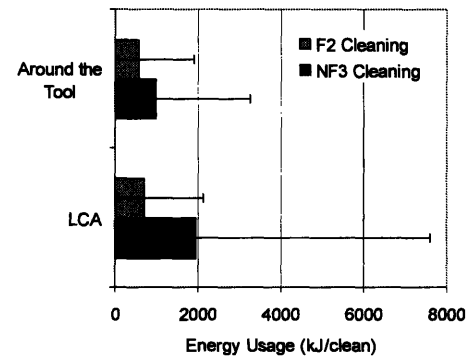

Figure 5.21 Comparison of the Energy Usage of the Two Cleaning Processes with Two System Boundaries

The analysis shows that in terms of LCA environmental impacts, using F_2 as the cleaning gas leads to less impacts than using NF_3. However, there are other complexities with F_2 such as worker health and safety. F_2 is very toxic. It has extremely low threshold limit value of 1, compared to 10 for NF_3 and 5 for silane. It is also highly reactive and can erode the pipes and fittings in the presence of moisture. It is also regulated by the EPA with a reportable quantity of 10 lbs [93]. Because of the reactivity and the toxicity of F_2, transportation of large amounts of F_2 is tightly regulated. POU generation has been tested as the means of supplying F_2 into the cleaning system. However, F_2 generators inside the fab are generate a large amount of explosive H_2 gas as a by-product, thus pose a safety threat. The generators also need frequent maintenance. Therefore, the decision of choosing between NF_3 and F_2 as the cleaning gas requires comprehensive considerations of these aspects.

- **Identification of Important Parameters at Second Round of Comparison**

In this work, no further research was done in comparing the two processes. For the completeness of the analysis, the important parameters that contribute to the uncertainty in the outputs will still be discussed here.

Figure 5.22 shows the three parameters with the largest absolute values of the Spearman rank correlation coefficients of the NF_3 cleaning etch rate. The temperature of the chamber inner surface is the most important factor. Although the heater temperature is well controlled, the temperatures of the shower head, the pumping plate, and other areas that need to be cleaned are not controlled or measured in practice. Hence, an estimation with a broad distribution was assigned to represent the average temperature of these surfaces. Its high correlation coefficient means that to reduce the variability in the simulated etch rate, a better account of the average temperature is needed. A more accurate way of modeling the etch rate is to find the temperature and the etch rate for each surface. Then average the mass change at each surface to get the average rates.

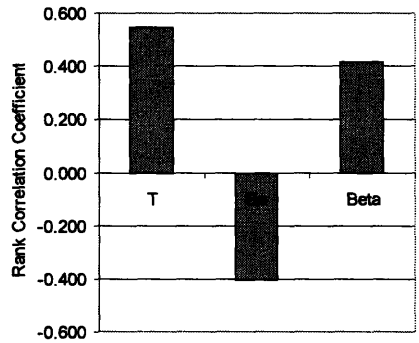

Figure 5.22 Top Three Rank Correlation Coefficients of the Etch Rate of the NF_3 Cleaning Process at the Second Process Modeling Level. T is the temperature of the surfaces that need to be cleaned. Ea is the activation energy in the SiO_2 etch rate equation (see Equation (5.16)). Beta is the power of the electron temperature of the NF_3 disassociation reaction in the plasma (see Equation (5.5)).

Table 5.4 lists the top 5 parameters with the highest rank correlation coefficient of the relative GWP at the second process modeling level. The largest part of uncertainty of the relative GWP comes from the power β to the electron temperature in the NF_3 disassociation reaction. β affects the etch rate, as can be seen in Figure 5.16, therefore the cleaning time, the power used in the plasma generator, and the cleaning gas usage. The second most important parameter is the power consumption in the plasma generator. The NF_3 efficiency in NF_3 production and the energy usage in F_2 production directly drives the overall energy usage in the life cycle of the NF_3 and F_2 processes, which in turn determines the relative impacts. Based on this sensitivity analysis, gathering more information on the plasma system and the upstream of NF_3 production will be the most effective in increasing decision confidence from this modeling level on, rather than researching the GWP factors.

Table 5.4 Parameters with the Highest Rank Correlation Coefficients of the Relative GWP of the NF_3 and F_2 Cleaning Processes at the Second Process Modeling Level

Parameter	Rank Correlation Coefficient
Power β to the Electron Temperature in the NF_3 Disassociation Reaction (See (29))	-0.55
NF_3 Efficiency in NF_3 Production from NH_3 and HF	-0.46
Power Used in Plasma Generator (W)	0.40
Power β to the Electron Temperature in the NF_2 Disassociation Reaction (See (30))	-0.24
Energy Used in HF Production (J)	0.22

5.3 Summary

This chapter discusses the methodology that can address the uncertainty in data and ease the integration of environmental considerations into technology selections under multiple criteria and tight time frame. By using probability distribution functions to describe the uncertain inputs and apply appropriate non-linear global sensitivity analysis methods, the variability in outputs due to the model and variability in inputs can be captured. The parameters that contribute to the most of the variability in outputs can be identified. When the uncertainty analysis is coupled with hierarchical modeling and the value of information analysis, it can economically allocate data collection effort and reduce analysis time. Hierarchal modeling and the value of information analysis are based on the concept that the amount of information needed for an analysis depends closely on the decision context. The case study of comparing two chamber cleaning gases exemplifies the framework. A case study comparing NF_3 and F_2 as the cleaning gas in chemical vapor deposition chambers illustrates the application of the framework. The distributions of the LCA global warming potentials of the NF_3 cleaning and that of the F_2 cleaning were calculated, with the most likely value of the ratio of the two around 2.5 given the same etch rates. The study shows that with uncertainty analysis, large variability in inputs does not necessarily lead to low confidence level in decisions. When higher accuracy in inputs is desirable, data collection and model refining effort should

focus on factors that contribute the most to the uncertainty in decision. Hierarchical modeling in combination with uncertainty analysis and value of information analysis is efficient in supporting the decision making and resource allocation process.

Chapter 6 Uniformed Modeling Platform

6.1 Description of the Platform

One of the major obstacles for integrating LCA into process design and optimization is that these two functions are segregated despite much overlap in their data requirement, as seen in Figure 6.1. This large overlap in data shows that the data collected for better understanding of the environment can be used for cost analysis, and vise versa. In order for the LCA to provide useful and actionable suggestions on process design and optimization, the effects of process recipes and tool selections on life cycle impacts need to be clear.

The process modeling in most of the existing LCA studies are ad hoc [15]. Researchers use various programs and languages to develop process models. Existing LCA software does not have extensive physical and chemical databases, nor process modules dedicated for the semiconductor industry that can be easily customized. On the other hand, existing process modeling software does not have extensive life cycle information, nor environmental/health exposure and impact data. Without a uniform modeling platform, models built by one researcher are hard to be used by other researchers or the industry.

To overcome these difficulties, a unified modeling platform was designed. It consists of an LCA simulator, a process simulator, chemical/physical databases, LCA databases, and an uncertainty analysis tool. A relationship diagram of the system is shown in Figure 6.2.

The system was realized by existing commercial software. The software programs used are: Aspen Plus® [94] for process modeling, Microsoft® Excel 2002 for LCA modeling, Microsoft® Access 2002 for LCA database, and @Risk® [95] for Monte Carlo simulations. The programs are connected through Visual Basic to perform a process model-driven LCA. This integrated system reduces the cost and time for developing a process modeling platform that is compatible with LCA from scratch. It also allows uncertainty analysis on both the LCA models and process models simultaneously. The importance of including uncertainty analysis has gradually gained recognition in the LCA community due to the large uncertainty in the LCA data [96-99].

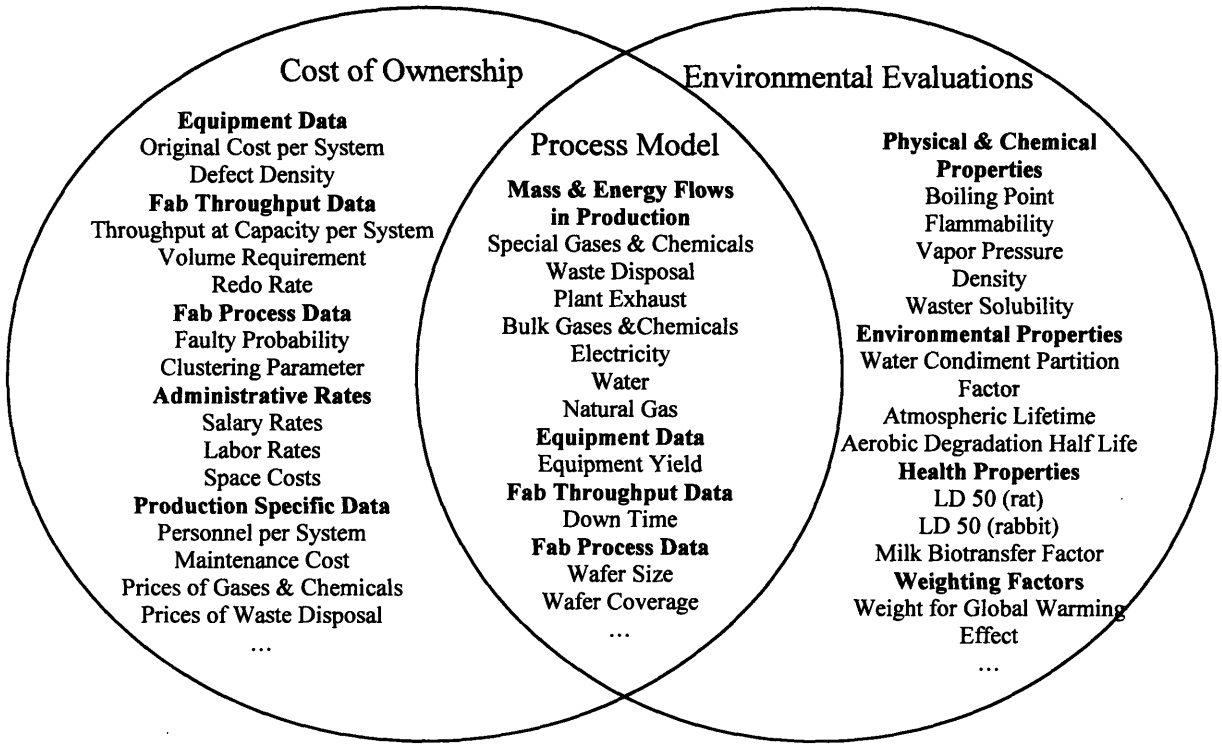

Figure 6.1 Overlapping of Data Requirements in an economic valuation and an environmental valuation

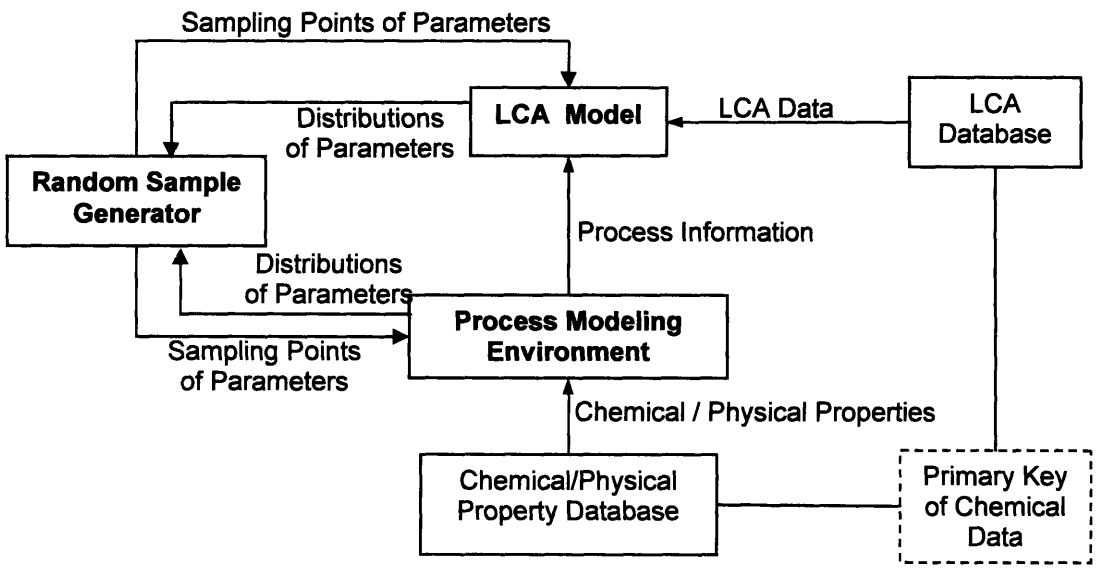

Figure 6.2 Relationship Diagram of Components in the Unified Modeling Platform

6.2 Case Study of the Chamber Cleaning Process

A case study of comparing NF_3 and F_2 as the chamber cleaning gas is used here to illustrate the integrated system. Its process model was built in Aspen Plus®. Aspen

Plus® is commonly used by the chemical industry in process design. It provides an integrated flowsheeting environment for sequential-modular, equation-oriented simulation and optimization, data reconciliation, parameter estimation and optimization [100]. The flowsheet of the chamber cleaning case is shown in Figure 6.3. In the actual process, SiO_2 is inside the chamber before the etching starts. However, due to limitations of the version of Aspen Plus that was available to the author at the time of the study, the model represents the SiO_2 as continuously fed into the chamber. The flow rate of SiO_2 in the model is equal to the etch rate in moles per second for real situations. In calculating the inlet conditions of the etch chamber and downstream waste treatment, the reactions of the process were fed into the software. The design requirements were specified such as the etch rate of the SiO_2 film and the outlet fluorine concentration of the downstream effluent. Then the imbedded physical and chemical databases in Aspen Plus were used to solve for the inlet conditions and determine the material and energy balances of the unit operations.

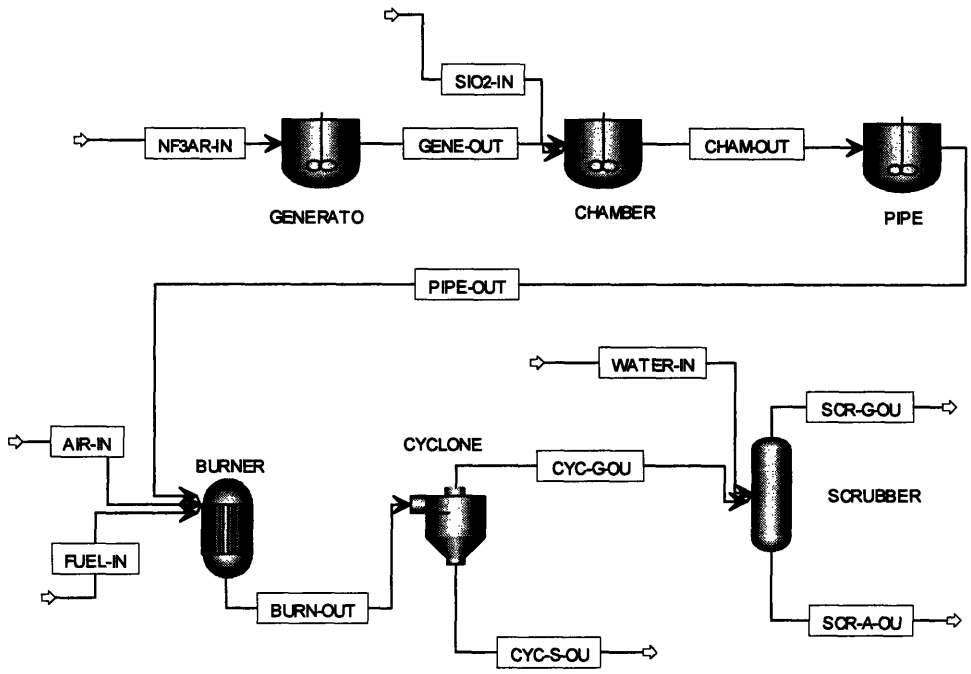

Figure 6.3 Aspen Plus Flow Sheet of Chamber Cleaning Process with Downstream Treatment

To show how the changes in etch rates affect the lifecycle impacts, a range of etch rates was selected. Different etch rates were achieved by varying the NF_3 flow rates while keeping the plasma power, the pressures and temperatures in the generator and the chamber, and the flow rates of other gases constant. This implicitly assumes that the set plasma power is sufficient to break down the NF_3 at different flow rates, which is generally valid because most of the power is used to ionize the gases. The NF_3 flow rates and the water usages to scrub the HF to 10 ppm were calculated by Aspen Plus. The former was then fed into the PIO-LCA model. The histogram of the ten life cycle impacts were generated by the LCA model in combination with the Monte Carlo

simulations ran in @Risk®. Visual Basic macros were used to connect the programs and automate the simulations. A Process-Product Input Output LCA (PIO-LCA) with supporting database [12, 63, 66] was used for the life cycle modeling. The set of indicators follow Eco-Indicator 99 [101].

6.3 Results of the Case Study

The global warming potential (GWP) is used as one example of the life cycle impacts to illustrate the effects of the changes of the etch rate requirements. Its result and the NF_3 usage per clean are shown in Figure 6.4. It can be seen that as the etch rate increases, the NF_3 needed to sustain the higher etch rate increases along with the GWP. However, the increase of the GWP is less steep than that of the NF3 usage. This is because a large portion of the GWP comes from generating energy for the plasma generator.

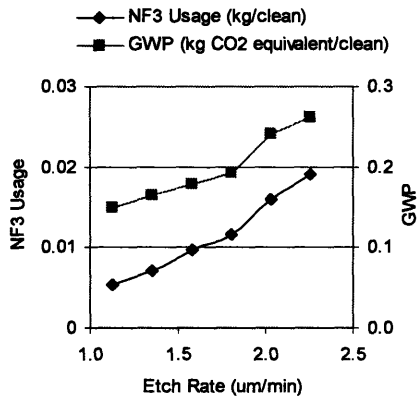

Figure 6.4 Changes of NF_3 Usages and GWP with Changes of Etch Rates

Given the large uncertainty in the life cycle data, it is necessary to look at the uncertainty of the results. Figure 6.5 shows the confidence levels of the GWP at different etch rates. It can be seen that the uncertainties in the GWP are significant. However, most of the uncertainty comes from emissions of power plants, the global warming potentials of emission gases, and the amount of raw materials and energy needed to produce NF_3. These factors are common to all of the scenarios studied here. Therefore, when relative GWPs are used for the comparison, the uncertainty is much smaller as the effects of these common factors cancel out. Relative GWP is defined here as

$$\text{Relative } GWP_i = GWP_{ri} / GWP_{r=1.2\ \text{um/min}},$$

where i – number of scenario.

The result can be seen in Figure 6.6, which shows that all of the relative GWP is greater than one (excluding Relative $GWP_{r\ =\ 1.2\ \text{um/min}}$, which is one). Hence, in comparison of two or more processes under uncertainty, the relative ratio rather than the absolute value should be studied.

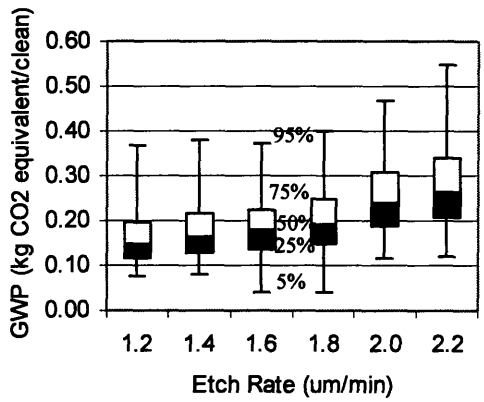

Figure 6.5 Comparison of GWPs of Different Etch Rates with Confidence Levels

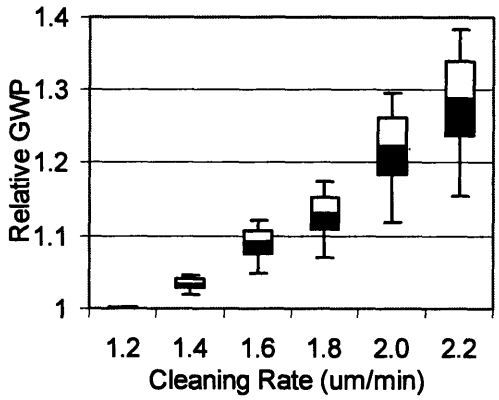

Figure 6.6 Comparison of Relative GWPs of Different Etch Rates with Confidence Levels

Water consumptions under different etch rate requirements were also modeled. The results are shown in Figure 6.7. Water is used to scrubbed the HF in the gas exhaust stream to be less than 10 ppm. Facility engineers can use this information to correctly size the abatement system and plan waste water treatment capacity.

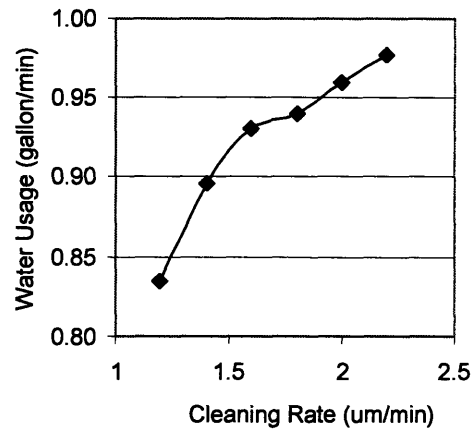

Figure 6.7 Changes of Water Usage with Changes of Etch Rates

6.4 Discussions

The set of commercial software used in this case study serves only as an example. The reason why Aspen Plus® was selected was that (a) it includes many build-in unit operations that can be customized; (b) it allows easy linkage between unit operations, therefore clusters of tools and even the whole fab can be modeled in one platform, as well as the downstream treatment processes. This makes it easier to study the impact of process designs on downstream and emissions; (c) it allows process models to be built at various hierarchy of details. Models of different detail level can be straightforwardly exchanged; (d) it also has databases of physical and chemical properties of common chemicals and estimation methods imbedded in the program. However, it is a program designed for the chemical industry. Its unit operations are not necessarily the most appropriate ones for semiconductor processes.

Another program that can be studied is TSUPREM-4 [102]. It is a computer program for simulating the processing steps used in the manufacture of silicon integrated circuits and discrete devices. It can simulate the incorporation and redistribution of impurities in a two-dimensional device [103]. It has an extensive pool of common processing steps used in the semiconductor manufacturing. Its drawback is that it does not model material and energy usages, nor emissions. However, these can be calculated from the parameters that describe the film transformation.

Aspen Plus® has extensive physical and chemical property databases. These databases provide necessary information for modeling reactions, products, and reactor conditions. These databases need to be linked to the LCA database by sharing the same primary key for the same chemical. Eventually we can imagine a highly integrated system in which once chemicals are called in process models, the system will automatically call the LCA data of these chemicals and generate the LCA model. This will greatly facilitate the use of LCA in process design and optimization.

The method and system used in this case study is generic and can be used for comparison of alternative technologies, such as NF_3 vs. C_2F_8. Over time, models of unit operations can be developed and accumulated. These models can help both process and facility engineers in designing the processes and facility, as well as ESH personnel in understanding/predicting the impacts. More importantly, this integrated system can facilitate the communication between the parties and resolve the shortcoming of "un-actionable" of LCAs. Eventually the goal is the integration of several design criteria: technical performance, profit, and sustainability.

6.5 Summary

An integrated system of process and LCA modeling platform can be used to understand both the technical performance and the life cycle environmental impacts of processes and facility. The effects of changes the process recipes on lifecycle impacts can be easily seen using this system. It can ease the communication between ESH engineers, process engineers, and facility engineers. A case study using existing commercial software illustrates the use of the system. To fully take advantage of existing physical/chemical and LCA databases, common primary keys need to be established for the same chemicals in different databases. More process modeling software should be studied to identify the most suitable one for the integrated system.

Chapter 7. Future Work

This thesis has laid a foundation for easing the integration of environmental considerations into technology selection under uncertainty. There is more work to be done to make the integration being fully practical in the industry routine decision making.

- **Identify areas for the most effective improvement on the ESH footprints**

The majority of the thesis has focuses on distinguishing among alternative processes. If the objective is to reduce the environmental footprint of the whole semiconductor and flat panel industry, the approach is still similar. Firstly, the processes, platform, infrastructure that have the largest footprints need to be identified. A hybrid Economic Input-output LCA and PIO-LCA can be used to include the upstream and downstream effects. Secondly, the ones that allow the largest flexibility in material substitution, process optimization, and downstream treatment optimization also need to be identified. The first areas are where the largest potential benefit lies. The second areas are where the lowest cost lies. The most effective improvement areas should be the shared part of the two. Special attention should be put into the flat panel industry which is more cost-sensitive and has larger leeway in changing process receipts to lower costs.

The framework and tools proposed in this work can be directly implement into the identification of the two areas. Due to the large number of processes involved, only rough estimations on materials and energy inflow and outflow can be used. Proper documentation and propagation of the uncertainty through the study are important in the speed and credibility of the results.

- **Generate alternatives with smaller footprints in the most effective areas**

Besides for the good of the environment, there have been cases where an investigation to a new material or process was prompted by ESH causes, yet the results of the alternative turned out to be superior performance wise. An example for this is the discovery of C_4F_8 as an etching gas. C_4F_8 was first studied for its higher disassociation rates in the plasma compared to C_2F_6 which was widely used in the industry, therefore lower global warming gas emissions. It was then found that C_4F_8 also has a higher etching rate than C_2F_6. This should not be surprising because higher disassociation rates mean higher percentages of input materials are turned into radicals to react with photoresists, which in turn leads to higher etch rates. The adoption of C_4F_8 ultimately resulted from its better performance. Yet without the motivation to study it form the environmental perspective, it probably would not have been discovered.

- **Construct models of the most effective areas**

To facilitate the generation of alternatives with smaller footprints and other comparison type of analyses, models that describe these most effective areas can be constructed at different levels of sophistication. These models can then be used as off-the-shelf prototypes for further customized analyses or give directions to experiment designs.

Future researchers should also pick a few industrially relevant case studies and work through them in detail, illustrate information needed at each stage and how should one use approximation, then generate technology transfer reports.

- **Develop training modules for practitioners to educate them to think probabilistically.**

The concept that the real world is probabilistic rather than deterministic is foreign and disturbing to many people, including well-educated engineers and managers whose decisions are concerned in this paper. In order for them to use the framework and tools, they first need to feel comfortable with them. Training modules and workshops need to be developed and conducted to educate the practitioners about the merits of observing and thinking about problems probabilistically. This also link back to the development of process models. The educational modules should use the processes and chemicals that are of practical interest to the practitioners. They should be available on-line. The workshops can be conducted in conferences.

- **Incorporate risk analysis technology assessment**

This work has only studied the environmental and cost impacts of technologies. In reality, another major concern is safety and risk. Here safety includes both personnel safety and damage to capital equipment. Risk includes regulation changes and how well the technologies will fare technically and commercially. Ensuring safety leads to additional costs, such as thicker cylinder wall for storing gases, special piping, lower on-site inventory, and compliance. Yet it reduces the likelihood of large costs once accidents happen. For the F_2 case, because it is much more reactive and toxic than NF_3, there will be extra requirement to ensure it being used safely in the fab. The cost, environmental impacts, and the benefits of these areas need to be considered. To capture the cost of risk management, real options theory can be used [104].

- **Make the framework and tools available on-line**

Given the current economical and political environment, it is highly unlikely to commercialize the tools in this paper. Therefore, in order to attract practitioner to use them, they should be made available on-line for free. A successful example of free on-line applications is the EIO-LCA [105]. To protect the intellectual properties of the authors of the tools and copy rights of the software used by the tools, a user can submit requests and input data to a web-based interface. The calculation and analysis can be done at the host server. The results are then transmitted back to the user. To do this, the connection between different software programs described in Chapter 6 also need to be automated.

Users are also encouraged to share their data such as processes, chemicals, lifecycle impacts. The host of the on-line application will collect the data and propagate them into the master database. A data management strategy that incorporates both proprietary data and public data has been proposed by Cano Ruiz [12].

Chapter 8. Conclusion

A new decision-making framework and related tools have been constructed to tackle the barriers in integrating environmental considerations into technology selections. It has the ability to vary system boundaries and provide distributions of adverse environmental impacts rather than single nominal values. It is a generic model and widely applicable to a variety of systems.

1. In order to address the barriers of low data availability and quality issue and long assessment time, an iterative decision process is proposed. The analysis should start with simple models and rough estimations. The uncertainties in the inputs need to be represented using probability distribution functions (PDFs). The uncertainties are then propagated through the evaluation models. The uncertainties in comparison criteria are also represented in PDFs. If the accuracy of the outputs is not satisfactory, appropriate global non-linear sensitivity analysis can be conducted to identify the factors that contribute the most to the uncertainties of the outputs. Given that there is a cost associated with collecting new information, the value of the new information needs to justify the cost. If the VOI is larger than the cost of the information, resources should be allocated in refining models or gathering more data according to the importance of the factors. Otherwise, the decision maker needs to reassess his/her risk preference or end the analysis. This hierarchical modeling procedure can prevent excessive spending on collecting information and building models, and reduce the time and resources used on technology assessments.

2. To make the business case of considering environmental impacts in this economic environment, economical analyses should be conducted along side of environmental analyses. To address the barrier of disengaged environmental and economical analysis, a unified modeling platform has been built using existing commercial software. This platform links the environmental and economical evaluation simulators, the databases for both evaluations, and random number generators together. It allow the effects of changes in the process recipes on lifecycle impacts can be easily seen using this system. It can ease the communication between ESH engineers, process engineers, and facility engineers.

3. For a non-linear non-monotonic system, local sensitivity analysis cannot accurately capture the effects of the inputs on the uncertainties of the outputs. More sophisticated methods are needed to attribute the uncertainties of the outputs to the inputs. Methods can be chose based on their ease to use, representation power, and computation requirements.

4. The case study of using NF_3 and F_2 as the chamber cleaning gas shows that with proper treatment of uncertainty, large variability in inputs does not necessarily lead to low confidence level in decisions.

Uncertainty ≠ Ignorance

Appendix A Cu CVD Model

The following description follows the model developed by [61].

A.1 Mathematical Formula of the Model

- **Mass Balance**

The mass balance for the precursor is:

$$N_{pi} = N_{po} + N_{pr} = N_{po} + N_{rx} \tag{A.1}$$

where N_{pi} –Mole of precursor that comes into the reactor, mole;
N_{po} – Mole of precursor that leaves the reactor, mole;
N_{pr} – Mole of precursor that remains in the chamber, mole;
N_{rx} – Mole of reacted precursor, mole.

$$N_{pi} = \int_0^t \frac{TP_{pv}}{760 \cdot 22.4} dt \tag{A.2}$$

$$N_{po} = \int_0^t \frac{TP_{pp}}{760 \cdot 22.4} dt \tag{A.3}$$

$$N_{pc} = \int_0^t \frac{TP_{pc}}{760 \cdot 22.4} dt \tag{A.4}$$

$$N_{pr} = N_{pi} - N_{po} \tag{A.5}$$

where TP_{pv} – Precursor throughput in the vapor phase, torr-l/sec;
TP_{pp} – Precursor pumping throughput, torr-l/sec;
TP_{pc} – Precursor consumed throughput, torr-l/sec.

N_{pr} and N_{rx} are used as double check for the mass balance.

The precursor utilization percentage is defined as:

$$U = \frac{N_{pr}}{N_{pi}} \cdot 100\% \tag{A.6}$$

For carrier gas,

$$N_{cgi} = N_{cgo} + N_{cgr} \tag{A.7}$$

where N_{cgi} – Mole of carrier gas that comes into the reactor, mole;
N_{cgo} – Mole of carrier gas that leaves the reactor, mole;
N_{cgr} – Mole of carrier gas that remains in the chamber, mole.

$$N_{cgi} = \int_0^t \frac{TP_{cg}}{760 \cdot 22.4} dt \tag{A.8}$$

$$N_{cgo} = \int_0^t \frac{TP_{cgp}}{760 \cdot 22.4} dt \tag{A.9}$$

where TP_{cg} – Carrier gas throughput, torr-l/sec;

TP_{cgp} – Carrier gas pumping throughput, torr-l/sec.

For by-products,

$$N_{bpg} = N_{bpo} + N_{bpr} \tag{A.10}$$

where N_{bpg} – Mole of by-products that is generated inside the reactor, mole;
N_{bpo} – Mole of by-products that leaves the reactor, mole;
N_{bpr} – Mole of by-products that remains in the chamber, mole.

$$N_{bpg} = \int_0^t \frac{TP_{bpg}}{760 \cdot 22.4} dt \tag{A.11}$$

$$N_{bpo} = \int_0^t \frac{TP_{bpp}}{760 \cdot 22.4} dt \tag{A.12}$$

where TP_{bpg} – By-products throughput, torr-l/sec;
TP_{bpp} – By-product pumping throughput, torr-l/sec.

- **Throughputs**

Precursor

The precursor throughput in the vapor phase TP_{pv} is calculated as :

$$TP_{pv} = 0.0126667 * F_p \tag{A.13}$$

where F_p – Precursor flow rate as in vapor phase, sccm.
F_p is calculated as:

$$F_p = 22400 \times \frac{F_{plcon} \times \rho_p}{MW_p} \tag{A.14}$$

where F_{plcon} – Controlled precursor flow rate as in liquid phase, ccm;
ρ_p – Precursor density at 65 °C, g/cm3;
MW_p – Molecule weight of the precursor, g/mol;

The controlled precursor flow rate is determined by the film thickness: before the film thickness reaches the set point, the flow rate is the one set by the user; once the thickness reaches the set point, the flow rate is set to zero. In the model, to prevent divided by zero in the code, the flow rate is set to 10^{-9} instead of zero. The action of terminating the precursor flow can be set either manually, meaning the user would watch the film thickness and stop the simulation when the film thickness reaches the set point, which stops the precursor flow; or can be set automatically, meaning the program would watch the film growth and stop the simulation when the film thickness reaches the set point. Usually the simulator is set to automate the termination.

The precursor pumping throughput TP_{pp} is determined by the proportion of precursor in the gas phase and the R1-RBP1 throughput:

$$TP_{pp} = TP_{R1\text{-}RBP1} * PR_p = TP_{R1\text{-}RBP1} * P_p / P_t \tag{A.15}$$

where $TP_{R1\text{-}RBP1}$ – R1-RBP1 throughput, torr-l/sec;
PR_p – Proportion of the precursor in the gas phase;
R_1 – Reactor chamber;
P_t – Sum of the partial pressure of the precursor, carrier gas, and by-products, torr.

The precursor pressure is calculated as:

$$P_p = \int_0^{t_r} \frac{TP_{pv} - TP_{pp} - TP_{pc}}{V_{R1}} dt \quad (A.16)$$

where t_r – reaction time, sec. In theory, the integral time should start from zero. In the model, in order to avoid dividing by zero, the starting time is set to be 10^{-9}.

The precursor consumption throughput is calcualted as:

$$TP_{pc} = R_e * V_{R1} * 760 * 22.4 \quad (A.17)$$

Carrier Gas

The carrier gas throughput TP_{cg} is calculated as :

$$TP_{cg} = 0.0126667 * F_{cg} \quad (A.18)$$

where F_{cg} – Carrier gas flow rate, sccm. The carrier gas flow rate control is silimar to that of the precursor flow control.

The carrier gas pumping throughput is determined by the proportion of carrier gas in the gas phase and the R1-RBP1 throughput:

$$TP_{cgp} = TP_{R1\text{-}RBP1} * PR_{cg} \quad (A.19)$$

where PR_{cg} – Proportion of the carrier gas in the gas phase;

$$PR_{cg} = P_{cg} / P_t \quad (A.20)$$

where P_{cg} – Partial pressure of the carrier gas, torr.

$$P_{cg} = \int_0^{t_r} \frac{TP_{cg} - TP_{cgp}}{V_{R1}} dt \quad (A.21)$$

By-products

The by-products throughput is calcualted as:

$$TP_{bpg} = 1.5 * R_e * V_{R1} * 760 * 22.4 \quad (A.22)$$

The by-products pumping throughput is determined by the proportion of by-products in the gas phase and the R1-RBP1 throughput:

$$TP_{bpp} = TP_{R1\text{-}RBP1} * PR_{bp} \quad (A.23)$$

where PR_{bp} – Proportion of the by-products in the gas phase;

$$PR_{bp} = P_{bp} / P_t \quad (A.24)$$

where P_{bp} – Partial pressure of the by-product, torr.

$$P_{bp} = \int_0^{t_r} \frac{TP_{bpg} - TP_{bpp}}{V_{R1}} dt \quad (A.25)$$

- **Energy Consumption of Heating in the Cu CVD Process**

In the Maryland model, the energy consumed in the Cu CVD process only includes the energy to maintan the wafer temperature:

$$E = 1000 \cdot \int_0^{t_r} PO_h dt \quad (A.26)$$

where E – Total energy consumption, kJ;

PO_h – Power to maintain heater temperature, W.

PO_h is the sum of the heat lost by radiation and by conduction:

$$PO_h = PO_r + PO_c \tag{A.27}$$

where PO_r – Power lost by radiation, W;

PO_c -- Power lost by conduction, W.

PO_r is calculated as:

$$PO_r = E_m * C_{SB} * A_w * n_s * T_w^4 \tag{A.28}$$

where E_m – Emissivity of the precursor, which is 0.7;

C_{SB} – Stefan-Boltzmann Constant, which is $5.67*10^{-8}$ W/m^2-K^4;

A_w – Area of the wafer, which is 0.0706 m^2 for a 300 mm wafer;

N_s – Number of sides that radiate, which is 2;

T_w – Wafer Temperature, °C.

PO_c is determined by the amount of heat that conducts through the substrate bolts, which both support the wafer above the heater:

$$PO_c = Cv_s \cdot \frac{A_b}{L_b} \cdot n_b \cdot (T_h - 25) \tag{A.29}$$

where Cv_s – Conductivity of the substrate, which is set to be 0.3 W/cm-°C;

A_b – Area of one bolt, cm^2;

L_b – Length of the bolt, which is set to be 1cm;

n_b – Number of bolts;

T_h – Temperature of the heater, °C. It is set by the user.

The area of the bolt is calculated as:

$$A_b = \pi * r_b^2 \tag{A.30}$$

where r_b – Radiator of the bolt, cm.

A.2 Inputs and Outputs of the Model

The table below summarizes the inputs that can be specified by the user and the outputs of the model.

Table A.1 Summarization of the Inputs and Outputs of the Process Model

	Name	Symbol	Unit
Inputs	Precursor(l) Flow Rate	F_p	ccm
	Carrier Gas Flow Rate	F_{cg}	sccm
	Chamber Pressure	P	Torr
	Film Thickness	h_f	A
	Substrate Temperature	T	°C
Outputs	Total Precursor Going into the Chamber	N_{pi}	mole
	Total Carrier Gas Going into the Chamber	N_{cgi}	mole
	Reacted Precursor	N_{pr}	mole
	Precursor Utilization	U	%
	Energy for heating	E	kJ
	Process Time	t_r	minute

A.3 Using the Process Model in VisSim™

VisSim™ is a Windows-based program for the modeling and simulation of complex dynamic systems. It has an intuitive drag-and-drop block diagram interface with more than 110 function blocks. Its blocks include animation, integration, matrix operation, random variables generation, signal producer, optimization, and so on. It is capable of linear, nonlinear, continuous-time, and discrete-time simulation. The visual interface offers a simple method for constructing, modifying, and maintaining complex system models. "Cu CVD Unit Process" was developed on VisSim by the University of Maryland [61]. The section below gives the procedure of using this model.

- **System Specification**

The parameters that can be specified by a user are: the precursor and carrier gas flow rates, chamber pressure, film thickness, and the wafer temperature. Double click on the blue PROCESS CONTROL bottom on the up-left part of the main window. A "CENTRAL PROCESS CONTROL MODULE Properties" window will appear. The precursor and carrier gas flow rates, chamber pressure, and desired film thickness can be specified. Note that the unit of the precursor flow is in cm^3/min, because the precursor is liquid. After filling the values, pressure OK.

The wafer is also called the substrate. Double click on the blue SUBSTRATE EATER bottom on the main window. A "SUBSTRATE HEATER Properties" window will appear. The wafer temperature can then be specified.

- **Simulation**

The simulation can be run by either pressing the green triangle bottom on the tool bar, or going to the tool menu/Simulate/Go, or pressing F5. The five diagrams on the main window show the power of the process and the changes of the following parameters with time: total and partial pressures, precursor utilization, energy consumption, film thickness, and film growth rate. The boxes around the diagrams show the final values of these parameters.

To see the total usage of the precursor and the carrier gas, go to the left panel on the window and right click on the directory name. The list of directories will appear. Go to MASS BALANCE -- > Mass Balance: Precursor (moles) -- > Total Precursor In (moles). On the right end of the main window, there is a box coming out of the "Total Precursor In (moles)" box. The number in the box is the total precursor that comes into the chamber during the process. Note that the number is not the amount of precursor that is deposited on the wafer. MASS BALANCE -- > Mass Balance: Precursor (moles) -- > Total Precursor Rxted (moles) gives the amount of reacted precursor. Similarly, to see the total carrier gas used, go to MASS BALANCE -- > Mass Balance: CarrierGas (moles) -- > Total CarrierGas In (moles).

- **Navigating through the Model**

The simulation consists of several modules, shown as the blue bottoms on the top of the main window, or the directories on the left panel. By double clicking on the

bottoms or the directories, the user can see the details of the module. For example, by double clicking the MASS BALANCE directory, the main window will show the bellowing information:

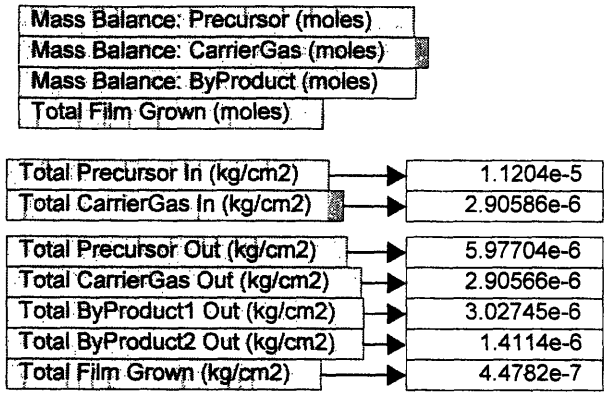

If the total precursor that goes into the chamber is of interest, the user can again double click on the "Total Precursor In (kg/cm2)" box. The main window will then show the below diagram:

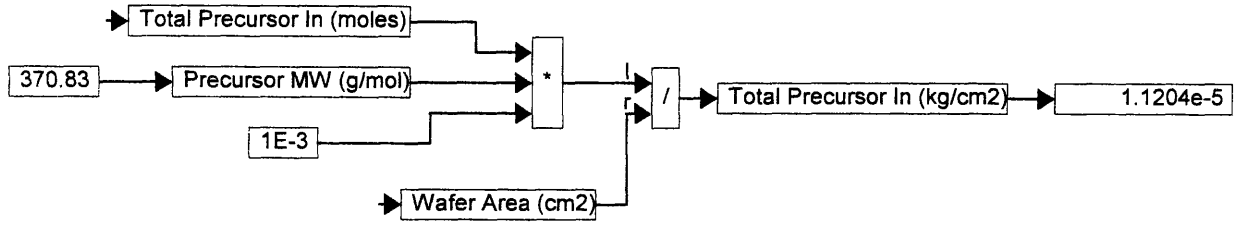

The "Total Precursor In (moles)", "Precursor MW (g/mol)", "Wafer Area (cm^2)", and "Total Precursor In (kg/cm^2)" boxes are variables. The user can trace where they are defined or referred to by double clicking on them, and then choose "Find Def" or "Find Ref".

Appendix B. Literature Review on Application of Supercritical Fluid Carbon Dioxide in Semiconductor Industry

B.1 Introduction

According to the prediction of Moore's Law—the number of components per chip doubles every 18 months, the International Technology Roadmap for Semiconductors set the goal for key lithography-related characteristics by product type, which is shown in Table B.1.

Table B.1 ITRS Table Structure—Key Lithography-Related Characteristics by Product Type: Near –Term Years

Technology Node	**180nm**	**130nm**			**100nm**	
Year	2001	2002	2003	2004	2005	Driver
DRAM Pitch (nm)	150	130	120	110	100	D
MPU Gate Length (nm)	100	85-90	80	70	65	M Gate
MPU/ASIC Pitch (nm)	180	160	145	130	115	M&A
ASIC Gate Length (nm)	150	130	120	110	100	A Gate

Long-Term Years

Technology Node	**70nm**	**50nm**	**35nm**	Driver
Year	2008	2011	2014	
DRAM Pitch (nm)	70	50	35	D
MPU Gate Length (nm)	45	30-32	20-22	M Gate
MPU/ASIC Pitch (nm)	80	55	40	M&A
ASIC Gate Length (nm)	70	50	35	A Gate

From this table, we can see that the scale of the characteristic lengths will decrease dramatically in the following years. In order to achieve the goals of ITRS, finer features on wafer surface are required. Besides the wavelength of developing lights, another factor that determines the feature size is the aspect ratio, which is strongly affected by the degree of pattern collapsing in lithography process.

There are two operations in lithography process that can cause pattern collapsing—the drying of wafers and the development of photoresist or dielectric. These two operations share the same purpose: removing unwanted materials from the surface of wafers. For the former operation, the unwanted material is water; for the latter one, the unwanted materials can be either photoresist or dielectric. Because of this similarity, both of them share the similar process procedure and also face the same problem of pattern collapsing. They are both discussed in this report so that they can be referenced to each other.

The cause of resist pattern collapsing is related to the surface tension (γ) of the rinse liquid and the resulting capillary forces acting on the resist walls [106]. Three different approaches have been followed during the last decade to overcome the problem of pattern collapsing. The first one was intended to increase the resist stiffness and therefore achieve better performance. The second approach focused on minimizing or eliminating γ during the drying stage. The third one is the use of supercritical fluid (SCF), which will be discussed in detail in this report. Using SCF CO_2 in extraction has been studied since in 1936. Now it is used as solvents in many commercial applications, including the extraction of caffeine from coffee, fats from foods, and essential oils from plants. However, the application of it in semiconductor industries did not appear until 1980s with the increasing demand for fine-pitch resist patterns.

- **Outline of the Report**

This report first describes the features and advantages of SCF CO2. Then the current research on applying SCF CO2 in drying and developing process is reviewed with some successful examples. Next, risk and safety issues associated with SCF CO2 are discussed briefly. Finally, suggestions to future research are presented.

B.2. Advantages of SCF CO_2 as Developer and Drying Solvent

B.2.1 Technical Consideration

The physical and chemical properties of SCF CO_2 make it appealing in semiconductor industry. Table B.2 illustrates the physical and chemical properties of SCF CO_2 compared to other liquids commonly used as surface cleaning solvents [107]. In the supercritical state, CO_2 behaves as a non-polar organic solvent, similar to hexane in its solvating properties. Consequently, SCF CO_2 is excellent for dissolving other organics, such as greases and oils. In addition, its negligible surface tension and low viscosity promote particulate removal by significantly reducing the thickness of the surface boundary flow layer. All these are desirable properties for developer and cleaning agent.

Table B.2 Physical chemical properties of SCF CO_2 and some fluids commonly used for drying and surface cleaning (Typical values at ambient conditions unless otherwise stated)

Solvent	Viscosity (mPa.s)	Surface Tension (mN/m)	Relative Dielectric Constant	Dipole moment (Debye)	Density (kg/m^3)
SCF CO_2	0.03 (35°C, 75atm)	$\equiv 0$ ($T \geq T_c$ & $P \geq P_c$)	1.1 (35°C, 75atm)	0	258 (35°C, 75atm)
Methyl chloroform	0.79	25.2	7.5	1.8	1339
Freon-113	0.66	17.8	2.4	0.9	1564
Methanol	0.54	22.1	32.7	1.7	791

Hexane	0.3	17.9	1.9	0	655
Water	1	72	78.5	1.8	1000

B.2.2 Environmental Consideration

SCF CO2 is of particular interest as an environmentally benign developing medium, as it is nontoxic, nonflammable, cost-effective and recyclable. It can also greatly reduce the need for hazardous chemicals, eliminate water consumption, eliminates the possibility of wafer damage from a plasma source, and reduce the number of process steps.

B.2.3 Economic Consideration

Using SCF CO_2 is also cost-effective. Its critical conditions are easily achievable with existing process equipment. By simple manipulation of pressure and temperature conditions, its density and hence solvating power can be easily controlled, which greatly reduces the operation cost. What's more, there is already an extensive transportation infrastructure of CO_2, as the food service industry relies on the use of solid and high-pressure gaseous CO_2 for food storage and carbonated drinks, respectively. This greatly lowers the cost of applying CO_2 in semiconductor industry comparing to building the infrastructure from scratch.

B.3 Applications of SCF CO_2 as Developer and Drying Solvent

B.3.1 SCF CO_2 as Drying Solvent

Most of the current resist systems are designed to work with aqueous-based developers. Because of the poor solubility of water in SCF CO_2, surfactants are added to increase the solubility of water. Surfactants are selected according to their emulsion formation properties and interfacial tension values. Sodium dioctylsulfosuccinate (AOT) was used in a SCF CO_2 drying stage on a polyhydroxystyrene-based chemically amplified resist (APEX-E) to demonstrate the feasibility of obtaining high aspect ratio structures without pattern collapsing [108]. Using SCF CO_2 as drying solvent is significant more effective than the normal nitrogen drying. A film thickness of 950 nm gave an aspect ratio of 6.8.

However, pattern deformation still exists in SCF CO_2 drying, especially for drying of photoresist. Using thermal desorption spectra (TDS) of H_2O and CO_2 in dried photoresist, Namatsu et al concluded that the deformation is resulted from the incorporation of H_2O molecules into the resist films during the SCF drying process [109]. Furthermore, CO_2 is also dissolved in H_2O and is released from the film when pressure is reduced. This pattern deformation was not observed in the SCF drying of the Si patterns because H_2O molecules cannot diffuse in Si. Therefore, avoidance of water contamination is the key factor in suppressing pattern deformation in supercritical drying.

This can be achieved by injecting supercritical CO_2 instead of liquid CO_2 into the drying chamber.

B.3.2 SCF CO_2 as Developer

The mechanism by which SCF CO_2 removes the photoresist has not yet been determined. However, it is well known that polymeric materials can be made to swell by diffusion of CO_2 molecules. It is likely that such a swelling occurs to effectively soften the photoresist.

Similar to the drying mechanism, a co-solvent with SCF CO_2 may also enhance the solubility of photoresist in SCF CO_2. Propylene carbonate (1,3-Dioxoland-2-one, 4-methyl; CAS# 108-32-7), hereafter referred to as PCO_3, was investigated to be the co-solvent [110]. Testing on positive photoresist from Si, GaAs, and GaP wafers showed that only of the PCO_3/CO_2 mixture could achieve complete photoresist removal, whereas pure SCF CO_2 and pure PCO_3 alone have no effect on the resist material. It is suspected that the reactive ester group of the PCO_3 acts to degrade the polymer, reducing its average molecular weight. Such a reduction promotes solubility in the supercritical fluid, facilitating its removal.

However, if the molecular weight of the dielectric layer can automatically be reduced to such an extent after exposure that the exposed part is soluble in SCF CO_2, no co-solvent and no photoresist are needed. This type of dielectric is called direct patternable dielectric. Using hexafluoropropylene oxide (HFPO) as the precursor gas, a new type of film that is spectroscopically similar to polytetrafluoroethylene (PTFE) was achieved by hot filament CVD (Weibel et al, 2000). This film was then developed in a commercial supercritical fluid extraction system under the operation conditions of 6000 psi and 80°C at a SCF CO_2 flow rate of 2-4 L/min. Lines/spaces ratio of 1.0 μm in pyrolytic CVD fluorocarbon films was attained. This patternable dielectric layer plus SCF CO_2 developer will significantly reduce the use of chemicals and associated waste stream volume, thus results in considerable savings on chemical supplies and disposal costs.

B.3.3 Industrial Example—ARROYO^{TM} System

ARROYO^{TM} is developed by SC Fluids, Inc. (Nashua, NH), which is a privately held subsidiary of GT Equipment Technologies. Its reactors—the pressure vessels can hold either 200 mm or 150 mm wafers and have been dynamically designed to eliminate stagnant zones and eddy-currents during dynamic fluid flow conditions. The vessels are rated at two different maximum operating conditions: 3,500 psi at 150 °C and 6,000 psi at 150 °C [111].

Besides ARROYO^{TM}, Supercritical Systems, Inc. (Fremont, CA) is also aiming at using SCF CO_2 in wafer cleaning. However, not enough information about this company is available yet.

B.4 Risk and Safety Issues Associated with SCF CO_2

From the previous discussion we can see that SCF CO_2 requires high pressure. Because the possibility of explosion, high-pressure vessels have always been regarded as a source of risk.

In the paper cited before, none of them mentioned the risk associated with SCF CO_2. The reason for this might be that all these experiments were carried out in either laboratory or pilot plant level, in which the scale of SCF CO_2 reactors is small. Thus the energy stored in these reactors is also small, which in turn means that even if an explosion does happen, the consequent loss is non-significant. However, once this technology is implemented in industrial scale, especially when a semiconductor fabricator (fab) that cost 2 billion dollars [112], the loss caused by one explosion will be enormous.

Using SCF CO_2 as an extraction solvent has been widely adopted. Because of the similarity of extraction, drying and developing, study and common regulations used in extraction process can be used as a guideline temporarily. Several books that related to this area are listed [113-115].

B.5 Future Research

There are two possible approaches of using SCF CO_2 as developer: one is to dissolve photoresist; the other one is to dissolve direct patternable dielectric. The former can be adopted by current industry quite fast, while the latter is the direction of next generation of semiconductor fabrication. No matter which approach is investigated, the mechanism by which SCF CO_2 removes the photoresist or dielectric needs to be studied further.

Before the application of SCF CO_2 in industrial practice, thorough study of safety issues needs to be carried out. Regulations and standard operation procedures focusing on the characteristic of semiconductor industry should be set up within the whole industry.

B.6 Conclusion

The physical and chemical properties of SCF CO_2 make it a desirable candidate as drying solvent and developer in semiconductor industry. The zero surface tension of SCF CO_2 prevents pattern collapsing in drying and developing process. If cooperated with co-solvents, satisfactory removal of water or photoresist can be achieved with high aspect ratio. Further research is needed to put SCF CO_2 into industrial practice.

Appendix C Supplemental Information on Industrial Survey

C.1 Questionnaires Used in Survey

Product Development Life Cycle

- Our understanding of the different stages of the development of a process and issues with ESH and cost decision making is outlined below. Do you agree with this view?

Table C.1 Stages of Development in Semiconductor Manufacturing

Time Frame	Development Stage	Chemical Development Stage	Length of Chemical Stage?	ESH and Cost Information Needed
4-6 yrs before high vol. mfg	University research in collaboration with equipment and chip manufactures	Bench-top prod. of chemicals for lab testing in universities		Screen out chemicals with toxicity and environment impacts of high concern, rough LCA of candidate chemicals
2-4 yrs before high vol. mfg	Equipment R&D, initial downstream treatment consideration	Bench-top production of chemicals by chemical suppliers		COO, EnV-COO, more detailed information on the ESH properties of chemicals, LCA of the process
0-2 yrs before high vol. mfg	Manufacturing R&D, in depth consideration of abatement	Small scale production		Same information as above on fewer chemical and process choices. The level of detail depends on the decision context
0+ yrs	Large vol. production, incremental decisions on abatement needs, maintenance	Large scale production		Same as above

Decisions to Be Made

- Which kind of ESH and cost choices do you make at different stages? How do you make these choices?
- How do you make decisions on chemical selection?
- How do ESH considerations affect chemical development?
- Do you have a check list in development/commercializing a chemical? If yes, what are the check points?

- How automated is the checking of new chemicals against all requirements? If it is not automated, would you like it to be automated? Do you think it is possible? If yes, which software do you use?
- How much time does it take to understand hazard of a product?
- How have you responded to ESH concerns that have emerged after product introduction? And how have ESH concerns modified product development processes?

Internal and External Communications

- Do your process engineers and R&D personnel estimate ESH impacts of chemicals and do they have any ESH impact assessment training?
- How much interaction do you have with chip manufacturers and equipment manufacturers?
- What criteria do your clients use to valuate a product?
- How do you reconcile issues of proprietary chemicals or formulations and the need to provide ESH information to your customers?
- Do you have concerns sharing non-proprietary ESH information about your products, such as water and energy consumption in production? Why?
- How have different requirements by the semiconductor industry, such as extremely high purity, high consistency, changed ESH issues related to these products compared to traditional chemicals?

Uncertainties and Risks

- Our definition of uncertainties and risks
- How do you deal with uncertainty/risk in technical, ESH, marketing, and purchasing decisions?
- How do you allocate resources to tackle risk?
- How would you like to see risk tackled?
- Do you use QSAR or other tools to estimate new chemical properties? Do you quantify the uncertainties in these extrapolations?

Existing Environmental Evaluation Tools

Table C.2 Comparison of Existing Environmental Tools

		CARRI®	Chemical Data Matrix	Cost Analysis Tool?	Other decision support tools?
If it is used in your company	Who use it?				
	In what decision context?				
	How often do they use it?				
	How do they like it?				
If it is not used in your	How do you do what the program is supposed to do?				

company	Barriers of implementation				
	Wish list				
	Anything good about it?				

C.2 Suggested from Industrial Surveys

There is a strong need for looking for emerging issues 6-8 years ahead: (i) A regulatory screening tool with the ability to predict regulations 6-8 years into the future on a global basis is needed. (ii) We need to develop methods to characterize chemicals based on little or no experimental data.

Researchers should also look at EHS decision making 3-4 years before large technology inflections. It is easier to make changes in ESH when there is a large technology inflection. For example, with the adoption of extreme ultraviolet where tools will be changing, there are opportunities to suggest changes that can improve both the environmental and technical performance.

The case studies that were suggested include:

- Cu CVD vs. Cu plating. The waste stream of Cu plating contains Cu, while a recycle loop for Cu CVD has been invented over a decade ago which can capture the total copper used. The organic part of the organometallic compound can be captured as well. Currently, Cu plating is in use but not Cu CVD.

- Spin on vs. CVD for low k dielectrics.

- F_2 POU vs. large scale F_2 manufacturing. The aspect to be studied is the savings from the economies of scale, meaning the reduced cost from high volume F_2 manufacturing as compared to point of use F_2 generation.

- Super-Critical (SC) CO_2. SC CO_2 has been proposed for photolithography development. Yet it is most likely to be used in plasma ash removal or a standard clean using chelators. It will be interested to study whether adoption of SC CO_2 will be an ESH improvement. Use of co-solvents may result in more solvents being emitted than currently in the fab. SC CO_2 could also use in the sub fab as a cooling system.

- Changes that have been made in the industry, such as NF_3 remote cleaning. It was suggested to study whether these decisions should have been made from an ESH point of view.

C.3 List of Companies Surveyed

Table C.3 List of Companies Interviewed for ESH Needs and Concerns

Date of Visit	Companies/Organizations Visited	Type of Activity	Names of People Visited	Contact
01/12/04	Texas Instruments, TX	Device Manufacturer	Tim Yeakley (ESH Process & Product Strategy Management, Worldwide ESH Services), Laura Pruette Losey, David Boudlin,	t-yeakley@ti.com, 972-927-3155
01/13/04	Motorola, TX	Device Manufacturer	Brett Davis	brett.davis@motorola.com
01/13/04	SEMATECH, TX	Industrial Consortium	Walter Worth (Environmental, Safety for Health Program Manager), Dawn Speraza, Stephen Burnett, Coleen C Regan, Ram Mallela	walter.worth@intl.sematech.org, 512-356-7199
01/13/04	TEL, TX	Device Manufacturer	Alan Krov	akrov@aus.telusa.com
01/14/04	DuPont, DE	Chemical Supplier	Mike Mocella (Senior Technical Consultant), Brian Engler, Carina Alles, Gary Loh, William Haaf	Michael.mocella@usa.dupont.com, 302.999.5072
01/27/04	AMD, CA	Device Manufacturer	Reed Content (Director of ESH), Shaye Hokinson, Julia Bosie, Donna Sadowy, Arturo Luiz, Dan Seif, Phil Trowbridge, John Ennals	reed.content@amd.com, 408-749-4449
01/27/04	Applied Materials, CA	Tool Supplier	Sebastien Raoux (Acting Director of Technology, Environmental Solutions Product Division)	sebastien_raoux@amat.com, 408.563.4923
01/27/04	SEMI, CA	Industrial	Rick Row (Project Manager, EHS	rrow@semi.org

		Consortium	Division), Ralph Kirk, Kenneth Schramko, Dave Biasotti	
01/28/04	Intel, PX	Device Manufacturer	Jim Jewett (Director of Materials)	Jim.jewett@intel.com, 480 5543621
01/29/04	Novellus, CA	Tool Supplier	John G. Langan (Director of Technology), William R. Entley, Susrut Kesari	John.langan@novellus.com, 408-570-6257
01/29/04	Silicon Valley Toxicity Coalition, CA	Advocacy Group	Ted Smith (Executive Director)	tsmith@igc.org
01/30/04	Air Products, CA	Chemical Supplier	Ralph Richardson (Director of Technology), Mary Majors, Monica Peters, John Norman	RICHARRJ@airproducts.com
01/30/04	ATMI, PX	Tool Supplier	Mike Scherer (Director, Business Development)	msherer@atmi.com, 602-549-8855
02/24/04	BOC Edwards	Chemical Supplier	Ken Lykins	Ken.Lykins@bocedwards.com

Appendix D User Manual for PIO-LCA Macro Version

Cano-Ruiz [63] developed a computerized tool—EnvEvalTool to implement the PIO-LCA method. The tool consists of a database implemented on Microsoft Access, an Excel spreadsheet, which loads data from the database and computes the evaluation model.

D.1 Overview of the PIO-LCA Macro Version 3.1

PIO-LCA Macro Version 3.1 is the Implementation of EnvEvalTool in Microsoft Excel [63]. It utilizes the seamless interface of Microsoft Access and Excel to load data that are exported from Access into the spreadsheets where the valuation calculation is carried. The data loading and calculation are realized by two macros "Load Data" and "Build PIO-LCA Tables".

After loading the data, there will be five spreadsheets. The first spreadsheet stores the input-output data in the Usage and Fabrication Matrices **B** and **C**, and the exchange data in the Environmental Exchange Matrix **E**. The second spreadsheet stores the price and demand data in the price vector **p** and demand vector **d**. Note that the demand vector is empty after loading the data, thus the user has to put in the demand. The third spreadsheet stores the characterization factors and valuation factors in the Characterization Factor Matrix **H** and the transpose of the evaluation factor vector **w**. The macro that creates **H** and **w** also adds the correlation coefficients in the distribution expressions for the data. The fourth spreadsheet stores the market share data in Market Share Matrix **F**. The last spreadsheet stores the correlation coefficients among the characterization factors and the valuation factors.

The PIO-LCA tables that will be generated by the Excel Macro include all the intermediate matrices, such as Matrix **G**, **D**, $\mathbf{A}_{\mathbf{prod}}$, **x**, and **q**. The valuation results are shown in several spreadsheets. The impacts divided according to environmental exchanges and processes are seen in spreadsheets "Valuation by exchange" and "Valuation by process", respectively. These two spreadsheets show the contribution of each exchange or process to the total impact indicator, which help the user understand the sources of impacts and set priorities for checking the quality of the input data. The different break-down of the total impact indicator $\boldsymbol{\Omega}$ can also be found in these two spreadsheets.

Similar to the unit prices of products being used to calculate the cost of a project, the unit impact indicators can be used in calculating the environmental "cost". The unit impact indicators for each unit process throughput, unit product demand, and unit environmental exchange are shown in spreadsheet "Unit Impacts". The exchange arisen from each unit process throughput and unit product demand can be found in spreadsheet "proc unit valuation contrib" and "prod unit valuation contrib." They can also help the

user to trace the exchange back to their source and set priorities for checking the quality of the input data.

D.2 Uncertainty Analysis of the Evaluation

As discussed in the earlier chapters, a major problem associated with these valuation models is their uncertainty. To address this issue, the EnvEvalTool was designed so that uncertainty analysis can be carried out easily with commercially available computer software. Instead of just using the nominal values, the data are expressed in their probability distribution functions using @Risk expression. To generate the distribution in the Excel, nominal values need to be multiplied by the @Risk expressions in the environmental evaluation database:

$$\text{PDF} = \text{Nominal Value} \times \text{@Risk expression} \tag{D.1}$$

For example, the nominal value of a normal distribution is a_N, its @Risk expression is RiskNormal(1,[Parameter1]/2), where Parameter 1 is 2×standard devaiation/mean. The PDF of the normal distribution is thus a_N × RiskNormal(1,[Parameter1]/2). Note that unlike most distributions whose nominal values are their arithmetic means, the nominal value of a lognormal distribution with mean μ and standard deviation (std) σ,

$$f(x) = \frac{1}{xb\sqrt{2\pi}} \exp\left(\frac{-(\ln(x)-a)^2}{2b^2}\right) \tag{D.2}$$

where

$$a = \ln\left(\frac{\mu^2}{\sqrt{\sigma^2+\mu^2}}\right), \tag{D.3}$$

$$b = \sqrt{\ln\left(\frac{\sigma^2+\mu^2}{\mu^2}\right)}, \tag{D.4}$$

is its geometric mean, while parameter 1 is its geometric std. In the database, the geometric mean is defined as e^a, the geometric std is defined as $(e^{2b})^2$, or e^{4b}. The geometric mean also equals to the 50th percentile of the lognormal distribution, and the geometric std equals the ratio of the 97.5th percentile divided by the 50th percentile. The mean μ, variance σ^2, geometric mean μ, and geometric std σ_g are related as:

$$\mu = e^{\ln\mu_g + 0.5(\ln\sigma_g)^2}, \tag{D.5}$$

$$\sigma = \sqrt{\sigma^2}, \tag{D.6}$$

$$\sigma^2 = e^{2\ln\mu_g^2 + (\ln\sigma_g)^2} \times \left(e^{(\ln\sigma_g)^2} - 1\right) \tag{D.7}$$

Because the calculation of characterization factors and valuation factors use many uncertain parameters in common, they are correlated with each other. In the uncertainty propagation through the valuation model, it is necessary to consider the correlations among the factors to avoid overestimation of uncertainty. This can be done through

direct use of Monte Carlo simulation, which is straightforward but time-consuming; or through the use of copula multivariate distributions. In this work, the second method is used due to the large number of uncertain factors considered.

D.3 Step-by-Step User's Manual of the Environmental Evaluation Tools

This manual follows [116].

1. Creating a New Case Study

1.1 Specify the Processes and Products

Open the "products" table and enter the name of the new product along with the units of measurement that will be used for entering input-output coefficients. Open the "processes" table and enter data for the new processes.

1.2 Specify the Input-Output Data

Each of the new products defined requires at least one entry in the "Make coefficients" table. Multi-product processes will have more than one entry in this table. Usage coefficient distributions also need to be entered in the "Use coefficients" table for each of the processes that make the products of interest. If a process uses a product not previously existing in the database, the product and the process that makes the product need to be defined first before you are able to use it as an entry in the "use coefficients" table. The "Make coefficients" and "Use coefficients" tables are corresponding to the Fabrication Matrix and the Usage Matrix mentioned in the text.

1.3 Define the Environmental Exchange Factors

The last thing in creating a new case study is to define its environmental exchange inventory. If the emission substance is not currently in the database, it needs to be added in the "chemical information" table. The characterization factors for this chemical also needs to be added in the "characterization factors" table, otherwise the emissions of that chemical will not be evaluated for impact. Similarly, new impact categories need to be defined in the "Impact Categories" table. The valuation factor for the new category should be defined in the "Valuation Factors" table. After the emissions, the characterization factors, and the impact categories are completed, emission inventories can be entered in the "Emission factors" table.

If there is correlation within the newly entered characterization factors or valuation factors, or among these two, their correlation coefficients need to be entered in "CF to CF correlation", "VF to VF correlation", and "CF to VF correlation" tables.

1.4 Define the Valuation Method

Open the "Case Studies (valuation)" table and enter the name of the new case study and the code of the valuation method you to be used. Valuation methods are defined in two tables. The "valuation method" table gives the valuation

method code, valuation method name, and reference. There are currently three defined valuation methods in the tool: The EPS method, the XLCA method, and the "Cano Thesis" method, which was used in this valuation. The distributions for the valuation factors used in each method are given in "valuation factors" table.

1.5 Specify the Final Product and Economic Information

Open the "Case Studies (products)" table and enter the name of the case study and the product code for the products to be included as final demand products in the study. If the study is to compare several different processes to make the same product, a market share scenario needs to be specified in the "market share" table. The distributions entered in this table are the market shares that different processes have in the production of the product of interest. For products produced in multi-product processes, prices of these products also need to be specified. The default price for all the products are 999 $/unit.

2. Export the Data into the PIO-LCA spreadsheet

2.1 Specify the Path for Output Files

Select "Modules" from the list of objects on the left side of the Access window. Double click on the "Export to spreadsheet" module. On the 11th line of the code, the pathname can be specified for where the exported file to be. The directory should exist before the exportation. It is recommended not to change the last part of the path (i.e. "\Environmental Evaluation Tool\Temp").

2.2 Export Data

Select "Macros" from the list of objects on the left side of the Access window. Double click on "Export to Spreadsheet". A dialogue window will pop up asking for the name of the case study. Input the case study name and hit "OK".

3. Read Data into PIO-LCA Model

After running successfully the "export to spreadsheet" macro, a series of Excel files will exist in the "Environmental Evaluation Tool\Temp" directory. Firstly, set the pathname used in the read-data macros to be consistent with the file structure of the computer. Go to the menu in Excel Tools→Macros→Visual Basic Editor and double click on the Sheet1 object under Project Explorer. Scroll down to the CommandButton2_Click() section and edit the Path Name. Then go to "PIO-LCA macros version 3.1" excel workbook and press the "Load Data" button in Sheet1. The files generated by the database will be read into the sheets.

4. Specify the Demand Vector

After loading the data, the demand vector remains zero for all the entries. The demand for the final product of interest needs to be specified.

D.4 Procedure of Drawing Distribution Box Plot

This procedure follows [116].

After running the Monte Carlo simulation using @Risk, the percentage of the simulation results that fall below a certain value will be obtained. These values can be seen by going to the @Risk window and press "statistics" button. Scroll down the "simulation statistics" window, these percentiles can be seen. Five series are needed: 25^{th} percentile, 50^{th} percentile minus 25^{th} percentile, 75^{th} percentile minus 50^{th} percentile, 25^{th} percentile minus 5^{th} percentile, and 95^{th} percentile minus 75^{th} percentile. With the first three series, create a stacked bar plot. Use the fourth series as the negative error for the 25^{th} percentile. Format the 25^{th} percentile to have no border or color. Use the fifth series as the positive error for the 75^{th} percentile minus 50^{th} percentile.

Bibliography

1. EU, *DIRECTIVE 2002/96/EC OF THE EUROPEAN PARLIAMENT AND OF THE COUNCIL of 27 January 2003 on waste electrical and electronic equipment (WEEE).* Official Journal of the European Union, 2003. **13**(2): p. 24-38.
2. Gutowski, T.G., et al., *WTEC Panel Report on Environmentally Benign Manufacturing.* 2001, International Technology Research Institute World Technology (WTEC) Division: Baltimore, MD. p. 31-32.
3. EU, *Press Release of European Commission on Integrated Product Policy (IPP).* 2003, European Commission.
4. EU, *DIRECTIVE 2002/95/EC OF THE EUROPEAN PARLIAMENT AND OF THE COUNCIL of 27 January 2003 on the restriction of the use of certain hazardous substances in electrical and electronic equipment.* Official Journal of the European Union, 2003. **13**(2): p. 19-23.
5. 3M, *Pollution Prevention Pays Program.* 2003, 3M Inc.
6. Ford, *Environmental Health and Safety.* 2003, Ford.
7. EU, *Proposal for a Regulation Of The European Parliament And Of The Council concerning the Registration, Evaluation, Authorisation and Restriction of Chemicals (REACH), establishing a European Chemicals Agency and amending Directive 1999/45/EC and Regulation (EC) {on Persistent Organic Pollutants}.* 2003, Commission Of The European Communities: Brussels.
8. *Perfluorooctyl Sulfonates; Proposed Significant New Use Rule*, in *40 CFR Part 721.* 2000. p. 62319-62333.
9. Lashbrook, W. and et al., *Design for Environment Tools for Management Decision Making -- A selected Case Study.* IEEE, 1997.
10. DeGenova, J., *UPW Recycle Strategy.* 2000, Texas Instruments Inc.
11. Bauer, D.J., N. Krishnan, and T. Francis. *Creating Win-Win: Leveraging Insight Into Industrial Environmental Decision-Making.* in *International Symposium on Environmental Issues with Materials and Processes for the Electronics and Semiconductor Industries, 199th Meeting of the Electrochemical Society.* 2001. Washington DC.
12. Cano-Ruiz, J.A., *Decision Support Tools for Environmentally Conscious Chemical Process Design*, in *Dept. Chem. Eng.* 2000, MIT: Cambridge, MA. p. 599.
13. Air Products and Chemicals, *Material Safety Data Sheet of Fluorine.*
14. Air Products and Chemicals, *Material Safety Data Sheet of Nitrogen Trifluoride.*
15. Schuppe, J. and H. Ho, *Lifecycle assessment (LCA) White Paper.* 2002, International SEMATECH: Austin, TX.
16. O'Hara, P., et al., *S70 Design for Environment, Safety, and Health (DFESH) Implementation Strategy for the Semiconductor Industry.* 1995, International SEMATECH: Austin, TX. p. 114.
17. Krishnan, N., J. Rosales, and D. Dornfeld, *Informing Design for Environment (DfE) in Semiconductor Manufacturing.* 2002, UC Berkeley: Berkeley, CA.
18. Krishnan, N. and U. Ayyagari, *A Hierarchical Framework for Integration of Fundamental Physical-Chemical Modeling to inform Environmental Decision*

Making: A Case study using the Environmental Value Systems Analysis. 2001, UC Berkeley: Berkeley, CA.
19. Thurwachter, S., *Environmental Value Analysis: Evaluating Manufacturing Product Process Design Trade-Offs*, in *Dept. Mech. Eng.* 2000, University of California, Berkeley: Berkeley, CA. p. 204.
20. Thurwachter, S., J. Schoening, and P. Sheng. *Environmental Value (EnV) Analysis*. in *the 1999 IEEE International Symposium on Electronics and the Environment*. 1999: IEEE.
21. *TEAM Impact Database*. 1999, Ecobilan, PricewaterhouseCoopers.
22. EORM, *Unit Operation Algorithm and Test Spreadsheets for SEMATECH's S70 Mass and Energy Balance Model*. 1997, SEMATECH International: Austin, TX.
23. Chen, Y., et al., *ERC_Stanford_Chen_McRae_Krishnan_Blowers_August_2004.ppt*. 2004: Stanford, CA.
24. Weisstein, E.W., *Monte Carlo Method*. 1999, MathWorld--A Wolfram Web Resource.
25. Hammersley, J.M., *Monte Carlo Methods for Solving Multivariable Problems*. Annals of the New York Academy of Sciences, 1960. **86**(3): p. 844-874.
26. Wozniakowski, H., *Average Case Complexity of Multivariate Integration*. Bulletin of the American Mathmatical Society, 1991. **24**(1): p. 185-194.
27. Sobol, I.M., *On the Systematic Search in a Hypercube*. SIAM Journal on Numerical Analysis, 1979. **16**(5): p. 790-793.
28. Papoulis, A., *Probability, Random Variables, and Stochastic Processes*. 3rd edition ed. Communications and Signal Processing, ed. S.W. Director. 1991, New York, NY: McGraw-Hill, Inc.
29. Frey, H.C. and S.R. Patil, *Identification and Review of Sensitivity Analysis Methods*. Risk Analysis, 2002. **22**(3): p. 553-578.
30. Helton, J.C., *Uncertainty and Sensitivity Analysis Techniques for Use in Performance Assessment for Radioactive Waste Disposal*. Reliability Engineering and System Safety, 1993. **42**: p. 327-367.
31. Iman, R.L. and J.C. Helton, *An Investigation of Uncertainty and Sensitivity Analysis Techniques for Comptuer Models*. Risk Analysis, 1988. **8**(1): p. 71-90.
32. Saltelli, A., T.H. Andres, and T. Homma, *Sensitivity Analysis of Model Output: An Investigation of New Techniques*. Computational Statistics and Data Analysis, 1993. **15**: p. 211-238.
33. Roussas, G.G., *A Course in Mathmatical Statistics*. 2nd ed. 1997, San Diego, CA: Academic Press.
34. Kendall, M.G., *Rank Correlation Methods*. 3rd ed. 1962, New York: Hafner Publishing Company.
35. Homma, T. and A. Saltelli, *Importance Measures in Global Sensitivity Analysis of Nonlinear Models*. Reliability Engineering and System Safety, 1996. **52**: p. 1-17.
36. Saltelli, A. and I.M. Sobol', *About the Use of Rank Transformation in Sensitivity Analysis of Model Output*. Reliability Engineering and System Safety, 1995. **50**: p. 225-239.

37. Cukier, R.I., C.M. Fortuin, and k.E. Shuler, *Study of the Sensitivity of Coupled Reaction System to Uncertainties in Rate Coefficients. I Theory.* The Journal of Chemical Physics, 1973. **59**(8): p. 3873-3878.
38. Cukier, R.I., J.H. Schaibly, and K.E. Shuler, *Study of the Sensitivity of Coupled Reaction Systems to Uncertainties in Rate Coefficients. III Analysis of the Approximations.* The Journal of Chemical Physics, 1975. **63**(3): p. 1140-1149.
39. Schaibly, J.H. and K.E. Shuler, *Study of the Sensitivity of Coupled Reaction Systems to Uncertainties in Rate Coefficients. II Applications.* The Journal of Chemical Physics, 1973. **59**(8): p. 3879-3888.
40. Cukier, R.I., H.B. Levine, and K.E. Shuler, *Nonlinear Sensitivity Analysis of Multiparameter Model Systems.* Journal of Computational Physics, 1978. **26**: p. 1-42.
41. McRae, G.J., J.W. Tilden, and J.H. Seinfeld, *Global Sensitivity Analysis -- A Computational Implementation of the Fourier Amplitude Sensitivity Test (FAST).* Computers & Chemical Engineering, 1982. **6**(1): p. 15-25.
42. Koda, M., G.J. McRae, and J.H. Seinfeld, *Automatic Sensitivity Analysis of Kinetic Mechanisms.* International Journal of Chemical Kinetics, 1979. **XI**: p. 427-444.
43. Weyl, H., *Mean Motion.* American Journal of Mathematics, 1938. **60**: p. 889-896.
44. Cadzow, R.A., *Discrete Time Systems.* 1973, Englewood Cliffs, NJ: Prentice-Hall.
45. Tatang, M.A., *Direct Incorporation of Uncertainty in Chemical and Environmental Engineering System*, in *Chemical Engineering.* 1995, MIT: Cambridge, MA. p. 538.
46. Villadsen, J. and M.L. Michelsen, *Solution of Differential Equation Models by Polynomial Approximation.* 1978, Englewood Cliffs: Prentice-Hall Inc.
47. Kakutani, S. *Spectral Analysis of Stationary Gaussian Processes.* in *the 4th Berkeley Symposium on Mathematical Statistics and Probability.* 1961. Berkeley, CA: University of Califronia Press.
48. Wiener, N., *The Homogeneous Chaos.* American Journal of Mathematics, 1938. **60**: p. 897-936.
49. Weisstein, E.W., *Gram-Schmidt Orthonormalization.* 2004, Mathworld -- A Worlfram web resource.
50. Pun, B.K., M.A. Tatang, and G.J. McRae, *Uncertainty Analysis of Chemical Mechanisms Using the Deterministic Equivalent Modeling Method.* 1997, MIT: Cambridge, MA.
51. Pun, K.K.-L., *Treatment of Uncertainties in Atmospheric Chemical Systems: A Combined Modeling and Experimental Approach*, in *Chemical Engineering.* 1998, MIT: Cambridge, MA.
52. Sobol', I.M., *Sensitivity Estimates for Nonlinear Mathematical Models.* Mathematical Modeling and Computational Experiment, 1993. **1**: p. 407-414.
53. Saltelli, A. *Global Sensitivity Analysis, An Introduction.* in *International Conference on Sensitivity Analysis.* 2004. Santa Fe, New Mexico.
54. Archer, G.E.B., A. Saltelli, and I.M. Sobol', *Sensitivity Measures, ANOVA-Like Techniques and the Use of Boostrap.* Journal of Statistical Compuation and Simulation, 1997. **58**(2): p. 99-120.

55. Saltelli, A., *Sensitivity Analysis for Importance Assessment.* Risk Analysis, 2002. **22**(3): p. 579-590.
56. Saltelli, A., K. Chan, and E.M. Scott, eds. *Sensitivity Analysis*. 2000, Wiley: West Sussex, England.
57. Ishigami, T. and T. Homma. *An Importance Quantification Technique in Uncertainty Analysis for Computer Models*. in *First International Symposium on Uncertainty Modelling and Analysis*. 1990. University of Maryland, USA.
58. Saltelli, A., S. Tarantola, and K. Chan, *A Quantitative Model-Independent Method for Global Sensitivity Analysis of Model Output.* Technometrics, 1999. **41**(1): p. 39-56.
59. Norman, J.A.T., *Advances in Copper CVD for the Semiconductor Industry.* Journal of Physics IV France, 2001. **11**: p. 497-503.
60. Xia, L. and et al., *Chemcial Vapor Deposition*, in *Handbook of Semiconductor Manufacturing Technology*, Y.D. Nishi, R., Editor. 2000, marcel Dekker, Inc.: New York. p. 309.
61. Chu, S., *CuCVD_ESH_Simulator.Cho_022602.vsm*. 2002: College Park, MD.
62. Keoleian, G.A. and D. Menerey, *Life Cycle Design Guidance Manual*. 1993, U. S. Environmental Protection Agency: Washington, D. C.
63. Cano-Ruiz, J.A., *PIO-LCA macros version 3.1 revised.xls*. 2000: Cambridge.
64. Pan, W., *The role of aerosols in the troposphere : radioative forcing, model response, and uncertainty analysis*, in *Dept. of Earth, Atmospheric, and Planetary Sciences*. 1996, Massachusetts Institute of Technology,: Cambridge, MA.
65. Gomei, Y. and M. Suzuki, *A Cost-of-Ownership Study On Lithography Systems.* Semiconductor International, 1998. **July**.
66. Cano-Ruiz, J.A., *New Environmental Evaluation.mdb*. 2000: Cambridge, MA.
67. *A Memorandum of Understanding (MOU) between the United States Environmental Protection Agency (EPA) and individual semiconductor manufacturing companies -- The PFC Emission Reduction Partnership for the Semiconductor Industry*. 1996: Washington, D. C.
68. Pruette, L.C., et al., *Evaluation of a dilute nitrogen trifluoride plasma clean in a dielectric PECVD reactor.* Electrochemical and Solid-State Letters, 1999. **2**(11): p. 592-594.
69. Raoux, S. and J.G. Langan, *Remote NF_3 Chamber Clean Virtually Eliminates PFC Emissions from CVD Chambers and Improves System Productivity.* Semiconductor Fabtech, 1999. **9**.
70. Pruette, L.C. and et al., *Evaluation of C_4F_8O as an Alternative Plasma-Enhanced Chemical Vapor Deposition Chamber Clean Chemistry.* Journal of The Electrochemical Society, 2000. **147**(3): p. 1149-1153.
71. Pruette, L.C., *Oxide Etching with NF_3/Hydrocarbon Chemistries for Global Warming Emissions Reduction*, in *Dept. Eletrical Eng. and Computer Sci.* 2001, MIT: Cambridge, MA. p. 52.
72. Lester, M.A., *Remote NF3 Plasma Processes for CVD Chamber Cleans.* Semiconductor International, 2001. **October 1**.
73. Lester, M.A., *No More PFC Emissions in Plasma Chamber Cleaning?* Semiconductor International, 2000.

74. Aitchison, K.A., *Simultaneous Resolution of Multiple Environmental Issues: the Development of In-Situ RF Plasma Chamber Clean Processes Using Dilute NF_3/He Mixtures.* Semiconductor Fabtech, 2000. **11**.
75. Krishnan, N., *EnV-S_pre_release_draft.* 2001: Berkeley, CA.
76. Hines, C.M., et al., *Reducing Perfluorinated Compound Emissions.* IEEE/SEMI Advanced Semiconductor Manufacturing Conference, 1998: p. 203-207.
77. Gravley, R.J., *Understanding Fluorine Gas Emissions and Control.* 2002: SEMI.
78. Taiariol, F., et al. *Lifecycle Assessment of an Integrated Circuit Product.* in *IEEE International Symposium on Electronics and the Environment.* 2001. Denver, CO: IEEE.
79. Schischke, K., et al. *Lifecycle Inventory Analysis and Identification of Environmentally Significant Aspects and Semiconductor Manufacturing.* in *IEEE International Symposium on Electronics and the Environment.* 2001. Denver, CO: IEEE.
80. Williams, E., R. Ayres, and M. Heller, *The 1.7 kilogram microchip: Energy and material use in the production of semiconductor devices.* Environmental Science and Technology, 2002. **36**(24): p. 5504-5510.
81. Hermanns, S. and M. Dainz, *Evaluating Life Cycle Assessment (LCA) Methodology at AMD Saxony for Identifying Resources Conservation Priorities.* 2002, AMD Saxony - Feb 30: Dresden, Germany.
82. Reu, R.Y.B., et al. *Life Cycle Inventory and Streamed Analysis of 64Mb DRAM Manufacture.* in *International Semiconductor ESH.* 2002. San Diego: ISESH.
83. Walling, T., A. Tran, and B. Ridgeway, *Evaluation of an Edwards TPU4214 and an Ecosys Phoenix IV for CF_4 Abatement.* 1997, SEMATECH International: Austin, TX.
84. Gilliland, T., B. Cummins, and B. Ridgeway, *S69 Evaluation of an Edwards/Alzeta Thermal Processing Unit (TPU) Designed to Abate Perfluorocompounds (PFCs).* 1995, SEMATECH International: Austin, TX.
85. Jaccaud, M., et al., *Ullmann's Encyclopedia of Industrial Chemistry.* 2002, Wiley-VCH Verlag GmbH, Weinheim, Germany.
86. Coronell, D.G., et al., *Process for nitrogen trifluoride synthesis.* 1996, Air Products and Chemicals, Inc (Allentown, PA): US.
87. Dance, D.L., D.W. Jimenez, and A.L. Levine, *Understand Equipment Cost-of-Ownership,* in *Semiconductor International.* 1998.
88. eCO2.com, *Emission Trading of CO2*, Y. Chen, Editor. 2005.
89. Chen, X., et al., *Advances in Remote Plasma Sources For Cleaning 300 mm and Flat Panel CVD Systems,* in *Semiconductor Magaznie.* 2003.
90. Meeks, E., et al., *Results from Modeling and Simulation of Chemical Downstream Etch Systems.* 1996, Sandia National Laboratories: Albuquerque, NM.
91. Flamm, D.L., C.J. Mogab, and E.R. Sklaver, *Reaction of Fluorine-Atoms with SiO_2.* Journal of Applied Physics, 1979. **50**(10): p. 6211-6213.
92. Kasner, M., *Personal Communication: Chamber Cleaning Process*, Y. Chen, Editor. 2002: Cambridge, MA.
93. *Comprehensive Environmental Response, Compensation, and Liability Act (Superfund),* in *US Law.* 1980.
94. AspenTech, *Aspen.* 2001, AspenTech Inc.: Cambridge, MA.

95. Palisade, *@Risk*. 1996, Palisade Corporation: Newfield, NY.
96. Steen, B., *On uncertainty and sensitivity of LCA-based priority setting.* Journal of Cleaner Production, 1997. **5**(4): p. 255-262.
97. Gonzalez, B., B. Adenso-Diaz, and P.L. Gonzalez-Torre, *A fuzzy logic approach for the impact assessment in LCA.* Resources, Conservation and Recycling, 2002. **00**(2002): p. 1-20.
98. Ardente, F., M. Beccali, and M. Cellura, *F.A.L.C.A.D.E.: a fuzzy software for the energy and environmental balances of products.* Ecological Modelling, 2004. **176**(3-4): p. 359-379.
99. Petersen, A.K. and B. Solberg, *Greenhouse gas emissions, life-cycle inventory and cost-efficiency of using laminated wood instead of steel construction.* Environmental Science & Policy, 2001. **5**(2): p. 169-182.
100. AspenTech, *ReadMe.txt for AES Version 11.1 of Aspen Engineering Suite(tm) 11.1*. 2001, Aspen Tecch: Cambridge, MA.
101. Goedkoop, M. and R. Spriensma, *The Eco-Indicator 99, a damage oriented method for LCIA: Methodology Report*. 2000, PRe Consultant: Amersfoort, the Netherlands.
102. Avant!, *TSUPREM-4*. 1999, Avant! Corporation: Fremont, CA.
103. Avant!, *TSUPREM-4 Manual*. 1999, Avant!: Fremont, CA.
104. Trigeorgis, L., *Real options: managerial flexibility and strategy in resource allocation*. 1996, Cambridge, MA: MIT Press.
105. Garrett, J., et al., *Economic Input-Output Life Cycle Assessment*, Carnegie Mellon Green Design Initiative.
106. Suzuki, K., *Sub-100 nm focused ion beam lithography using ladder silicone spin-on glass.* Journal of Vacuum Science and Technology B, 1996. **14**(6): p. 3916-3919.
107. Rubin, J.B. and L.B. Davenhall. *Carbon Dioxide-based Supercritical Fluids as IC Manufacturing Solvents*. in *of the 1999 IEEE International Symposium on Electronics and the Environment*. 1999.
108. Goldfarb, D., J. Pablo, and e. al., *Aquesous-based Photoresist Drying Using Supercritical Carbon Dioxide to Prevent Pattern Collapse.* Journal of Vacuum Science and Technology B, 2000. **18**(6): p. 1-5.
109. Namatsu, H. and K. Yamazaki, *Supercritical Drying for Nanostructure Fabrication without Pattern Collapse.* Microelectronic Engineering, 1994. **46**: p. 129-132.
110. Rubin, J.B. and L.B. Davenhall. *A Comparison of Chilled DI Water/Ozone and CO2-Based Supercritical Fluids as Replacements for -Stripping Solvents*. in *the 1998 IEEE/CPMT International Electronics Manufacturing Technology Symposium*. 1998.
111. Mount, D., *ARROYO^{TM} System Description*. 2001, SC Fluids, Inc.
112. Schmidt, M., Y. Chen, Editor. 2001: Cambridge, MA.
113. Crawley, F., M. Preston, and B. Tyler, *HAZOP: Guide to Best Practice*. 2000, Rugby, UK: Institution of Chemical Engineers.
114. Kletz, T., *HAZOP and HAZAN*. 1992, Bristol, PA: Hemisphere Publishing Corporation.

115. McHugh, M. and V. Krukonis, *Supercritical Fluid Extraction.* 2nd ed. 1994, Stoneham, MA: Butterworth-Heinemann.
116. Cano-Ruiz, J.A., *Alejandro_GettingStarted_LCA Tool.doc*, Y. Chen, Editor. 2002: Cambridge, MA.